ISTANBUL TECHNICAL UNIVERSITY ★ GRADUATE SCHOOL OF SCIENCE ENGINEERING AND TECHNOLOGY

MODELING THE MECHANISM OF ESTER-SUBSTITUTED ALKYNES IN ACYLOXY MIGRATION FOLLOWED BY VARIOUS CYCLOADDITION REACTIONS

Ph.D. THESIS

Dilek COŞKUN

Department of Chemistry

Chemistry Programme

JANUARY 2018

ISTANBUL TECHNICAL UNIVERSITY ★ GRADUATE SCHOOL OF SCIENCE ENGINEERING AND TECHNOLOGY

MODELING THE MECHANISM OF ESTER-SUBSTITUTED ALKYNES IN ACYLOXY MIGRATION FOLLOWED BY VARIOUS CYCLOADDITION REACTIONS

Ph. D. THESIS

Dilek COŞKUN
(509102053)

Department of Chemistry

Chemistry Programme

Thesis Advisor: Prof. Dr. Nurcan Ş. TÜZÜN

JANUARY 2018

İSTANBUL TEKNİK ÜNİVERSİTESİ ★ FEN BİLİMLERİ ENSTİTÜSÜ

ESTER SÜBSTİTÜYE ALKİNLERİN ASİLOKSİ GÖÇÜ VE ARDINDAN ÇEŞİTLİ HALKA KATILMA REAKSİYON MEKANİZMALARININ MODELLENMESİ

DOKTORA TEZİ

Dilek COŞKUN
(509102053)

Kimya Anabilim Dalı

Kimya Programı

Tez Danışmanı: Prof. Dr. Nurcan Ş. TÜZÜN

OCAK 2018

Dilek COŞKUN, a Ph.D. student of ITU Institute of Graduate School Of Science Engineering And Technology student ID 509102053, successfully defended the thesis entitled "Modeling the Mechanism of Ester-Substituted Alkynes in Acyloxy Migration Followed by Various Cycloaddition Reactions", which she prepared after fulfilling the requirements specified in the associated legislations, before the jury whose signatures are below.

Thesis Advisor :	**Prof. Dr. Nurcan Ş. TÜZÜN** Istanbul Technical University	.....
Jury Members :	**Prof. Dr. Safiye SAĞ ERDEM** Marmara University	.....
	Assis. Prof. Dr. Bülent BALTA Istanbul Technical University	.....
	Prof. Dr. İlknur DOĞAN Boğaziçi University	.....
	Assoc. Prof. Dr. Barış YÜCEL Istanbul Technical University	.....

Date of Submission : 13 December 2017
Date of Defense : 03 January 2018

To my beloved spouse,

FOREWORD

I would like to thank my supervisor Prof. Dr. Nurcan Tüzün for her excellent guidance, tolerance, patience and support during my PhD process. Also I owe my best thanks to Prof. Dr. Safiye Sağ Erdem and Asst. Prof. Dr. Bülent Balta for their scientific and constructive guidance.

Moreover, I am very grateful to my spouse and my parents for all of their help. Especially, my spouse deserves a particular note of thanks for his support and patience. If I ever lost interest, my husband kept me motivated.

I gratefully acknowledge the financial support and the scholarship received towards my PhD from The Scientific and Technologic Research Council of Turkey (TUBITAK). I also thank to High Performance Computing Center for the computational infrastructure to my projects.

December 2017

Dilek COŞKUN
(Chemistry)

TABLE OF CONTENTS

Page

ABBREVIATIONS

ACE	**:** 3-Acyloxy 1,4-Enyne Ester
ACP	**:** Allenylcyclopropane
B3LYP	**:** Becke-Lee-Yang-Parr Gradient Three Parameter Corrected Exchange-Correlation Functional
DCM	**:** Dichloromethane
DFT	**:** Density Functional Theory
ECP	**:** Effective Core Potential
GGA	**:** Generalized Gradient Approximation
GTO	**:** Gaussian Type Orbital
HF	**:** Hartree-Fock
IEFPCM	**:** Integral Equation Formalism Polarizable Continuum Model
IRC	**:** Intrinsic Reaction Coordinate
LANL	**:** Los Alamos National Laboratory
LDA	**:** Local Density Approximation
LYP	**:** Lee-Yang-Parr Gradient Corrected Correlation Functional
MEP	**:** Minimum Energy Path
M06-L	**:** Minnesota 06 Local functional
PCM	**:** Polarizable Continuum Model
PP	: Pseudopotential
PW91	: Perdew–Wang 1991
SCRF	**:** Self-Consistent Reaction Field
STO	**:** Slater Type Orbital
TDI	**:** Turnover Frequency Determining Intermediate
TDTS	**:** Turnover Frequency Determining Transition State
TOF	**:** Turnover Frequency
TS	**:** Transition State
VCP	**:** Vinylcyclopropane

LIST OF TABLES

Page

LIST OF FIGURES

Page

MODELING THE MECHANISM OF ESTER-SUBSTITUTED ALKYNES IN ACYLOXY MIGRATION FOLLOWED BY VARIOUS CYCLOADDITION REACTIONS

SUMMARY

In the present thesis quantum chemical methods have been used to model the mechanism of Rh-catalyzed acyloxy migrations followed by cycloaddition reactions of propargyl esters. The necessary background information and the literature are introduced in Chapter 1. The theoretical framework of quantum chemistry is presented in Chapter 2. The results of the thesis are discussed in Chapter 3 and Chapter 4. Finally, the main conclusions are summarized in Chapter 5.

One of the main targets of synthetic chemistry is an effective production of desired compounds. In this respect, metal catalyzed reactions have contributed to this area by enabling many synthetic utilities including regioselective or stereoselective synthesis. However, in most of these cases, the mechanism of the metal catalyzed reactions are recondite. At this point, mechanistic studies, especially quantum mechanical modelling of reactions are very valuable as they exhibit wide range of information on the dynamics of a reaction, including the structural factors that affect product distribution, transition state structures, ligand effect, metal's contibution to mechanism. The main aim of this study is to investigate the reaction mechanisms for the formation of functionalized cyclohexenone and cyclopentenone derivatives via tandem acyloxy migration and cycloaddition via Rh catalyst. This thesis consists of two parts of work. In the first part, the two competitive 1,2- and 1,3-acyloxy migrations have been discussed and the effect of the nature of alkynes, terminal vs internal, in regioselectivity has been investigated by considering [4+1] and [5+1] cycloadditions of 3-acyloxy 1,4-enynes (ACEs) with terminal and internal alkynes. In the second part, the mechanism of a tandem 1,3-acyloxy migration [5+1] cycloaddition of cyclopropyl substituted propargyl esters has been investigated. The effect of the substituent in the cyclopropane has been studied to elucidate the mechanism of cyclopropyl ring opening which leads to product distribution.

In the first part of the thesis, the mechanisms of the $[RhCl(CO)_2]_2$-catalyzed intramolecular cycloadditions of ACEs with a cyclohexene moiety by CO with concominant acyloxy (OAc) migrations have been extensively investigated using density functional theory (DFT) calculations. All geometries were optimized at the B3LYP/6-31+G(d) level (LANL2DZ for Rh). The effect of the nature of alkynes has been rationalized by modelling possible intermediates and transition states for competitive 1,2- vs 1,3-migrations of acyloxy group and for further possible transformations with terminal and methyl substituted starting enynes. Experimental

and mechanistic studies indicate that the formation of cyclohexadienones proceeded by a [5+1] type cycloaddition of ACEs with terminal alkynes involving a Rautenstrauch 1,2-OAc migration by carbonylation while the formation reaction of functionalized cyclopentenones involved a Saucy-Marbet 1,3-OAc migration of ACEs of substituted alkynes and subsequent [4 + 1] cycloaddition with CO.

The reaction initiates with two isomers of ACE-RhCl(CO) π-complex by switching the positions of CO and Cl ligands. The isomer in which CO is trans to the alkyl group has been found to be more stable because Rh metal coordinates to both alkyne and alkene fragments strongly. The acyloxy migration is found to be the rate determining step from the DFT study and the predicted regioselectivity is in harmony with the experimental result. The ~5 kcal/mol of Gibbs free energy difference between 1,2 and 1,3-acyloxy migration transition states favor 1,2-acyloxy migration for terminal or H-substituted alkynes which is consistent with the experimental and theoretical findings.

The Rh-allyl complex, can undergo CO insertion with two possible reaction pathways. In the first path, CO addition to rhodium in Rh-allyl complex and then CO insertion to the cycle take place. In the second path, isomerization takes place before CO addition which leads to a more stable isomer. The following CO insertion steps prove that the isomerized intermediate is energetically favored through the reaction mechanism. On the other hand, the insertion of carbonyl group from cyclohexane side is found to be favored compared to the alkene side which leads to the ketene formation when Rh is expelled from the system by complexing to another ACE. The rhodacycloheptadienone which is obtained through CO insertion from cyclohexane side undergoes reductive elimination. The cyclohexadienone product is obtained when the catalyst leaves the system by coordinating with another ACE molecule and the starting Rh-ACE complex is regenerated.

In internal alkynes, the preference of 1,3- is not strong as compared to 1,2-acyloxy migration, therefore, both mechanisms were modeled. The barrier heights for the following steps of 1,2-migration are found to be higher than that of 1,3-acyloxy migration. Furthermore, a probable equilibrium between Rh-allyl complex and Rh-ACE complex indicates that 1,2-acyloxy migration is a less facile path for internal alkynes. Additionally, 1,3-acyloxy migration intermediate called Rh-allenyl complex is also experimentally proposed. As it is discussed in the terminal part, calculations have shown that the isomerization step is energetically preferable compared to a direct CO addition and CO insertion from the cyclohexane side is energetically favored. The resulting rhodacyclohexenone undergoes reductive elimination and the catalyst leaves the system by coordinating with another ACE.

The calculations presented herein have contributed to understanding and thus will lead to controlling this effective Rh (I) catalyzed transformation reactions of 1,2 and 1,3-acyloxy migration followed by cycloaddition for further cyclohexadienone and cyclopentenone derivatives in obtaining custom made products.

In the second part of the thesis, the carbonylation mechanism of cyclopropyl substituted propargyl esters has been modeled with DFT at WB97XD/6-31+G(d) level (LANL2DZ for Rh). Although B3LYP functional was used in the fist part of the thesis, it was not succesful enough to investigate 1,3-acyloxy migration of cyclopropyl substituted propargyl esters in solution. On the other hand, a long range WB97XD functional is found to be good at highlighting the acyloxy migration. The cleavage of different cyclopropane C-C σ-bonds led to different isomers for the unsymmetrically substituted cyclopropanes. The regioselectivity for the cleavage of C-C σ-bonds is

found to be dependent on the stereochemistry of the cyclopropyl group, the metal catalysts and the electronic properties of the substituents.

In this thesis, cis and trans conformers of 3-(2-Hydroxymethyl-cyclopropyl)-1,1-dimethyl-prop-2-ynyl ester and trans conformer of 3-(2-Phenyl-cyclopropyl)-1,1-dimethyl-prop-2-ynyl ester have been modeled to highlight the reaction mechanism and explain the product distribution. Although both trans- and cis-disubstituted cyclopropanes with hydroxymethyl moiety prefer the cleavage of the less hindered C-C σ-bond of cyclopropane, a higher regioselectivity is observed in cis-substituted cyclopropane than the corresponding trans-counterpart. Moreover, trans conformers with hydroxymethyl and phenyl substituted cyclopropanes have opposite regioselectivities.

1,3-acyloxy migration of cyclopropyl substituted propargyl esters is a step-wise process which takes place in the first two transition states. The formed Rh-allenyl complex undergoes isomerization, CO addition and then ring opening. The resulting metallacycle undergoes CO insertion followed by reductive elimination. In the last step, alkylidene cyclohexenone product forms when the catalyst leaves the system by coordinating with another ACE. The energies of the intermediates formed by direct CO addition or isomerization followed by CO addition have been compared. As in the first part of the thesis, the resulting isomer is exothermically preferred. Isomerization leads to a lower energy transition state and an intermediate for the following CO insertion.

Furthermore, CO insertion has been investigated in terms of the positions of carbonyl group to the cleavaged C-C σ-bond of cyclopropane. The calculations herein show that the initial reactant energies and the barrier heights for CO insertion have a large effect on product distribution for trans and cis conformers. The 4.9 kcal/mol of energy difference in CO insertions of trans-disubstituted cyclopropanes favors the cleavage of the least substituted C-C σ-bond, leading to the major product. While the high selectivity of the least substituted C-C σ-bond in cis conformers have been explained by 3 kcal/mol of energy difference in the initial complexes and 4.9 kcal/mol of energy difference in CO insertions.

The opposite selectivity of trans-disubstituted cyclopropanes with phenyl group in which the most substituted C-C σ-bond is cleaved for ring expansion is due to the electronic effect of the adjacent π-system. Finally, the results in this study are consistent with the experimental findings.

As a part of this thesis, a poster has been presented in an international symposium and a paper has been published in a SCI indexed peer-reviewed journal (10.1016/j.jorganchem.2017.09.017).

ESTER SÜBSTİTÜYE ALKİNLERİN ASİLOKSİ GÖÇÜ VE ARDINDAN ÇEŞİTLİ HALKA KATILMA REAKSİYON MEKANİZMALARININ MODELLENMESİ

ÖZET

Metal katalizörlü sentezler organik kimyacıların sıkça kullandığı metodlardandır. Elde edilen ürün ya da ürünler katalizörün kimliğine, ligandlara, tepkenlere ve deney şartlarına çoğu zaman bağlılık göstermekte fakat hangi aşamalardan geçerek ürün elde edildiği bilinememektedir. Mekanizmanın bilinmesi, ürün dağılımına etki eden faktörlerin anlaşılması, o tepkimenin kontrolüne ve isteğe özel ürün elde edilmesine olanak sağlayacaktır.

Bu tez kapsamında bir seri propargil esterlerin Rh katalizör varlığında gerçekleşen asiloksi göç ve ardından siklokatılma tepkimelerinin hangi mekanizma üzerinden ilerlediği ve hangi ürünü verdiği kuantum mekanik yöntemlerle incelenmiştir. İlk bölümde konuya ilişkin literatür bilgisi verilmektedir. İkinci bölümde, kuantum kimyası teorik çerçevede sunulmuştur. Üçüncü ve dördüncü bölümlerde bu tez kapsamında yapılan çalışmaların sonuçları tartışılmıştır. Son bölümde ise tezin sonuçları özetlenmiştir.

Bu çalışmanın amacı asiloksi göçü ve halka katılması ile oluşan fonksiyonelleştirilmiş siklohekzenon ve siklopentenon reaksiyon mekanizmalarını kuantum mekaniksel yöntemlerle detaylı olarak aydınlatılmasıdır. Elde edilen yapılar bir çok kullanım alanına sahip olduklarından organik sentez açısından kıymetli ürünlerdir. Bu tez iki çalışmadan oluşmaktadır. İlk çalışmada, birbiriyle yarışan 1,2- ve 1,3-asiloksi göçleri tartışılmıştır. Alkinlerin yapısının regio seçiliğe etkisini incelemek için uç ve iç alkinli 3-asiloksi 1,4-enin esterlerin (ACE) [4+1] ve [5+1] siklokatılmaları araştırılmıştır. İkinci çalışmada ise, siklopropil sübstitüye propargil esterlerin ardarda gerçekleşen 1,3-asiloksi göçü ve [5+1] siklokatılma mekanizmaları araştırılmıştır. Ürün dağılımına neden olan siklopropil halka açılma mekanizmasını açıklayabilmek için siklopropile bağlı grupların etkisi üzerinde çalışılmıştır.

Bu tezin ilk aşamasında, siklohekzen sübstitüye ACElerin $[RhCl(CO)_2]_2$-katalizörlü molekül içi asilosi göç eşliğinde halka katılma mekanizmaları Yoğunluk Fonksiyoneli Teorisi (YFT) ile B3LYP/6-31+G(d) baz seti kullanılarak detaylı bir şekilde incelenmiştir. Rh atomu için LANL2DZ kullanılmıştır. Birbiriyle yarışan 1,2- ve 1,3-asiloksi göçleri ile uç ve metil sübstitüye başlangıç eninlerinin geçiş ve ara ürünleri modellenerek alkinlerin yapısının etkisi açıklanmaya çalışılmıştır. Deneysel ve mekaniksel çalışmalar göstermektedir ki uç alkinli ACEler Rautenstrauch 1,2-asiloksi göçü ve [5+1] katılması ile siklohekzadienon oluşumunu sağlarken, iç alkinli

ACE'lerle Saucy-Marbet 1,3-asiloksi göçü ve [4+1] katılması ile siklopentenon elde edilmektedir.

Reaksiyon ACE-RhCl(CO)-π bileşiğinin CO ve Cl ligandların pozisyonuna göre iki izomer ile başlamaktadır. Hem uç hem iç alkinlerde karbonilin alkin grubuna trans olduğu izomer enerjik olarak daha kararlıdır çünkü Rh metali hem alkin hem de alken yapısına koordine olmuştur. Diğer izomerde ise rodyum alkin yapısıyla güçlü bir bağ kurarken alken yapısından uzakta olmayı tercih etmiştir. YFT çalışması ile asiloksi göçünün hem uç hem de iç alkinlerin halkalaşma reaksiyonlarında tepkimenin hızını belirleyen basamak olduğu ve regio seçiciliğin deneysel sonuçlarla uyum içinde olduğu gözlemlenmiştir. 1,2- ve 1,3-asiloksi göçü arasındaki ~5 kcal/mol Gibbs serbest enerji farkı, uç alkinler için 1,2-asiloksi göçünün tercih edildiğini göstermektedir. Bu durum deneysel ve teorik bulgular ile de tutarlıdır.

1,2-asiloksi göç ürünü olan Rh-allil bileşiğine karbonil katılması için iki yol önerilmiştir: rodyum katalizörüne CO eklenmesi ve ardından CO grubunun halkaya katılması ya da CO eklenmesinden önce daha düşük enerjili izomer oluşumu. CO katılması ve ardından gelen reaksiyon basamaklar izomer ürününü takip eden mekanizmanın enerji bakımında tercih edildiği göstermektedir. Diğer yandan, karbonil grubunun keten oluşumuna neden olan alken tarafı yerine siklohekzan tarafından katıldığı gösterilmiştir. Oluşan rodyum-sikloheptadienon indirgeyici eliminasyona uğramış ve katalizörün farklı bir ACE ile koordine olup ayrılmasıyla siklohekzadienon elde edilmiştir.

İç alkinlerin 1,3-asiloksi göçü tercihi 1,2-asiloksi göçüne göre yeterince kuvvetli olmadığı için her iki mekanizma da modellenmiştir. 1,2-asiloksi göçünü takip eden basamakların bariyerlerinin 1,3-asiloksi göçünü takip eden basamaklara göre daha yüksek olduğu bulunmuştur. Aynı zamanda 1,2- göç ürünü olan Rh-allil bileşiği ile tepkenin enerjisi hemen hemen aynı olduğu için bir denge durumundan bahsedilebilir. Diğer yandan, 1,3-asiloksi göçü sonrası oluşan Rh-allenil bileşiği daha düşük enerjiye sahip ve daha kararlıdır. Aynı zamanda deneysel olarak da gözlemlenmiştir. Uç alkinlerde olduğu gibi, direk CO eklenmesi yerine önce izomerleşmenin gerçekleşmesinin ve karbonil grubunun siklohekzana yakın kısımdan katılmasının enerjik olarak tercih edildiği görülmüştür. Oluşan rhodasiklohekzenon indirgeyici eliminasyona uğramış ve katalizör başka bir ACE molekülü ile koordinasyona girerek sistemi terk etmiştir.

Olefinik karbonların yüklerinin asiloksi göçü etkilediği literatürde bahsedilmektedir. Bunu incelemek için uç ve iç alkinlerin tepkenlerinin olefinik karbon yükleri karşılaştırılmıştır. Buna göre asiloksi grubunun negatif yüklü karbonil oksijeni olefinik karbonlardan daha pozitif yüklü olana saldırmaktadır. Uç alkinlerde 1,2-asiloksi göçünün gerçekleşmesine neden olan karbonun daha pozitif olduğu görülürken, iç alkinlerde ise 1,3-asiloksi göçüne sebep olan karbon atomunun daha pozitif olduğu görülmüştür. Bu bulgular ile literatürde altın analoğu ile yapılan çalışmanın uyum sağladığı görülmektedir.

Bunun dışında, iç alkinler üzerinde sübstitüentin etkisini araştırmak için metil grubu fenil, para-metoksifenil ve vinil gruplarıyla değiştirilmiş fakat baskın bir 1,3-asiloksi göçü tercihi görülmemiştir. Diğer yandan bu yapıların 1,3-asiloksi göçü ile oluşan Rh-allenil bileşiklerinin 1,2-asiloksi göçü ile oluşan Rh-allil bileşiklerine göre daha kararlı olduğu enerji değerlerinden anlaşılmaktadır. Bu da iç alkinlerin 1,3- göç tercihinin oluşan allen yapısının daha kararlı olmasıyla açıklanabilir. 1,3-göç verimliliğini artırmak için, deneysel çalışma yapanların rezonans kararlığını kolaylaştıran uygun

sübstitüyeli gruplar ile daha kararlı allen elde etmeye odaklanabilirler. Ayrıca, çözücünün mekanizma üzerinde etkisi gözlemlenmemiştir.

Birinci kısımda sunulan sonuçlar Rh-katalizörlü 1,2- ve 1,3-asiloksi göç ve ardından gerçekleşen halka katılmaları ile istenen bisiklik siklohekzadienon ve siklopentenon türevlerinin elde edilmesine olanak sağlamaya ve oluşan ürünü kontrol etmeye katkı sağlamaktadır.

Tez çalışmasının ikinci kısmında, siklopropil sübstitüye propargil esterlerin siklokarbonlaşma mekanizması YFT ile WB97XD/6-31+G(d) baz seti kullanılarak detaylı bir şekilde incelenmiştir. Rh atomu için LANL2DZ kullanılmıştır. İlk çalışmada kullanılan B3LYP fonksiyonunun bu mekanizmanın aydınlatılmasında yeterince başarılı olmadığı, WB97XD fonksiyonunun asiloksi göçünün aydınlatılmasında etkili olduğu görülmüştür. Asimetrik sübstitüye siklopropanların farklı C-C σ-bağlarının koparılması ile farklı isomerler elde edilmektedir. Koparılan C-C σ-bağların regio seçiciliğinin siklopropil grubun stereokimyasına, metal katalizörün yapısına ve sübstitüyentlerin elektronik özelliklerine bağlı olduğu bulunmuştur.

Bu çalışmada, 3-(2-Hidroksimetil-siklopropil)-1,1-dimetil-prop-2-ynil esterin cis ve trans konformerleri ile 3-(2-Fenil-siklopropil)-1,1-dimetil-prop-2-ynil esterin trans konformeri için reaksiyon mekanizması aydınlatılmış ve ürün dağılımı incelenmiştir. Daha az veya daha fazla sübstitüye C-C σ-bağının kopmasını tercih eden ikişer konformer bulunmaktadır. Reaksiyon mekanizmasını aydınlatmak ve seçiciliği göstermek için her izomer için bu dört konformerin reaksiyon mekanizması modellenmiştir. Cis-sübstitüye siklopropanın halka açılımı trans benzeri gibi sübstitüyente sahip olmayan ya da daha az sübstitüyente sahip olan C-C σ-bağının kopmasıyla meydana gelmektedir. Diğer yandan, cis yapısı trans yapısına göre daha yüksek regio seçiciliğe sahip olduğu deneysel olarak gözlemlemiştir. Ayrıca, hidroksimetil ve fenil sübsitüye siklopropanların trans konformerlerinin karşıt regio seçiciliğe sahip olduğu görülmüştür.

Siklopropil sübstitüye propargil esterlerin 1,3-asiloksi göçü iki aşamada gerçekleşen bir işlemdir. Oluşan Rh-allenil bileşiği sırasıyla izomerizasyona, CO eklenmesine ve en son olarak halka açılmasına uğrar. Yeni oluşan metal içeren halka önce CO katılması sonra indirgeyici eliminasyon geçirir. Son basamakta, katalizör başka bir ACE molekülü ile koordine olarak sistemi terk eder ve alkilidin siklohekzenon ürünü oluşur. Ana mekanizmaya alternatif olup siklohekzenon ürünü verebilecek mekanizmalar da dikkate alınıp incelenmiştir. İlk olarak halka açılmasının CO eklenmesinden önce geldiği mekanizma modellenmiştir. İkinci olarak ise önce CO eklenmesi ardından halka açılması incelenmiştir. İlk alternatif başarısız olduğu için ikinci mekanizma ile reaksiyonun aydınlatılmasına devam edilmiştir.

İlk çalışmada olduğu gibi allen bileğişinin izomerizasyona uğrayarak daha kararlı bir yapıya dönüştüğü izomere karbonil katılmasının, direk karbonil katılmasına göre daha düşük bariyer ile gerçekleştiği görülmüştür. Ayrıca, CO katılması hem siklopropan tarafından hem de alken tarafından modellenmiştir. Siklopropan tarafından katılma daha düşük enerjiyle gerçekleşirken, alken tarafından katılma rodyumun π-bağlarını kaybederek daha yüksek enerjili rodasiklohexene dönüşmesi ile gerçekleşmektedir. Bu yüzden, karbonilin siklopropan tarafından katıldığı kabul edilmektedir.

Ayrıca, karbonil katılmasının siklopropilin C-C σ-bağları arası seçiciliği de incelenmiştir. Hesaplamalar başlangıç tepkeni enerjilerinin ve karbonil katılması için gerekli enerji bariyerinin cis ve trans konformerlerin ürün dağılımında büyük bir etkisi

olduğunu göstermektedir. Trans-hidroksimetillerin daha az sübstitüye C-C σ-bağı tercihi CO katılması geçiş durumdaki 4.9 kcal/mol enerji farkı ile açıklanırken, cis benzerinin daha az sübstitüye C-C σ-bağı tercihinin hem tepkenler arası 3 kcal/mol enerji farkı hem de CO katılması durumdaki 4.8 kcal/mol enerji farkından kaynaklandığı görülmektedir. Bu da cis izomerin trans benzerine göre neden daha yüksek seçiciliğe sahip olduğunu açıklamaktadır.

Trans- fenil siklopropil propargil esterlerin daha fazla sübstitüye C-C σ-bağını tercih ederek halka genişlemesi gerçekleştirmesinin nedeni C-C bağına bitişik fenil grubunun π-elektron sisteminin elektronik etkisiyle açıklanmaktadır. Her iki ürüne neden olan konformerlerin enerjileri birbirine yakın olmakla birlikte daha fazla sübstitüye C-C σ-bağını tercih eden konformerin tepken ve allen bileşikleri biraz daha kararlıdır. Bu da trans- fenil siklopropil propargil esterlerin diğer yapılara göre aksi seçiciliğe neden olmasına karşın seçiciliğin çok da baskın olmadığını enerji değerleri de göstermektedir.

Bu çalışmada, Rh-katalizörlü ard arda gerçekleşen 1,3-asiloksi göçü ve [5+1] siklokatılma reaksiyonu siklopropil propargil esterlerin mekanizması aydınlatılmış ve siklopropana bağlı grupların trans ve cis izomerlerinin regio seçiciliğe etkisi incelenmiştir.

Bu tez kapsamında uluslararası kongrede bir poster bildiri sunumu ile , SCI indeksli hakemli dergide bir yayın (10.1016/j.jorganchem.2017.09.017) gerçekleştirilmiştir.

1. INTRODUCTION

The development of new, efficient methods in synthetic chemistry represents an important ongoing challenge for organic and inorganic chemists. Among a variety of synthetic transformations, reactions catalyzed by transition metals are some of the most efficient tools to access several types of cyclic or acyclic structures. Many natural or synthetic compounds used as drug substances for their biological activities are carbo- or heterocycles. Therefore, transition metal catalyzed cycloaddition has recently attracted considerable attention for producing highly functionalized carbocyclic and heterocyclic compounds [1-5].

One of the most recently studied methods involve transition metal catalyzed cycloaddition of 1,n-enynes to access a wide range of cyclic structures [6-8]. The electrophilic activation of alkynes or alkyne derivatives (such as enynes, yne-benzenes) by transition metal complexes and the formation of metallacycle or metal vinylidene complexes have been proposed as the key steps in most of the cycloisomerization reactions [9]. Therefore, the understanding of the reaction mechanisms of intra and intermolecular cycloadditions of alkynes with alkenes using π-acidic metals can provide important insights in the construction of various cyclic products including natural or non-natural compounds in this regard.

Rhodium is one of the most notable platinum group metals which are chemically stable at high temperatures and resistant to corrosion. Rh catalysts are mainly used for emission-control in vehichles which reduce smog and acid rains [10]. Over the past decade, many Rh-catalyzed methods have been developed for the synthetically useful reactions employing C-H bond activation and applied to natural products and drug synthesis [11]. In addition, Rh catalyst has been used to the direct catalytic conversion of methane to acetic acid in aqueous solution which provides a great improvement to reach industrially useful organic compunds [12].

Murai et. al. reported the skeletal reorganization of enynes to 1-vinylcycloalkenes catalyzed by different transition metals, such as $[Ru(Cl)_2CO_3]_2$, $PtCl_2$, $[IrCl(CO)_2]_n$,

$GaCl_3$ [13-16]. On the other hand, acyloxy substituted enynes or propargyl esters have gained much interest over the last decade thanks to their ability to form a great diversity of substituted rings via acyloxy migration [17-21].

1,3-acyloxy migration of propargyl esters was first discovered in 1959 by Saucy and Marbet in the presence of a silver catalyst [22]. Allene followed by alkene products were obtained from acyloxy substituted alkyne via acyloxy migration. The first 1,2-acyloxy migration and then cyclization where palladium complexes catalyzed the formation of cyclopentenones from propargyl esters (Figure 1.1) were reported in 1984 by Rautenstrauch [23] .

Saucy-Marbet (1959)

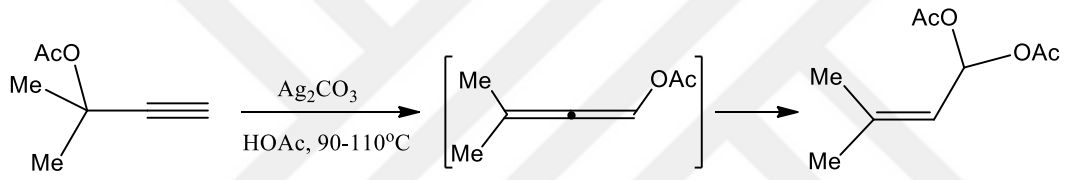

Rautenstrauch (1981)

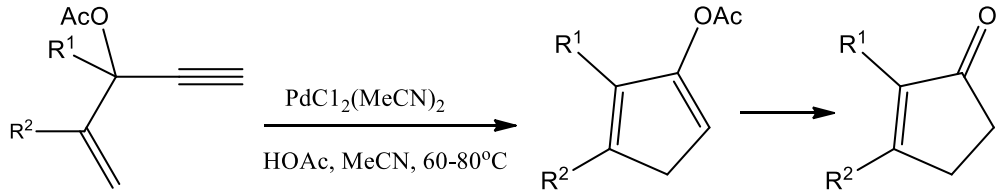

Figure 1.1 : Saucy and Marbet 1,3-acyloxy migration and Rautenstrauch 1,2-acyloxy migration.

These rearrangement reactions have been broadened significantly by the use of different substrates and transition metals, such as gold, [24-28] platinum, [29-32] ruthenium, [33-35] copper [36-38] and more recently rhodium [17,20-21,39-41]. The regioselectivity in these transformations is observed to be governed mostly by the nature of the catalyst and the substituents. Experimental and computational investigations on elucidating their effects are involved in the literature. Toste et al. reported the gold(I)-catalyzed Rautenstrauch rearrangement of enantioenriched propargyl pivaloates for the synthesis of 2-cyclopentenones with high enantioselectivites. In their recent study, a ketal is used in place of the acetoxy group to control the cyclization by ligand and form extensive enantioselective cyclopentenones [24-26]. In a detailed examination of 1,2- vs 1,3-acyloxy migration of secondary vs tertiary cyclopropyl substituted propargyl acetates by Nevado et al., the cyclopentannulation products were obtained in the presence of gold catalyst through cyclopropyl ring opening [19]. In another study, Soriano et.al. have suggested cyclopropanation and then 1,2-migration instead of 1,2-acyl migration followed by a cyclization step in order to obtain bicyclic adducts with $PtCl_2$ catalyst [42]. Indene synthesis via Pt-catalyzed cyclization of propargyl esters via 1,2-acyloxy migration were reported by Sarpong et al. [43]. On the other hand, Nolan and coworkers used gold catalyst to synthesize indene via 1,3-acyloxy migration in propargyl esters [17].

Au-catalyzed rearrangement of propargyl esters (I) proposed that the two competitive 1,2 and 1,3 acyloxy migrations are mechanistically related (Figure 1.2). 1,2-migration goes through metal carbene (III) while [3,3]-sigmatropic rearrangement proceeds via allenyl acetate (V) in a single process or stepwise by a second 1,2-migration from III [19].

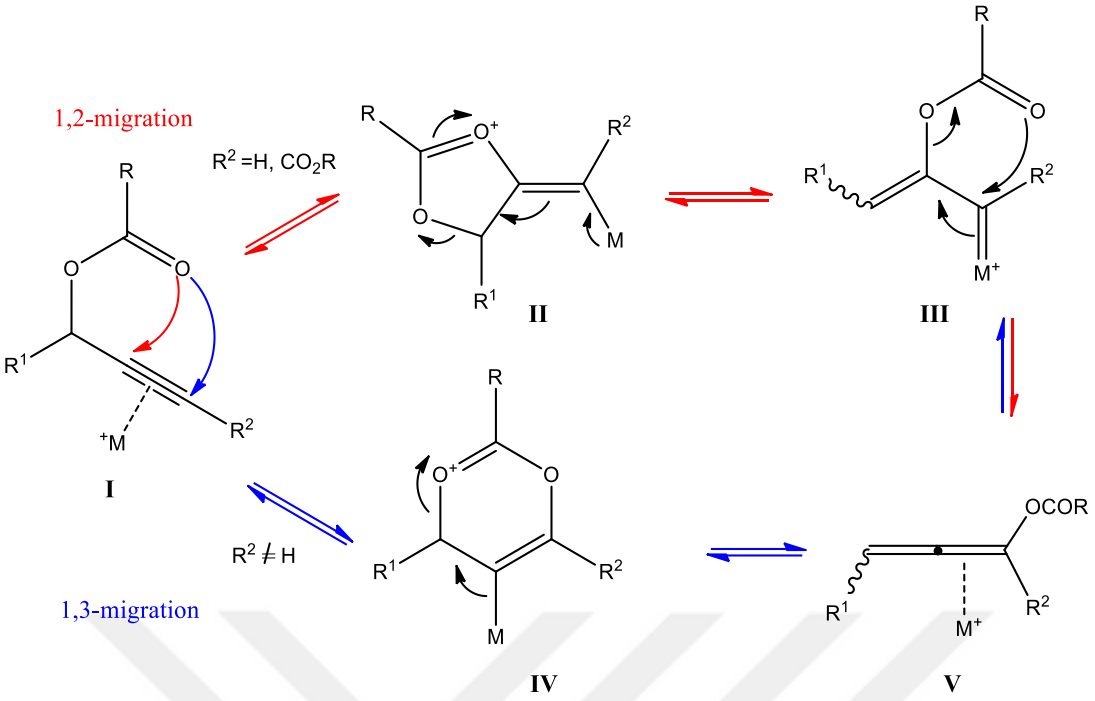

Figure 1.2 : The proposed mechanism for 1,2- vs 1,3-acyloxy migration.

Although numerous reports on acyloxy migrations of propargyl esters have been published with gold catalyst, rhodium metal is still well known for traditional organometallic reactivities such as oxidative addition, migratory insertion, reductive elimination, carbonylation and it has been successfully used in the literature for many types of transformations [21].

Rh-catalyzed various cycloadditions of propargyl esters via 1,3 acyloxy migrations have been reported in the literature. [4+1] cycloaddition of vinylallene and CO addition was first studied by Murakami et al. and a mixture of alkylidene cyclopentenone isomers was observed [44]. Malacria and Tang groups independently reported 1,3-acyloxy migration followed by [4+1] cycloaddition by $Rh(COD)Cl_2$ catalyst [39-40]. Aromatic benzene derivatives were obtained via intermolecular [4+2] cycloaddition of vinylallene and alkyne by Murakami et al. [45]. On the other hand, Tang studied an intramolecular [4+2] cycloaddition of propargyl esters via acyloxy migration by $[Rh(CO)_2Cl]$ catalyst. In their studies the three important roles of acyloxy group in the propargyl ester were explained as follows: (1) the preparation for allene moiety is not needed; (2) the inhibition of aromatization process and the isolation of isotoluenes may be achieved by acyloxy group; (3) it differentiated the olefins for further functionalization [46]. Additionally, [5+1] cycloaddition of cyclopropyl substituted propargyl ester by CO was reported with regioselective ring expansion of

cyclopropanes by Tang's group [41]. Yu et al. synthesized cylohexenone from vinylcyclopropanes in a CO atmosphere with Rh(dppp)SbF_6 catalyst [47].

The synthesis of cyclooctadienones was achieved via Rh-catalyzed [7+1] cycloaddition of buta-1,3-dienycyclopropanes with CO by Yu et al. [48]. A mixture of seven- and eight-membered carbocycles was obtained from allenylvinylcyclopropane via Rh-catalyzed 1,3-acyloxy migration ring expansion and [7+1] cycloaddition by Tang et al. [49].

Rh-catalyzed 1,2-acyloxy migration of propargyl esters followed by [3+2] cycloaddition was first reported by Tanaka et al. [50]. Functionalized cyclohexadienone and resorcinol derivatives from 3-acyloxy 1,4-enynes (ACEs) were developed by Malacria et al. via a tandem 1,2-acyloxy migration [5+1] cycloaddition of ACEs with CO [20,28]. Tang et al. reported Rh-promoted [5+2] cycloaddition of propargylic esters with alkynes accompanied by 1,2-acyloxy migration [51-52].

Among a variety of rhodium catalysts, the intra and intermolecular cycloaddition reactions have been reported to be efficiently catalyzed by the rhodium dimer, $[RhCl(CO)_2]_2$[18,19,20]. In this thesis work, $[RhCl(CO)_2]_2$ catalyzed tandem acyloxy migration and intramolecular cycloadditions of propargyl esters with CO have been carried out.

1.1 Rh-Catalyzed Competitive 1,2- versus 1,3-Acyloxy Migration Followed by [5+1] and [4+1] Cycloadditions of 3-Acyloxy-1,4-Enynes with CO

Transition-metal catalyst has promoted the transformations of propargylic esters to a variety of valuable substances effectively. 1,3 and 1,2-acyloxy migration of 3-acyloxy-1,4-enynes (ACEs) by transition metals allow the formation of a wide range of molecular constituents and natural products from simple and readily available starting structures. Resorcinols, cyclopentenone, cyclohexanone and cycloheptenone derivatives are some essential products of cycloaddition reactions [20,39]. Especially, resorcinols as natural compounds which have been isolated from plant sources [53] display important biological activities [53-54], such as, efficiently meditating DNA cleavage under oxidative conditions, as well as antibacterial activities [55].

Over the last decade, transition metal catalyzed 1,3- and 1,2-acyloxy migration of propargylic esters have become popular when their synthetic potential was realized.

However, the reaction mechanism of 1,3- and 1,2-migration of acyloxy group in propargyl esters is still controversial [21]. Soriano and Marco-Contelles reported that 1,2-acyloxy migration was considerably kinetically favored for terminal alkynes while alkyl substituted internal alkyne enhances the electrophilicity of that acetylenic atom, and allows a faster 1,3-acyloxy migration [11]. Fensterbank, Malacria and, Nolan et al reported that Au-catalyzed 1,3-acyloxy migration might be preferred to take place via a double 1,2-shift comparing to a direct 1,3-shift [56]. On the other hand, Toste et al. showed that the formation of allene intermediate was obtained from a direct 1,3-acyloxy migration by gold catalysis [57]. You and Pu have found that Rh-promoted a tandem 1,3-acyloxy migration [4+1] cycloaddition of vinyl allene intermediates with CO generated cyclopentenone products by providing good diastereoselectivity for the enyne substrates bearing an aromatic ring at the propargylic carbon with electron-withdrawing or o-substituents [58].

In the first part of the thesis work, Rh catalyzed [5+1] and [4+1] cycloadditions of 3-acyloxy-1,4-enyne esters (ACEs) to obtain functionalized resorcinols and cyclopentenones, reported by Malacria M. et. al., have been studied [39]. The investigation of the reaction mechanism and the selectivity of acyloxy migration have been evaluated for both terminal and internal alkynes. According to the literature, 1,3- vs 1,2-acyloxy migration selectivity depends on the substitution pattern of the propargyl moiety (the type of alkynes) and the metal catalyst. The selectivity of 1,3- or 1,2-acyloxy migration by Rh(I)-catalysis has shown similar trend with Au- and Pt-catalyzed reactions [21].

The ACEs with terminal alkynes or electronically demanding alkynes favor 1,2-acyloxy migration whereas ACEs with other internal alkynes prefer 1,3- acyloxy migration by the catalysis of various metals [20,27-28,39,59-60]. In particular, Rh(I)-catalyzed cycloaddition of 3-acyloxy 1,4-enyne ester (a) with CO leads to functionalized cyclohexadienones (b), resorcinols (c) via 1,2-acyloxy shift and alkylidene cyclopentenones (d, e) via 1,3-acyloxy shift (Figure 1.3) [20-21,39-41].

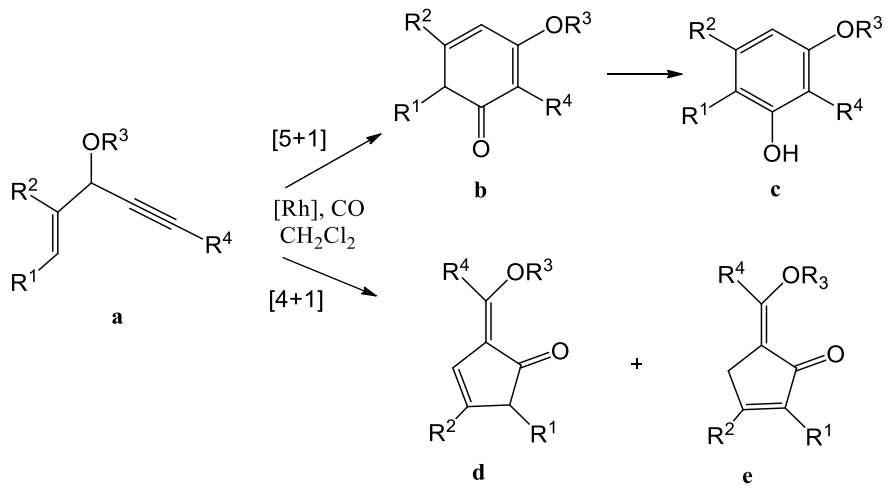

Figure 1.3 : Rh(I)-catalyzed carbonylation of 3-acyloxy-1,4-enyne in the synthesis of cylohexadienone and cyclopentenone derivatives.

In the first part of the study, the cycloaddition reaction mechanisms have been investigated by quantum mechanical calculations for the formation of bicyclic [5+1] and [4+1] type cycloaddition products. The competing 1,2- vs 1,3-acyloxy migrations of ACEs with terminal alkynes and internal (methyl substituted) alkynes have been modeled in the presence of $[RhCl(CO)_2]_2$ catalyst.

1.2 Rh-Catalyzed Tandem 1,3-Acyloxy Migration [5+1] Cycloaddition of Cyclopropyl Substituted Propargyl Esters

Cycloaddition reactions have been essential tools in organic synthesis since the development of Diels−Alder reaction (specifically, a [4+2] cycloaddition) which are useful and reliable methods for forming six-membered rings [61-66]. In the past decades, transition metal cycloadditions have opened many new cycloaddition manifolds to provide efficient syntheses of six membered carbo or heterocycles, such [3+3], [3+2+1], [2+2+2], and [5+1] [67]. Recently, the use of various transition metals to catalyze new cycloaddition reactions between unactivated alkenes, alkynes, and other unsaturated molecules has attracted more attention [68-71]. Comparing to the more classical approaches, the carbocylization reactions have at least one carbometalation step. The formation of multiple carbon–carbon or carbon–heteroatom bonds in a single operation makes carbocyclization strategies a highly attractive approach, specially for the reduction of chemical waste in synthetic applications. Furthermore, cyclic structures containing a wide variety of ring sizes, degrees of unsaturation, and substitution patterns can be obtained from acyclic substrates under

relatively mild conditions for a target-directed synthesis [72]. The carbocyclization reaction is still an efficient way to synthesize cyclohexenones which is widely found in many natural products and pharmaceuticals as a structural skeleton like saudin [73], antroquinonol [74], gabosines [75], etc., displaying important biological activities such as anticancer agents [76] and pheromones [77-79]. In the first part of the thesis, we have investigated Rh-catalyzed [4+1] and [5+1] carbocyclization of 3-acyloxy 1,4-eneynes for the synthesis of alkylidene cyclopentenone and cyclohexadienone derivatives. In the second part, Rh-catalyzed [5+1] carbocyclization of cyclopropyl-substituted propargyl esters for the synthesis of alkylidene cyclohexenones via cyclopropyl ring opening has been discussed.

The transition metal-mediated [5+1] cyclocarbonylations of vinylcyclopropanes (VCPs) and allenylcyclopropanes (ACPs) with CO have emerged as attractive and effective ways for the construction of cyclohexenones in Figure 1.4 [67]. In early studies, the synthesis of cyclohexenones from VCP has been studied with $Fe(CO)_5$ catalyst by Sarel et al. [80-82] and Aumann [83]. In 1987, the first rhodium-catalyzed [5+1] reaction of cyclopropenyl esters and ketones has been reported by Liebeskind [84]. [5+1] cocyclizations of VCPs with carbon monoxide mediated by octacarbonyldicobalt, $Co_2(CO)_8$, and $[Rh(CO)_2Cl]_2$ have been examined with different substituents on vinyl and cyclopropyl by Meijere in Figure 1.4(a) [85]. Recently, a cheap and safe $Fe_2(CO)_9$ catalyst was used by Yu et al [86]. Yu's group has also reported Rh-catalyzed [5+1] reactions of VCPs and CO for the synthesis of α, β-and β, γ-cyclohexenones [87-88]. Although [5+1] cycloadditions have mainly concentrated on VCPs, there are few examples involving allenylcylopropanes (ACPs).

Functionalized alkylidene cyclohexenones have been obtained from ACP via Iridium [89] and Rhodium [88,90]-catalyzed [5+1] cycloaddition as in Figure 1.4(b). The release of cyclopropane ring strain with π-coordination to allenyl group facilitates the oxidative addition of cyclopropane moiety to the metal. Carbonyl insertion to the formed metallocyclohexene and then reductive elimination provides the product, alkylidene cyclohexenone.

Recently, acyloxy migration have been suggested as a prominent mechanism to obtain allenylcylopropane (ACP) and then cyclohexenone product from cyclopropyl substituted propargyl esters as in Figure 1.4(c) [41,66]. The formation of allene from

propargyl ester via acyloxy migration was first discovered in 1959 by Saucy and Marbet in the presence of a silver catalyst [22].

Although Au-catalyzed rearrangement of propargyl esters have gained much interest due to the accessibility of the starting materials, the mild reaction conditions required for conversion and the very rich chemistry, Rh-catalysts have been proven to be excellent catalysts for cycloaddition and cyclocarbonylation reactions, and they readily coordinate to a wide variety of substrates and ligands.

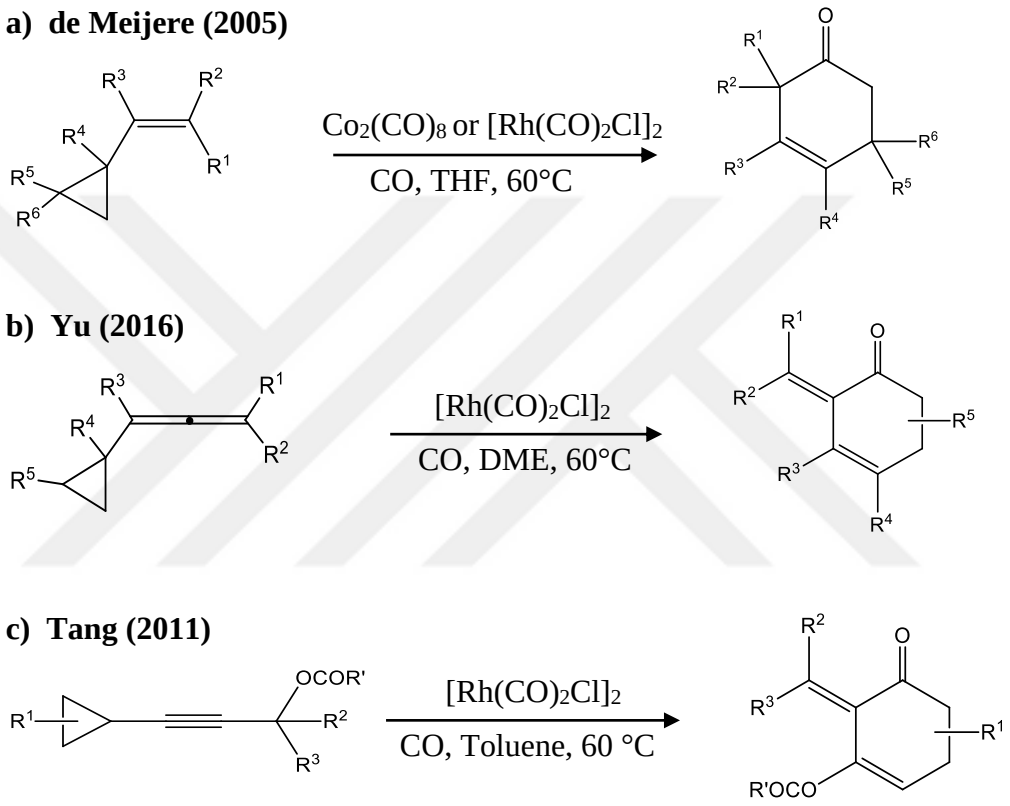

Figure 1.4 : Functionalized cyclohexenones starting with different initial substrates via [5 + 1] cycloaddition.

In the second part of this thesis work, the mechanism of rhodium catalyzed carbonylation of cyclopropyl substituted propargyl esters via a tandem 1,3-acyloxy migration [5+1] cycloaddition has been investigated by using quantum mechanical calculations. For this purpose, the experimental results of Tang et. al. have been considered in Figure 1.4(c) [41,66].

The reaction mechanism has been studied for both trans- and cis-disubstituted cyclopropanes. Trans and cis positions of R^1 and propargyl ester group with respect to each other give rise to the different ratio of regioisomers of alkylidene cyclohexenone

due to the cleavage of different cyclopropane C−C σ-bonds. The studies showed that the regioselectivity for the cleavage of C−C σ-bonds in cyclopropanes depends on the stereochemistry of the cyclopropane ring, the electronic and steric properties of the substituents, and the metal catalysts [41]. In this respect, C-C bond activation was investigated for both trans- and cis-disubstituted cyclopropanes.

According to the experimental studies of Tang et al., the opposite regioselectivity was found for trans-disubtituted cyclopropanes with a phenyl vs an alkyl substitutent on the cyclopropane ring. Furthermore, high regioselectivity was observed for substrates with an alkyl substituent cis to the propargyl ester group than its corresponding trans-substituent [41].

In the second part of the thesis, the reaction mechanism of tandem 1,3-acyloxy migration [5+1] cycloaddition reaction will be modeled and the regioselectivity of trans- and cis-disubstituted of cyclopropanes will be discussed for phenyl and hydroxymethyl substituents in cyclopropane.

2. THEORY

In the present thesis electronic structure methods have been used to model cycloaddition reactions with CO accompanied by acyloxy migration. In this chapter the theory that quantum chemistry is based on will be briefly presented.

2.1 Calculation Methods

The goal of quantum chemical approaches is to find the approximate solution of the time-independent, non-relativistic Schrödinger equation.

$$H\,\Psi = E\,\Psi \tag{2.1}$$

where, H is the Hamiltonian operator, E is the total energy of the system, Ψ is the wavefunction which describes the x, y, and z Cartesian coordinates specific to each particle. By solving equation (2.1) for the wavefunction Ψ, information on structure, properties and energies of the molecular system can be obtained.

The Hamiltonian operator, H, contains all the terms that contribute to the energy of the system: the kinetic energies of the electrons and nuclei, the attractions of the electrons to the nuclei, and the electron-electron and nuclear-nuclear repulsions.

$$H = T_e + T_n + V_{ne} + V_{ee} + V_{nn}$$

$$H = -\sum_i \frac{\hbar^2}{2m_e}\nabla_i^2 - \sum_k \frac{\hbar^2}{2m_k}\nabla_k^2 - \sum_i \sum_k \frac{e^2 Z_k}{r_{ik}} + \sum_{i<j} \frac{e^2}{r_{ij}} + \sum_k \frac{e^2 Z_k Z_l}{r_{kl}} \tag{2.2}$$

The Born-Oppenheimer approximation states that the electronic and nuclear wavefunctions can be solved separately since nuclei are much heavier than electrons and therefore travel much more slowly. It is assumed that electrons can react instantaneously to any motion of the nuclei. This assumption allows computing electronic energies for fixed nuclear positions. The nuclear kinetic energy term is taken

to be independent of the electrons and the nuclear-nuclear potential energy term is a constant for the given geometry.

The electronic Schrödinger equation does not have an analytical solution for systems consisting of more than two sub-atomic particles. In order to solve the electronic Schrödinger equation, some approximations must be used:

- Semi-empirical methods; use parameters derived from the experimental data.
- Ab-initio methods; are wavefunction methods with no experimental parameters.
- Density functional methods; are an alternative to wave-function based methods and the total energy of the system depends on the electron density not the wavefunction [91].

2.1.1 Wavefunction methods

Hartree-Fock (HF) Theory is the simplest wavefunction-based method. The electronic wave function is expressed as a Slater determinant of one-electron orbitals. Each molecular orbital contains a spatial orbital and a spin part. For each spatial orbital, there are two spin orbitals. The one-electron molecular orbitals can be written as a linear combination of atomic orbitals. There are predefined sets of atomic orbitals, or basis sets. The accuracy of basis sets depends on the number of functions used. The larger basis set brings about more accurate results in general, but less efficient and more expensive calculations.

According to variational theorem, the energy obtained from any approximate wavefunction will always be greater than the energy determined from the exact wavefunction. The HF energy will be minimized until the-self consistent solution is obtained. In HF theory, each electron sees all of the others as an average field which is called the mean-field theory. Neglect of electron correlation is the major problem in this approximation. On the other hand, there exists wavefunction methods for computing the correlation energy [91].

2.1.2 Density functional theory

In Density Functional Theory, the electron density, ρ, is computed instead of the wavefunction. It is based on the Hohenberg-Kohn theorems [92-93] which state that the electron density function determines the ground states properties of an atom or molecule. The first Hohenberg-Kohn [92] theorem says that any ground state of a molecule is a function of the ground state electron density function but it does not tell how to find that functional. The second Hohenberg-Kohn [93] theorem says that any trial electron density function will give an energy higher than or equal to the ground state energy. That means, any value of molecular energy calculated from Kohn-Sham equations (obtained by minimizing energy with respect to electron density) will be greater or equal to the true energy. This is true only if the functional used were exact [94].

The overall energy of the system can be divided into three parts: the electronic kinetic energy, E_T, the nuclei-electron attraction E_V, the electron-electron interaction which contains Coulomb repulsion E_J and the exchange-correlation term E_{XC}.

$$E = E_T + E_V + E_J + E_{XC} \tag{2.3}$$

Kohn-Sham introduced the electronic kinetic energy expression, $T_S[\rho]$, which is a determinantal wavefunction of N orbitals, $\emptyset_i$, to describe a system of non-interacting electrons [93].

$$T_S = \sum_{i=1}^{N} < \emptyset_i | -\frac{1}{2}\nabla^2 | \emptyset_i > \tag{2.4}$$

The difference between the kinetic energy in real system (or interacting system), T, and the kinetic energy in noninteracting system, T_S, can be absorbed as a correction term in exchange-correlation term.

The electronic energy for the systems with interacting electrons, $E[\rho]$, can be written as a functional of electron density where $E_{Ne}[\rho]$ is the nuclei-electron interaction, $J[\rho]$ is the electron-electron Coulomb interaction and E_{XC} is the exchange-correlation energy functional.

$$E[\rho] = E_{Ne}[\rho] + T_S[\rho] + J[\rho] + E_{XC}[\rho] \tag{2.5}$$

$$J[\rho] = \frac{1}{2}\iint \frac{\rho(r_1)\rho(r_2)}{|r_2 - r_1|} dr_1 dr_2 \tag{2.6}$$

$$E_{Ne}[\rho] = \sum_A \int \frac{Z_A}{|R_A - r|}\rho(r)dr \tag{2.7}$$

$$E_{XC}[\rho] = (T[\rho] - T_S[\rho]) + (E_{ee}[\rho] - J[\rho]) \tag{2.8}$$

E_{XC} is the sum of error made in using a noninteracting kinetic energy and the non-classical part of the electron-electron interaction. The challenge of DFT is to find an expression for $E_{XC}[\rho]$. The exchange-correlation functional is divided into an exchange, $E_X[\rho]$, and a correlation part, $E_C[\rho]$.

$$E_{XC}[\rho] = E_X[\rho] + E_C[\rho] \tag{2.9}$$

Most functionals have been developed to improve exchange and correlation terms in order to increase the accuracy of DFT methods. While local functionals depends only on electron density, gradient corrected functionals depend on both electron density and its gradient. The performance of DFT methods was further improved by including Hartree-Fock exchange functional, E_X^{HF}. These models are called hybrid functionals which include exact exchange.

The most update and dominating hybrid functional is B3LYP [95,96] which yields very good structural and thermochemical properties.

$$E_{XC}^{B3LYP} = (1-a)E_X^{LDA} + aE_X^{HF} + b\nabla E_X^{B88} + (1-c)E_C^{VWN} + cE_c^{LYP} \tag{2.10}$$

where a, b and c were optimized to 0.2, 0.72 and 0.81, respectively. The same values were in B3PW91 functional but B3LYP was improved by using LYP instead of PW91. LYP is constructed to improve the full correlation energy, not a correction to LDA. The local exchange function is referred as Slater exchange, E_X^{LDA}[97]. Vosko, Wilk and Nusair developed an interpolation formula to get an approximate correction term, E_C^{VWN}[98]. Becke added a correction term ∇E_X^{B88} to the Slater exchange which includes gradient correction of energy density [99,100]. Lee, Young and Parr introduced local and gradient correction in the functional, E_c^{LYP} [101].

B3LYP do not include long-range electron correlation, such as London dispersion interactions between unbound chemical species. On the other hand, wB97XD [102] which is a new class of DFT functional known as range-separated functional, which is

capable of capturing both short-range and long-range interactions. Also, Minnesota functionals including many parameters fitted to many sets of properties have been developed by Truhlar. M06-L (Minnesota 06 Local functional), a meta-GGA functional, which does not include HF exchange (thus, it cannot be considered as hybrid functional) is proposed to be fast, good for transition metals, inorganic and organometalics [103].

2.1.3 Basis sets

A basis set is the set of mathematical functions to describe molecular orbitals. The basis functions are divided into two functional forms, Slater Type Orbitals (STO) and Gaussian Type Orbitals (GTO). The functional form of STO is,

$$\emptyset(x, y, z; \alpha, i, j, k) = Nx^i y^j z^k e^{-\alpha(i+j+k)} \tag{2.11}$$

N is the normalization constant, i, j and k are nonnegative integers that dictate the nature of orbital in Cartesian sense and α is an exponent controlling the width of the STO or GTO. Gaussian type orbitals can be written as,

$$\emptyset(x, y, z; \alpha, i, j, k) = Nx^i y^j z^k e^{-\alpha(i^2+j^2+k^2)} \tag{2.12}$$

With the split valence basis set developed by Pople, the more flexibility is gained in the valence basis functions. In such basis sets, valence orbitals are split into arbitrarily many functions while core orbitals still continue to be represented by a single (contracted) basis function. Pople-type basis sets include 3-21G, 6-21G, 4-31G, 6-31G and 6-311G. The first number symbolizes the number of primitives used for core orbitals and the numbers after the hyphen indicate the number of primitives used for the valence orbitals [91].

2.1.4 Effective core potential

The large number of basis functions have been required to desribe very heavy elements which have large number of electrons. The extra electrons are mostly core electrons and the function modelling the core electrons is called Effective Core Potential (ECP) or Pseudopotential (PP). ECP will replace the core electrons with an effective potential. The neglect of an explicit treatment of the core electrons reduce the scope of electronic structure problem for heavy elements and the computational cost. Also, ECPs can be parametrized to take account of the relativity. The use of ECPs provides a large gain for the elements in the lower part of the periodic table where relativistic effects are important. Gaussian functions are used to describe the core potential as well as the valence orbitals. ECP is determined by the number of electrons to include in the core potential. Large-core ECP includes everyting but the outermost (valence) shell while small-core ECP scales back to the next lower shell. With the latter one, better results can be obtained though leading to an increase in the computational cost. Los Alamos National Laboratory (or LANL) ECPs are one of the most popular pseudopotentials in use. [91,104].

2.1.5 Intrinsic reaction coordinate

The minimum energy path (MEP) which is also called intrinsic reaction coordinate (IRC) [105-106] is defined as the steepest descent in the mass-weighted Cartesian coordinate [107]. IRC calculations are used to check that the given transition state is the expected transition state for the reaction of the interest.

The IRC path is defined by the differential equation:

$$\frac{dx(s)}{ds} = -\frac{g}{|g|} = t \tag{2.13}$$

Here x is the mass-weighted coordinates, s is the path length amd t is the tangent to reaction path, defined by the normalized gradient. Solving equation (2.13) starting from a TS geometry slightly displaced along the normal coordinate for the imaginary frequency.

The Euler method is the simplest method for integrating equation (2.13). The reaction coordinate is calculated in a number of steps that are taken along the tangent direction at the current geometry x_n:

$$x_{n+1} = x_n + \Delta s t(x_n) \quad (2.14)$$

This is a simply steepest-descent method with a fixed step size Δs. The points chosen by the steepest-descent algorithms tend to oscillate around the reaction coordinate unless very small steps are taken [104].

2.1.6 Solvation model

There are two methodologies for introducing the effects of solvation: explicit solvation and implicit (or continuum) solvation. In explicit solvation, solvent molecules place around the solute molecule. In continuum solvation, the solvent is considered as a continuum medium with a given dielectric constant.

The solvation energy is decomposed into four terms, electrostatic energy, dispersion energy, cavity creation energy and repulsion energy [104].

$$\Delta G_{solvation} = \Delta G_{elec} + \Delta G_{disp} + \Delta G_{cav} + \Delta G_{rep} \quad (2.15)$$

Relevant to solute-solvent interactions, the charge distribution of the solute molecule polarizes the solvent cavity wall, which in turn changes the charge distribution and so on. Due to the polarization of the cavity wall, these methods are called polarized continuum models (PCM). Also, the final iteration must be calculated by iterative procedure, leading to a self-consistent reaction field (SCRF) calculation. SCRF calculations have been implemented in ab initio, semiempirical and DFT calculations [94].

Among the variations on the PCM model, an integral equation formalism for solving the SCRF equations which facilitates computation of gradients and molecular response properties is developed by Tomasi et al [91,108]. The integral equation formalism polarized continuum model (IEFPCM) creates the solute cavity via a set of overlapping spheres.

3. THE MECHANISM OF Rh-CATALYZED COMPETITIVE 1,2- VERSUS 1,3-ACYLOXY MIGRATION FOLLOWED BY [5+1] AND [4+1] CYCLOADDITIONS OF 1,4-ENYNES WITH CO

In this part of the study, the mechanism for the formation of bicyclic [5+1] and [4+1] type cycloaddition products via competing 1,2- and 1,3-acyloxy migrations of ACEs in the presence of $[RhCl(CO)_2]_2$ catalyst for both internal and terminal alkynes have been investigated by using quantum mechanical calculations (Figure 3.1). For this purpose, the experimental results of Malacria et al. has been considered [39]. The mechanistic studies in the literature have mainly concentrated on 1,2-acyloxy migration. To our knowledge, there is no report on Rh-catalyzed 1,3-acyloxy migration of ACE with internal alkynes.

The whole mechanism has been considered at the molecular level so that the experimentally observed product distribution could be explained. The design or discovery of new reactions can be stimulated through the acyloxy migration and the subsequent reactions; oxidative addition, migratory insertion, and reductive elimination. In this respect, understanding the mechanistic details will enable synthesizing custom made products with the desired substituents.

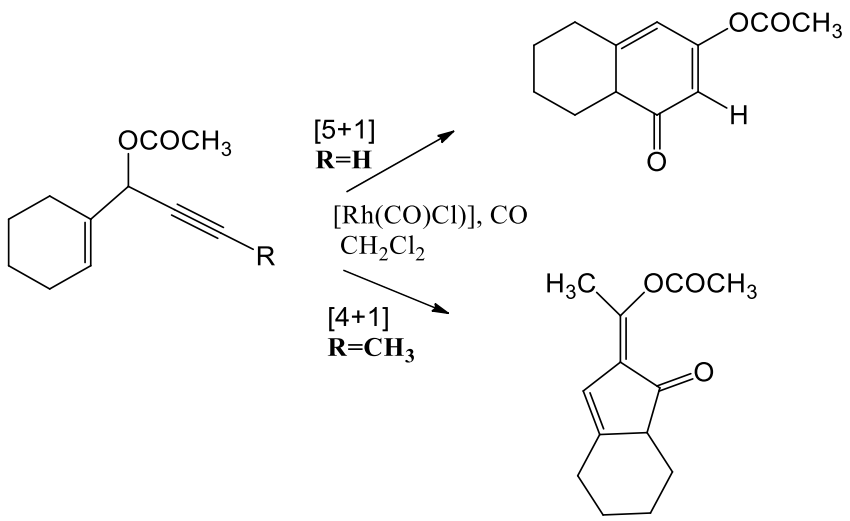

Figure 3.1 : The mechanism of bicyclic [5+1] and [4+1] type cycloaddition products via competing 1,2- and 1,3-acyloxy migrations of ACEs with terminal (R=H) and internal ($R=CH_3$).

3.1 Computational method

Quantum mechanical calculations were performed with Density Fuctional Theory (DFT). Geometry optimizations and frequency analyses were performed in gas phase using the B3LYP functional. B3LYP is one of the most widely utilized functionals which has been reported to be successful for many transition metal systems as well [60,109]. For Rh, LANL2DZ effective core basis and for the other atoms 6-31+G(d) basis set have been used [110-112]. Rhodium metal has an electron configuration of $[Kr]4d^8 5s^1$. Square planar Rh(I) complex is used in its singlet state. Single-point solvation energies were calculated in dichloromethane (DCM) solvent (ε=8.93) with the Polarizable Continuum Model (PCM) [108] on gas-phase optimized geometries using the B3LYP [95,96,101] and M06-L [103] functionals with the 6-31+G(d) basis set. Truhlar's functional M06-L has been developed especially for transition metal containing systems [103]. All calculations were carried out with Gaussian 09 [113]. Frequency calculations have been performed to verify all stationary points and transition states. To every stationary point, conformational search was performed manually to find the lowest energy conformer by considering a number of isomers and rotamers. Intrinsic reaction coordinate (IRC) calculations are performed on the transition states in order to confirm the expected reactant and product on both sides [114,115]. The energies discussed in the manuscript are Gibbs Free energies from gas

phase calculations unless otherwise stated. In order to have the same number of atoms in free energy comparisons (Figure 3.3 and Figure 3.8), all the structures' energies on the paths are compared relative to the sum of ACE-RhCl(CO)-π complex (1t or 1i), an ACE (will be used to regenerate the starting Rh-ACE complex) and a CO group that is later inserted in the mechanism. Throughout the manuscript, the suffixes t and i refer to terminal and internal alkynes, respectively.

3.2 Results and Discussion

3.2.1 Tandem 1,2- and 1,3-acyloxy migration and cyclization pathways of ACE with terminal alkynes

The reaction initiates with the two isomers of ACE-RhCl(CO)-π complex in which the CO and Cl ligands switch positions as shown in Figure 3.2. The isomer where CO is trans to the alkyne moiety (1t) is energetically more favorable than 21t by 2.9 kcal/mol. In these two structures, the strentghs of the π-bonds are different. In 1t, the Rh center coordinates to both alkyne and alkene fragments strongly whereas, in 21t, Rh favors to position itself away from the alkene fragment while bonding more strongly with the alkyne, as seen in the bond distances in Figure 3.2.

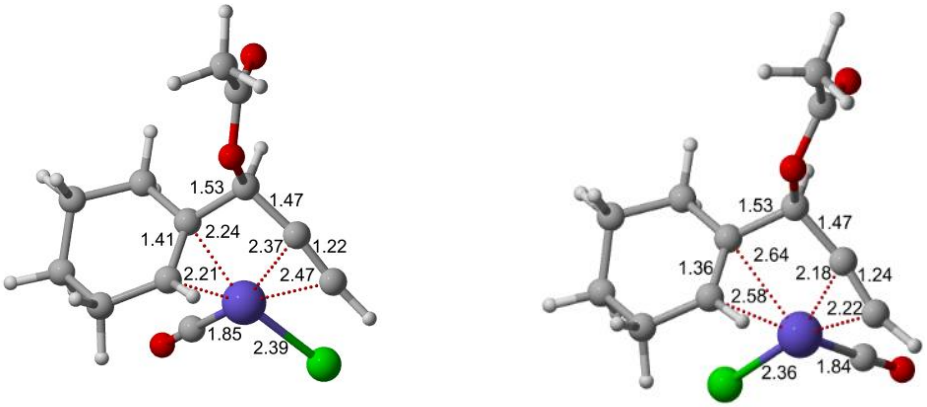

1t (0.0 kcal/mol) **21t** (2.9 kcal/mol)

Figure 3.2 : 3D representation of ACE-RhCl(CO) π-complexes.

The computed Gibbs free energy profiles of several possible reaction pathways of $[RhCl(CO)_2]_2$ catalyzed [5+1] cycloaddition with concomitant 1,2-acyloxy migration in ACE with terminal alkyne are shown in Figure 3.3.

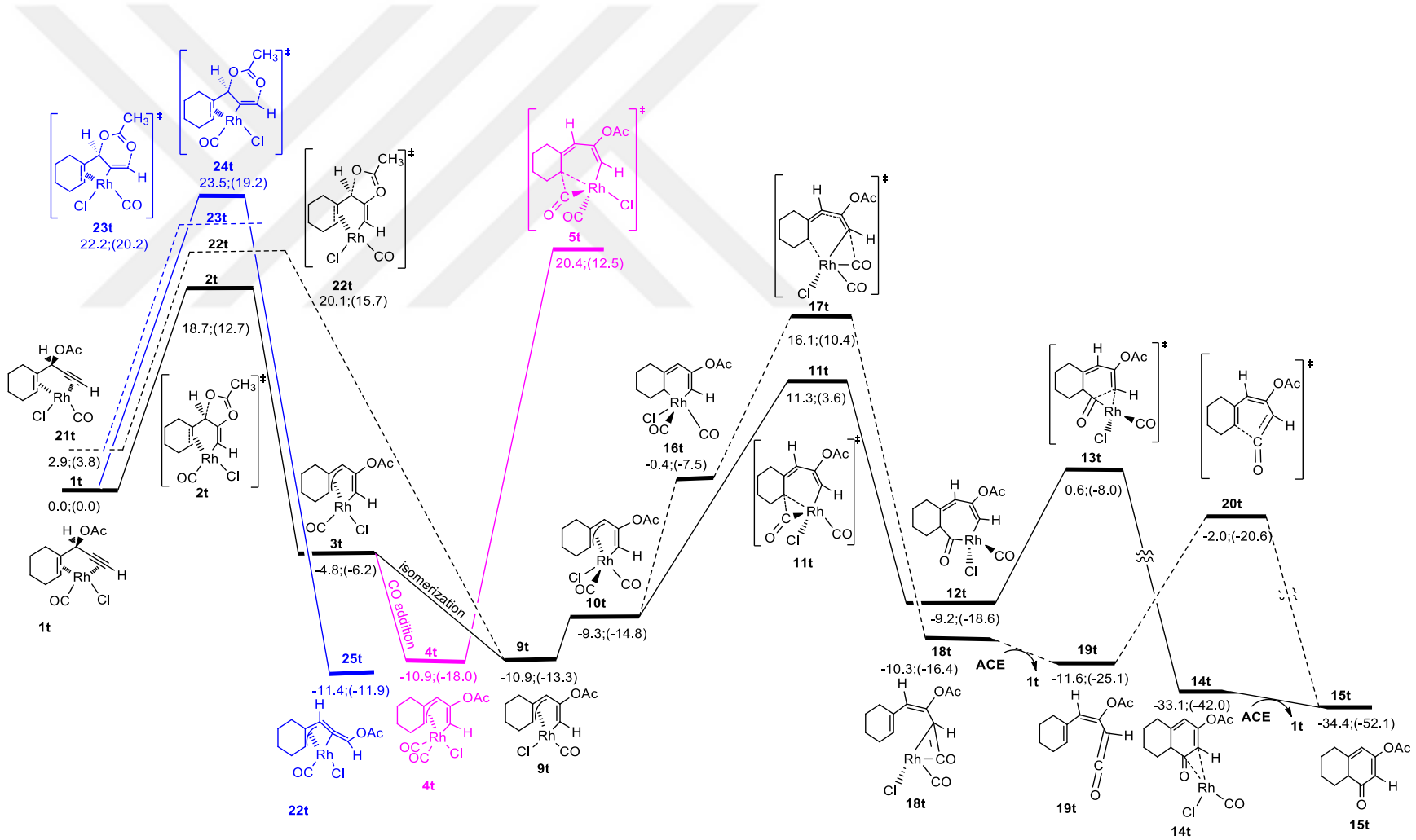

Figure 3.3 : The Gibbs free energy profile of the $[Rh(CO)_2Cl]_2$-catalyzed [5+1] cycloaddition reaction of ACE with terminal alkynes by CO in gas phase. The energy values in parentheses are single point energies in dichloromethane. Energies are in kcal/mol. Energies are not to scale. The solid black line shows the more favorable pathway.

ACE with terminal alkynes favor to undergo a 1,2-acyloxy migration triggering subsequent [5+1] cycloaddition by carbonylation in the presence of π-acidic transition metal catalysts [20,21,24-26,39]. Although 1t is more stable than 21t, the reaction mechanisms were modeled with both isomers of the Rh-complex to check for the migration barriers. 1,2-acyloxy migration requires an activation barrier of 18.7 kcal/mol (2t) when initiated from 1t in which the CO is trans to the alkyne moiety while from the isomer 21t, migration takes place at a higher relative energy of 20.1 kcal/mol (22t) (Figure 3.4).

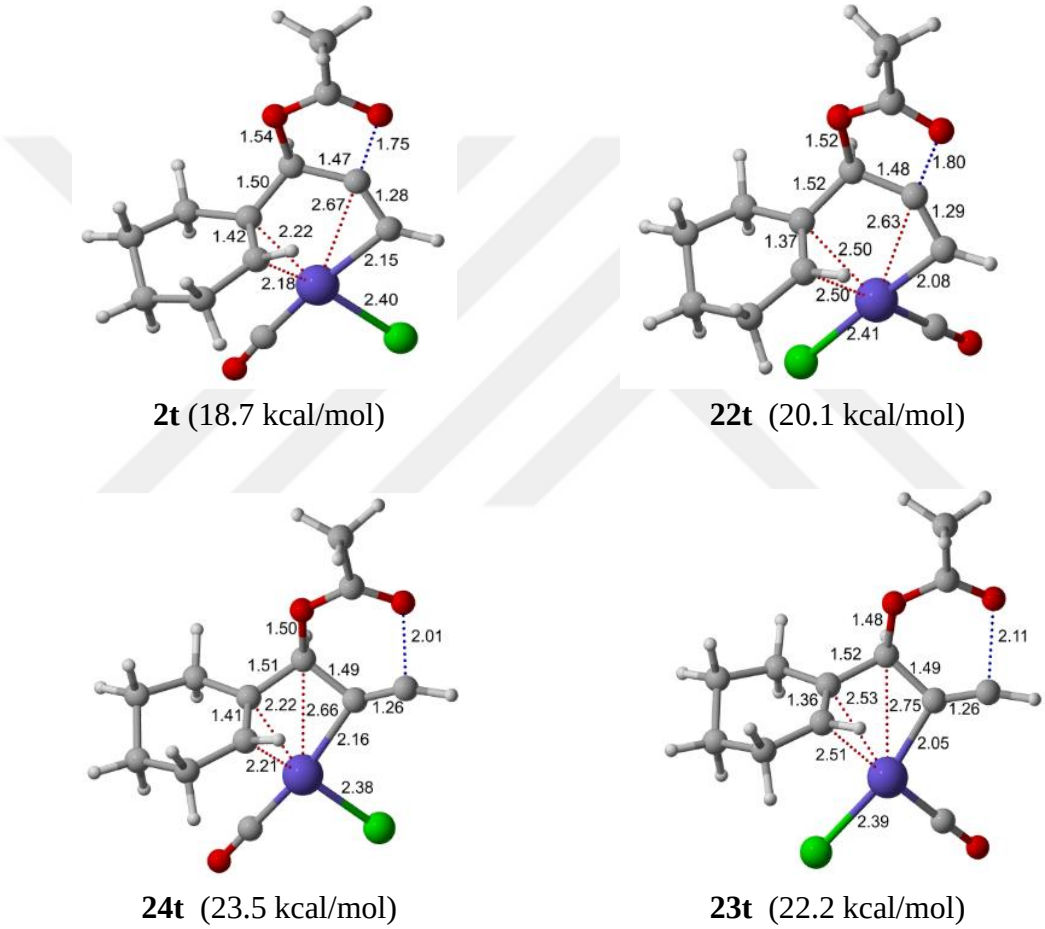

2t (18.7 kcal/mol) **22t** (20.1 kcal/mol)

24t (23.5 kcal/mol) **23t** (22.2 kcal/mol)

Figure 3.4 : 3D geometries and the relative Gibbs free energies of possible transition states for 1,2- and 1,3-acyloxy migration of ACE with terminal alkyne.

The CO ligand addition in 9t leads to the intermediate (10t) at a relative energy of -9.3 kcal/mol. The CO insertion to 10t from the cyclohexane side (11t) requires an activation energy of 20.6 kcal/mol. After the formation of seven-membered metallacycle (12t), Rh should be expelled from the ring system. The reductive elimination step via 13t has an activation energy of 9.7 kcal/mol which leads to 14t in

a highly exergonic way (-33.1 kcal/mol). Cyclohexadienone product (15t) is obtained when the catalyst leaves the system by coordinating with another ACE molecule and the starting Rh-ACE complex is regenerated.

Alternatively, CO can be the catalytically inserted to 10t from the other side of the rhodium atom (17t) as compared to 11t and ketene formation (19t) takes place (dashed lines following 10t in Figure 3.3). For ketene formation, Rh should be expelled essentially before the product formation by complexing to another ACE (18t to 19t). Afterwards, 6π electrocyclization of the ketene intermediate can take place (20t) and the cyclohexadienone product (15t) can be obtained exergonically.

Considering the possible paths, the transition states and intermediates on the reaction path of the CO insertion to 4t and the following reductive elimination (5t→6t→7t→8t, Figure 3.5) are all higher in energy than the transition states and the intermediates following isomerization. Thus, this path is unfavorable.

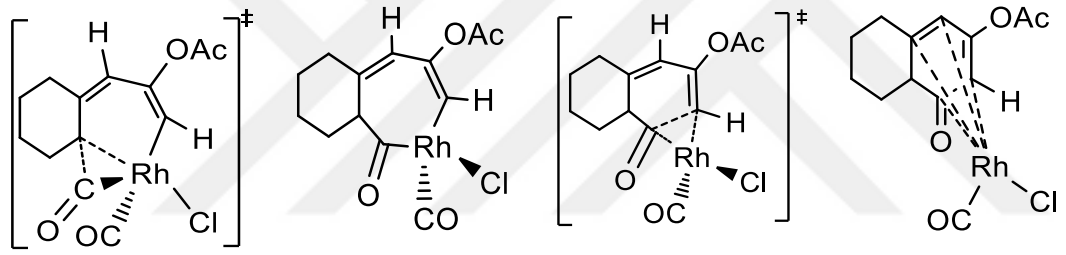

5t	**6t**	**7t**	**8t**
20.4; (7.4)	1.8; (-16.3)	9.1; (-8.3)	-29.7; (-48.7)

Figure 3.5 : The structures and the relative energies of the transition states and the intermediates following carbonyl insertion (5t). The energy values in parentheses are single point energies in dichloromethane. Energies are in kcal/mol.

Once isomerization takes place (from 3t to 9t), 17t and 11t are transition state structures for CO insertion. The 4.8 kcal/mol of energy difference between them renders the catalytic CO addition and the reductive elimination from the rhodacycloheptadienone (12t) which is a more favorable pathway (the black solid line) in this study. On the other hand, in their mechanistic study on a similar Rh catalyzed cycloaddition reaction, Tang et.al. have tried CO insertion from the alkyne side and suggested that the pathway through ketene formation (the dashed line) is the preferred mechanism [116]. In this study, we have considered CO insertion from both sides and ketene formation can take place only from 17t since it is not allowed from 11t.

In the experimental study of Malacria et al., 3-pivaloxy-1,4-enyne was used as substrate [20,39]. In this study, the pivaloxy group was replaced by the acyloxy group to reduce the computational cost since the tandem cyclization process was also successful when the ester was changed from pivaloate to acetate [20,39,66]. To test the model employed in this study, 1,2 vs 1,3-acyloxy migration barriers (2t *vs* 24t) in 3-pivaloxy 1,4-enyne ester with terminal alkyne are compared. The 1,2-shift is 5.4 kcal/mol more favorable than 1,3-shift with pivaloxy substitution. This has implied that the model considered herein is adequate for our comparative purpose.

In addition, the single point solvent calculations on gas phase optimized geometries were performed with B3LYP in the solvent (CH_2Cl_2, ε=8.93) used in the experiment. The solvent energies, as shown in parenthesis in schemes, have not made any differences in the preferred paths. To test the barriers, M06-L functional which has been reported to calculate the reaction kinetic parameters successfully was utilized. As with B3LYP, the calculations have shown a similar trend (Figure 3.6).

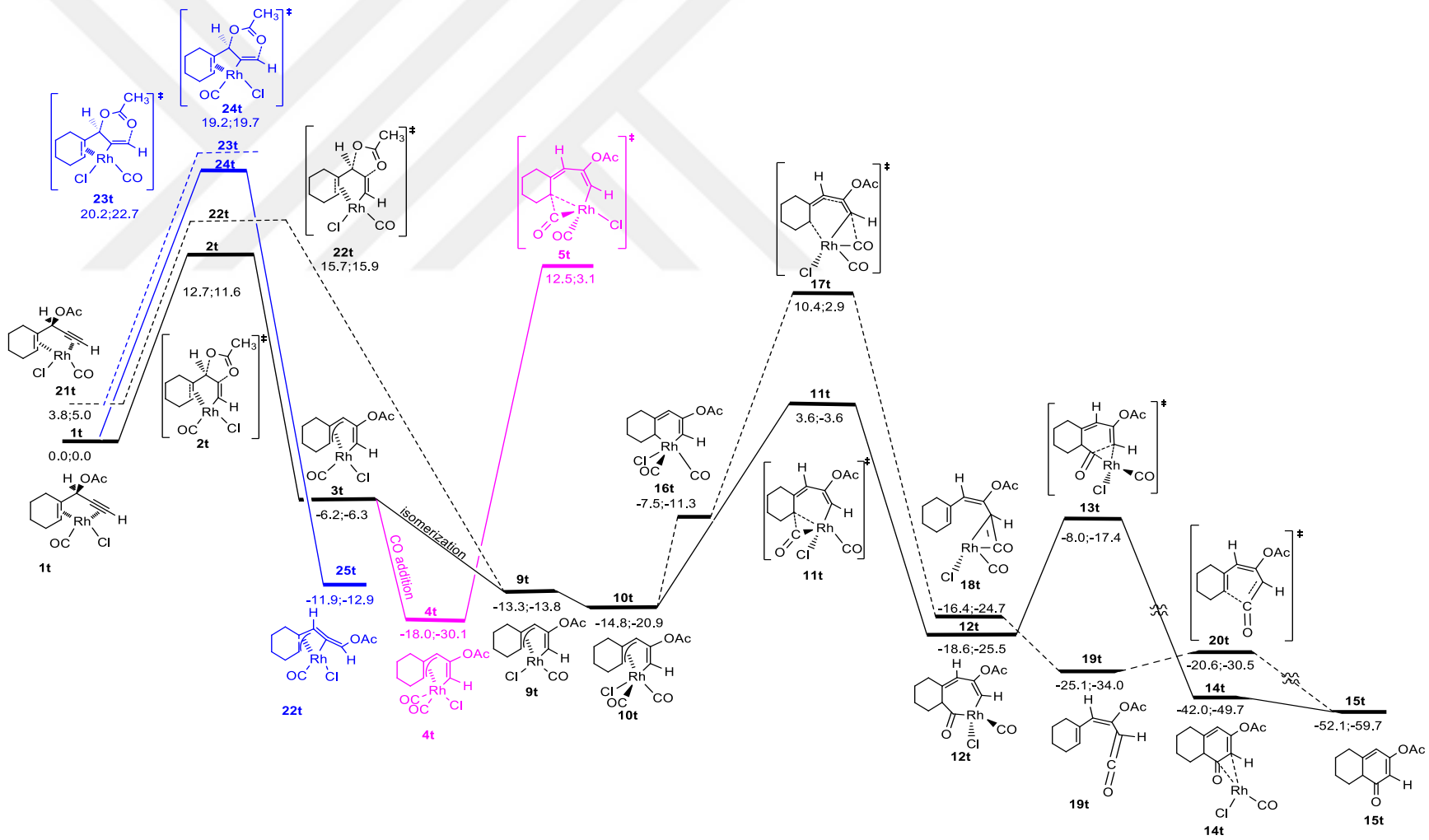

Figure 3.6 : Energy profile for terminal alkynes. Energies are single point energies (B3LYP; M06-L) in kcal/mol. ZPE corrections are included from the gas phase calculations. Energies are not to scale.

3.2.2 Tandem 1,2- and 1,3-acyloxy migration and cyclization pathways of ACE with internal alkynes

Internal alkynes of propargyl esters favor to undergo 1,3-acyloxy migration promoting [4+1] cycloaddition with CO in the presence of π-acidic transition metal catalysts, contrary to terminal alkynes [17,20,29,39-41]. The transition states for 1,2 vs 1,3-acyloxy migration reactions are modelled starting with the two isomers of methyl substituted ACE (Figure 3.8, 1i and 21i) [20,39].

The reactant complex 1i is 4.7 kcal/mol more stable than 21i, thus, the reaction path will be initially followed via 1i in which the CO is trans to the alkyne moiety. 1,3-acyloxy migration requires an activation barrier of 22.2 kcal/mol (24i) while the competing 1,2-acyloxy migration requires a slightly higher activation barrier (2i, 23.2 kcal/mol) (Figure 3.7). The preference of 1,3- is not strong as compared to 1,2-acyloxy migration, therefore both mechanisms were modeled and will be discussed in Figure 3.8 and Figure 3.11.

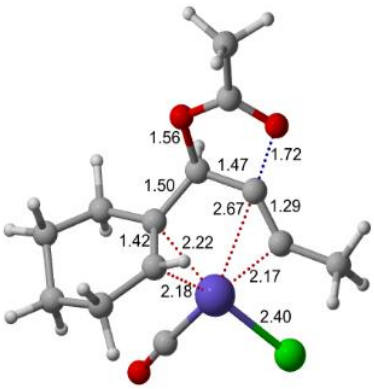

2i (23.2 kcal/mol)

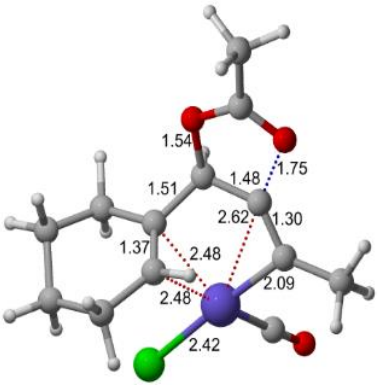

22i (25.2 kcal/mol)

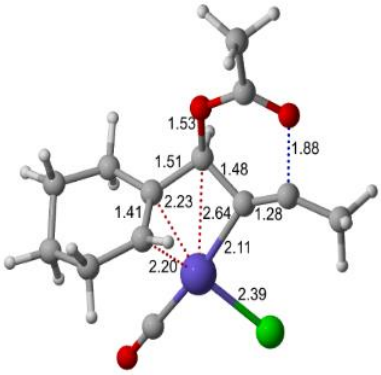

24i (22.2 kcal/mol)

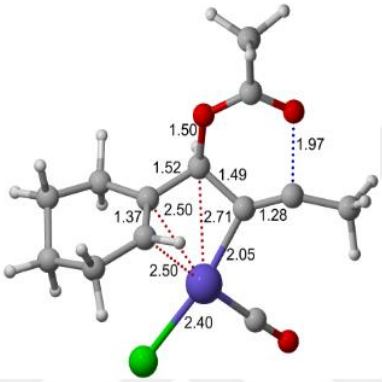

23i (22.6 kcal/mol)

Figure 3.7 : 3D geometries and the relative Gibbs free energies of possible transition states for 1,2- and 1,3-acyloxy migration of ACE with internal alkyne.

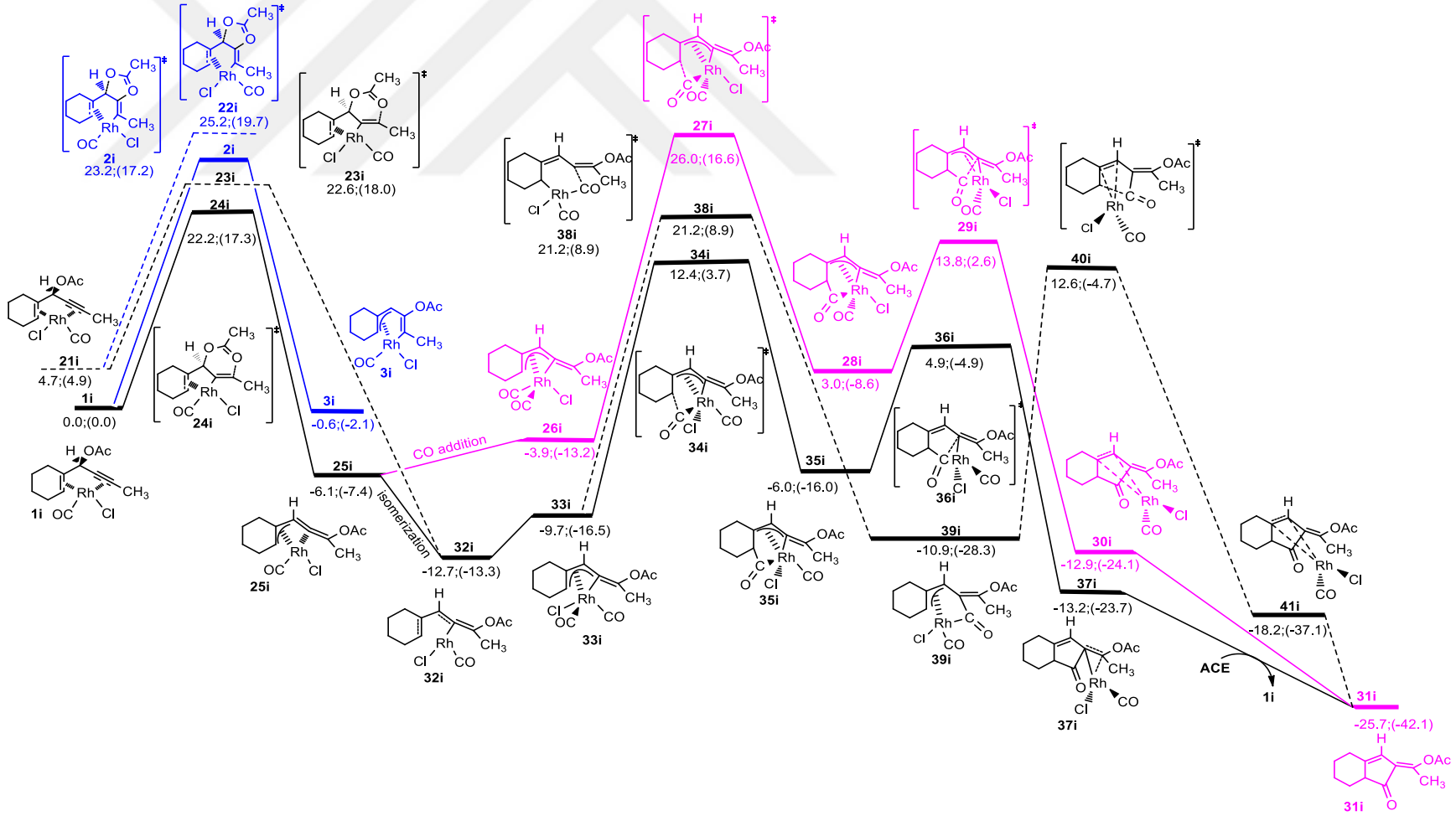

Figure 3.8 : The Gibbs free energy profile of the $[Rh(CO)_2Cl]_2$-catalyzed [4+1] cycloaddition reaction of ACE with internal alkynes by CO in gas phase. The energy values in parentheses are single point energies in dichloromethane. Energies are in kcal/mol. Energies are not to scale. The solid black line shows the more favorable pathway.

3.2.2.1 1,3-acyloxy migration for internal alkynes

In 1,3-migration, the allenyl-Rh complex 25i forms exergonically at a relative energy of -6.1 kcal/mol (Figure 3.8 and Figure 3.9). This allene structure was proposed as an intermediate in many experimental studies involving π-acidic transition metals [17,20,29,39-41].

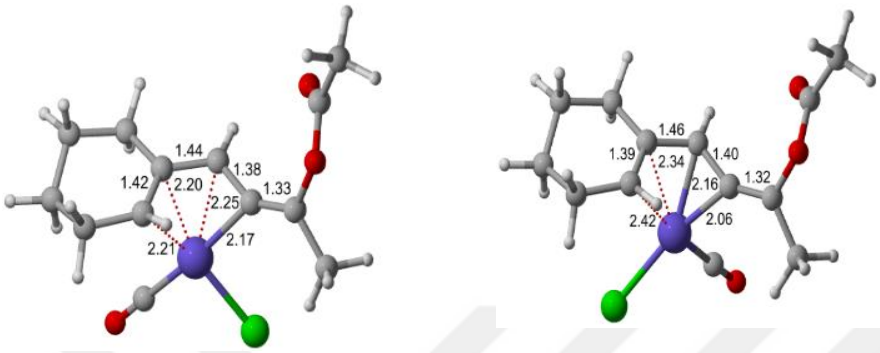

25i (-6.1 kcal/mol) **32i** (-12.8 kcal/mol)

Figure 3.9 : 3D figures of two isomers, 32i is the isomer of 25i.

As in 1,2-migration mechanism, the reaction can advance via the CO coordination or via isomerization followed by the CO coordination as it is discussed in the Part 3.2.1. If isomerization takes place, a 6.7 kcal/mol more stable isomer, 32i forms. Although the starting reactant complex 21i is high in energy with respect to 1i, if migration through transition state 23i takes place, it will lead to the same product (32i). If, on the other hand, the CO coordination to Rh in 25i takes place, 26i forms at a relatively higher energy (-3.9 kcal/mol). Additionally, the CO insertion to 26i via transition state 27i has a high activation energy barrier of 29.9 kcal/mol which renders it an unfavorable reaction as compared to the CO insertion to the isomerization product 33i via TS-34i ($\Delta G^{\ddagger}$= 22.1 kcal/mol). Therefore, following 1,3-acyloxy migration, isomerization of 25i is expected to occur in preference to the CO coordination to it, as in part I. Additionally, transition states and the intermediates following the CO coordination are also at relatively higher energies, rending the path (27i→28i→29i→30i) unfavorable.

In the more favorable pathway, rhodacyclopentadienone 35i which is formed through a TS-34i was proposed by Malacria et al. [20,39]. 37i is obtained by the reductive elimination through transition state 36i at an energy expense of 10.9 kcal/mol. The

desired cyclopentenone product 31i is obtained when another ACE molecule coordinates to complete the catalytic cycle. Alternatively, CO can be catalytically inserted to 33i from the other side of the rhodium atom (transition state 38i) as compared to 34i at a relatively higher energy of 30.9 kcal/mol (dashed lines following 33i in Figure 3.8). Rh catalyst can be expelled from the cyclic structure (39i) via TS-40i with an activation energy of 23.5 kcal/mol. Although 41i is more stable compared to 30i and 37i, the path through 38i is not energetically favorable for Rh-catalyzed carbonylation mechanism.

3.2.2.2 1,2-acyloxy migration for internal alkynes:

The 1,2-acyloxy migration from 1i will lead to intermediate 3i through a transition state (2i), at a barrier of 23.2 kcal/mol, which is very close to that of 1,3 (22.2 kcal/mol, Figure 3.8). The relative energies of 1i and 3i indicate a probable equilibrium between them (Figure 3.10). Thus, 1,2-migration is a less facile path in terms of the exergonicity of the reaction (-0.6 vs -6.1 kcal/mol for 3i and 25i, respectively).

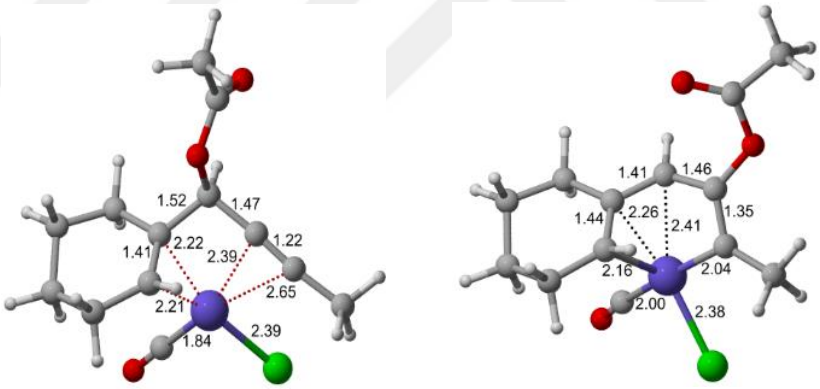

1i (0.0 kcal/mol) **3i** (-0.6 kcal/mol)

Figure 3.10 : 3D figures of the reactant complex (1i) and the product after 1,2-migration (3i).

Considering the small barrier differences between 1,2- and 1,3-migrations, the proceeding steps of 1,2-migration have also been modelled (Figure 3.11). As it is discussed, 3i can either undergo CO coordination (4i) or isomerization (9i). Although CO ligation to Rh in 3i is facile, following the CO insertion requires a high barrier (5i, $\Delta G^{\ddagger}$=30.4 kcal/mol), making it an improbable reaction path. Isomerization from 3i (9i) and further CO coordination to Rh (10i) decreases the relative energy of the

rhodacycle. Carbonyl insertion to this rhodacycle takes place via a smaller barrier (11i, 22.2 kcal/mol) as compared to the competing insertion TS-5i.

Although 1,3-migration is only slightly favored by barrier in the internal case, all the following intermediates via isomerization and the CO addition and the transition states are at relatively lower energies than their corresponding analogous in 1,2-migration throughout the path. Thus, the higher exergonicity of the 1,3-migration step and the relative energies of the intermediates on the preferred path render 1,3-shift a more facile process as compared to 1,2-shift. The results from our calculations are consistent with the experimental results where 1,3-acyloxy migration took place in ACE with internal alkynes [17,20,29,39-41].

Acyloxy migration transition states have been also modeled in dichloromethane to check the barrier heights for terminal and internal alkynes. For terminal alkynes, 1,2-acyloxy migration transition states (2t vs 22t) following through lower (1t) and higher (21t) energy isomers are 5.7 kcal/mol and 4.0 kcal/mol more stable than 1,3-acyloxy migration transition states (24t vs 23t). On the other hand, for internal alkynes, 1,3-acyloxy migration transition states (24i vs 23i) following through lower (1i) and higher (21i) energy isomers are 0.3 kcal/mol and 2.4 kcal/mol more stable than 1,2-acyloxy migration transition states (2i vs 22i). 1,3-acyloxy migration in internal alkynes is only slightly favored in solvent phase optimization as observed in gas phase calculations.

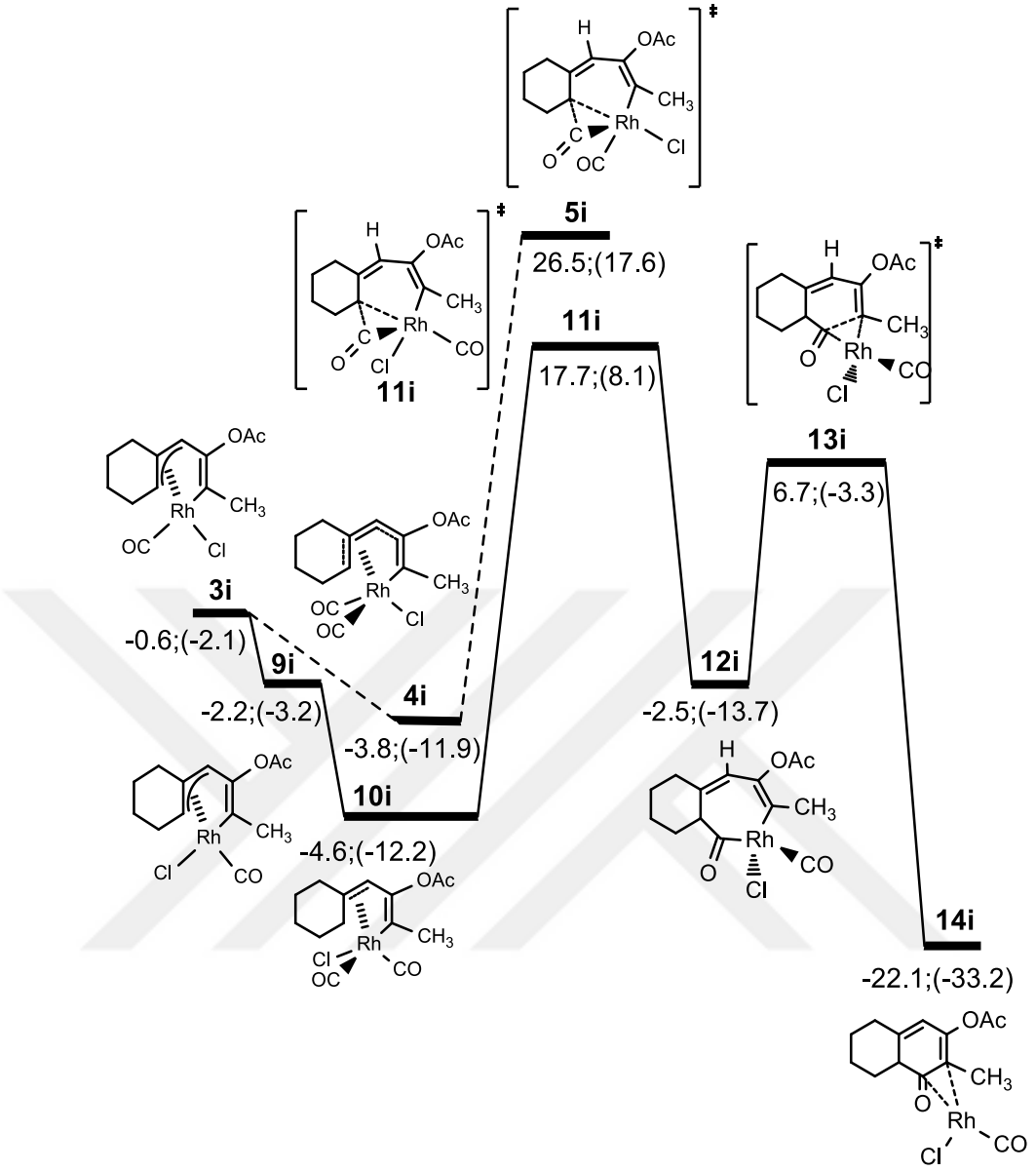

Figure 3.11 : The Gibbs free energy profile for 1,2-acyloxy migration reactions of ACE with internal alkynes in gas phase. The energy values in parentheses are single point energies in dichloromethane. Energies are in kcal/mol.

The competitive 1,2- vs 1,3-acyloxy migrations in internal alkynes have been modeled with different R groups to investigate the selectivity because 1,2 and 1,3 acyloxy migration transition states have close free energy values for methyl substituted ACE. Changing the substituent on alkyne of ACE to phenyl, p-methoxyphenyl or vinyl has not shown predominant 1,3-migration in terms of energy barriers as in the methyl case that is considered in detail (Figure 3.12, Table 3.1). The allene intermediates from the corresponding 1,3-migration transition states are more stable (7.6 to 2.2 kcal/mol) than the initial ACE-Rh catalyst complexes. Thus, the selectivity can be governed by the stability of the corresponding allene structures.

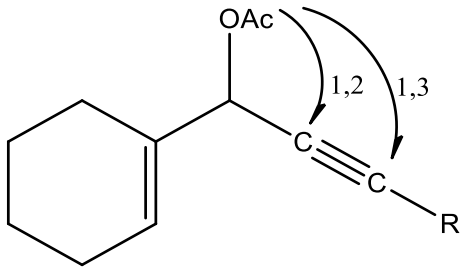

Figure 3.12 : 1,2- and 1,3-acyloxy migration of 3-acyloxy-1,4-enyne (ACE).

Table 3.1 : Gibbs free energies (in kcal/mol) for 1,2- and 1,3-migration transition states and their corresponding products relative to their R-substituted ACE-Rh complexes as calculated by B3LYP in gas phase.

R	**1,2-migration $\Delta G^{\ddagger}$**	**1,3-migration $\Delta G^{\ddagger}$**	**1,2-migration product**	**1,3-migration product**
H	18.7	23.5	-4.8	-11.4
CH_3	23.2	22.2	-0.6	-6.1
$CH{=}CH_2$	23.0	21.8	-1.4	-7.6
Ph	22.5	22.3	-0.6	-3.5
p-$OMeC_6H_4$	23.9	23.3	0.5	-2.2

As discussed in Part 3.2.1 and Part 3.2.2, the 1,3- vs 1,2-selectivity of the reaction is determined at the first step where acyloxy migration takes place. Besides the barriers and the energies of the forming complexes, the calculated charges also indicate the experimental preference for the migration of acyloxy group. The charges of the olefinic carbons, C4 and C5 are compared for both reactant complexes 1t and 1i. It is observed that among the two carbons, the more positively charged one is the experimentally preferred site of attack of the negatively charged carbonyl oxygen in the acyloxy group; such that C4 and C5 are the more positive carbons in 1t and 1i, respectively (Figure 3.13). This kind of observation has also been reported in detail in the case of Au catalyzed propargylic ester rearrangement in the literature [117].

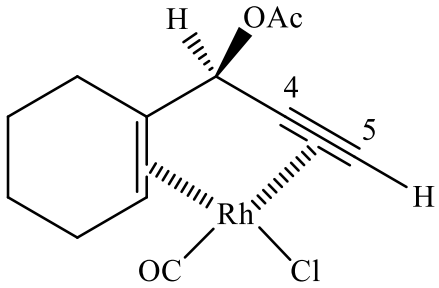

1t

Mulliken Charges C4&C5 : 0.11; -0.18

APT Charges C4&C5 : -0.05; -0.12

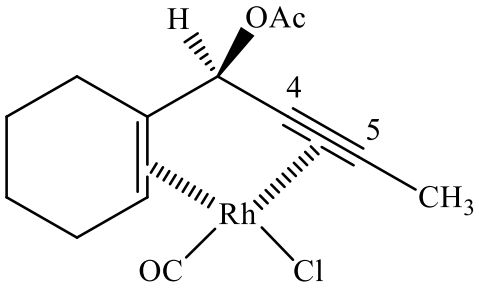

1i

Mulliken Charges C4&C5 : 0.25; 0.65

APT Charges C4&C5 : -0.28; 0.15

Figure 3.13 : Mulliken and APT charges of the olefinic carbons, C4&C5.

The single point solvent calculations on gas phase optimized geometries were performed with B3LYP and M06-L in the solvent (CH_2Cl_2, ε=8.93) used in the experiment. The solvent energies have not made any differences in the preferred paths. In addition, M06-L have shown a similar energy trend with B3LYP (Figure 3.14).

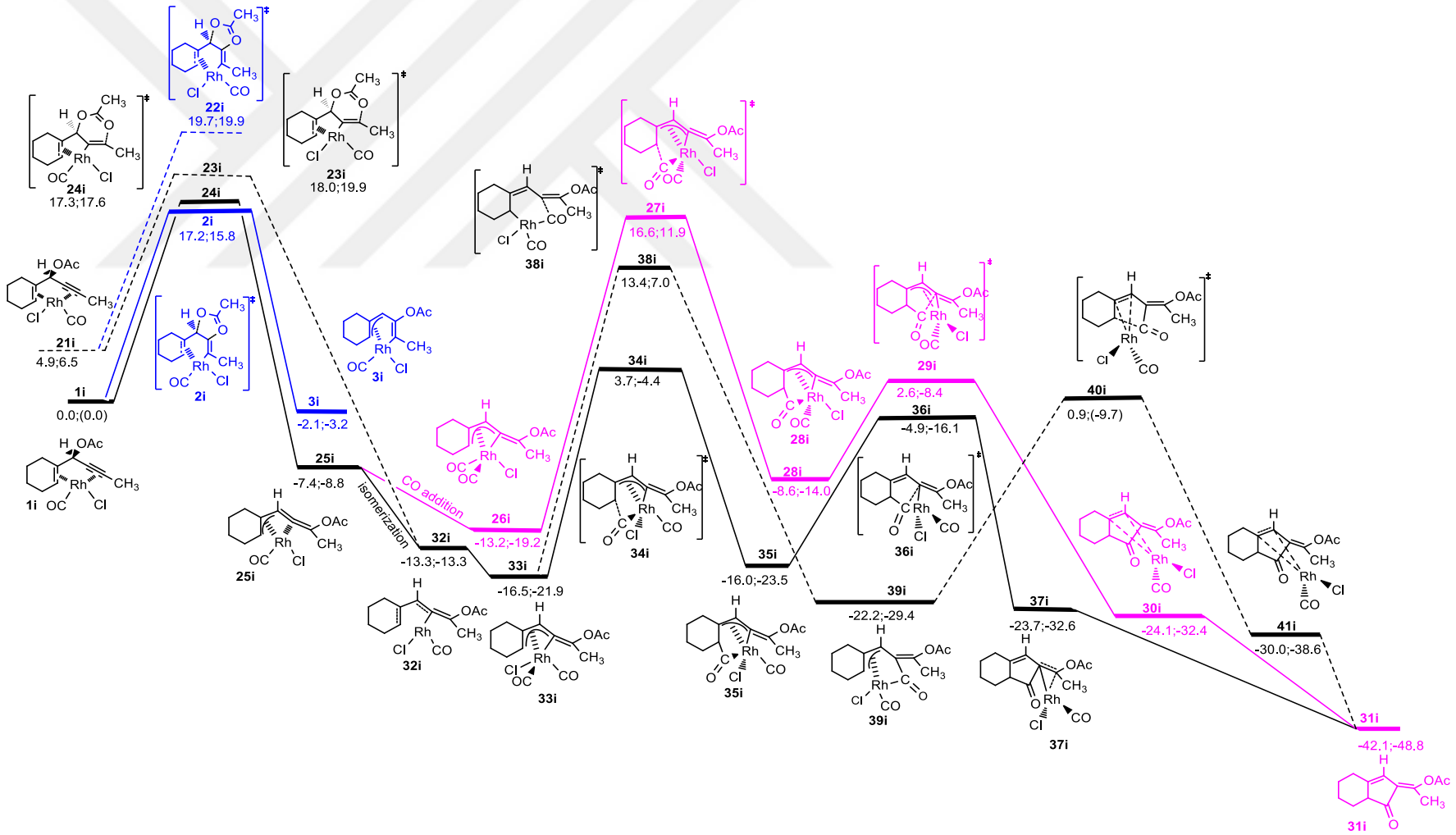

Figure 3.14 : Energy profile for internal alkynes. Energies are single point energies (B3LYP; M06-L) in kcal/mol. ZPE corrections are included from the gas phase calculations. Energies are not to scale.

4. THE MECHANISM OF Rh-CATALYZED [5+1] CYCLOADDITION OF CYCLOPROPYL SUBSTITUTED PROPARGYL ESTERS WITH CO

In the first part, a competitive study on Rh-catalyzed [5+1] and [4+1] cycloadditions of 3-acyloxy 1,4-enynes (ACEs) with terminal and internal alkynes with CO was reported [118]. In the second part of the thesis work, [5+1] cyclocarbonylation of cyclopropyl substituted propargyl esters has been investigated by using quantum mechanical calculations. Although a new DFT study was published to highlight the cycloaddition mechanism of vinylcyclopropane with Rh catalyst [121], there is no mechanistic study to discuss a tandem acyloxy migration cycloaddition of cyclopropyl substituted propargyl ester with CO. Also, the ring expansion of an allenylcyclopropane which is an intermediate formed in tandem acyloxy migration cycloaddition of cyclopropyl substituted propargyl esters has not been studied mechanistically to our knowledge. The similarity of the skeletal structures of vinylcyclopropanes and allenylcyclopropanes will help to highlight the carbocyclization mechanism. In this study, we have aimed to explain a consecutive acyloxy migration cycloaddition reaction and the selectivity of bond cleavage.

In the former studies, Taber et al. investigated the selectivity of the cyclopropane ring cleavage in ring expanding reactions of vinyl cyclopropanes in the presence of $Fe(CO)_5$ in Figure 4.1 [122]. The more stable metallacycle was obtained from an organometallic cleavage of the least substituted bond “a”. It is shown that the primary carbon metal bond is preferred rather the secondary carbon-metal bond in the cyclopropyl ring opening. Yu et. al. also reported in a similar study that the allenylcyclopropane preferred to undergo a cleavage of bond “a” [88].

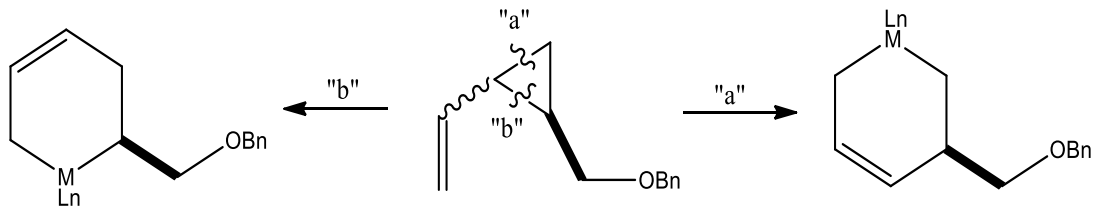

Figure 4.1 : Ring-expanding reactions of vinyl cyclopropanes with the cleavage of bond a vs b.

Herein, the experimental results of Tang et. al. have been considered to investigate the possible reaction mechanisms and the regioselectivity [41]. The proposed mechanism in Figure 4.2 is starting with the cleavage of dimeric rhodium catalyst, $[Rh(CO)_2Cl]_2$ by solvation and then RhCOCl which is formed by the dissociation of CO coordinates to cyclopropyl substituted propargyl ester (I) to give a π-complex. The following 1,3-acyloxy migration is the key step to obtain allenylcyclopropane (II). Rhodium alkylidene cyclohexene (III) is generated by the oxidative addition of cyclopropane preceded by CO addition to Rh-catalyst. Migratory insertion of CO to the cycle produced rhoda alkylidene cyclohexenone (IV) which is followed by reductive elimination to liberate the final product, alkylidene cyclohexenones (V) [41,66].

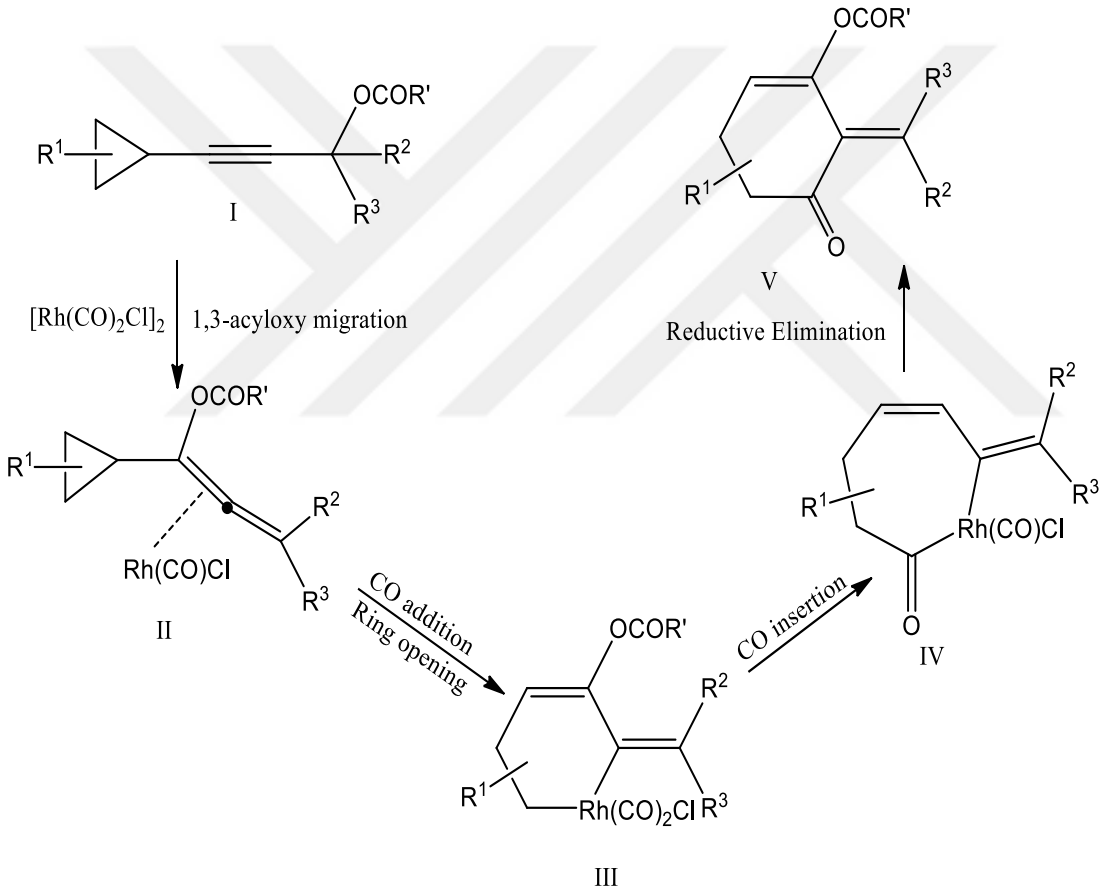

Figure 4.2 : The proposed mechanism of Rh-catalyzed tandem 1,3-acyloxy migration [5+1] cycloaddition by CO.

The cleavage of different cyclopropane C-C σ-bonds led to different isomers of V for the unsymmetrically substituted cyclopropanes. The regioselectivity for the cleavage of C-C σ-bonds is found to be dependent on the stereochemistry of the cyclopropyl group, the nature of the metal catalysts and the electronic properties of the substituents [41]. Numerous efforts have been devoted to the synthesis of natural products

including cyclohexenone skeleton via [5+1] cycloadditions such as the synthesis of functionalized cyclohexenone core of welwitindolinones C by Tang et al. [90] and (−)-galantamine by Yu et al [88]. Therefore, understanding the mechanistic details will enable synthesizing custom-made products with the desired substituents more efficiently.

4.1 Computational Method

Computations were performed using Gaussian 09 [113] suite of quantum chemical program. B3LYP [95,96,101] and wB97XD [102] functionals which have been demonstrated to be suitable for studying transition metal catalysis were used to optimize the geometries of all species in toluene (ε=2.38) with Polarizable Continuum Model (PCM) [108]. The LANL2DZ basis set was employed for Rh and the 6–31 G+(d) basis set was used for other atoms [110-112]. Rhodium is used in its singlet state. Frequency analysis at the same level was performed to ensure the stationary point as minimum or transition state. Intrinsic reaction coordinate (IRC) calculations were performed on the transition states to confirm the expected reactant and product on both sides [114,115].

The 3D structures were prepared using CYLView [120]. In naming the structures, C and T prefixes refer to *cis*- and *trans*-disubstituted-cyclopropanes with methoxy group and F refers to trans-disubstituent-cyclopropane with phenyl group. The conformers have been identified as a, b, c and d and the stereochemistry of trans and cis conformers have been defined in detail (Figure 4.4). The numbering of atoms is shown in Figure 4.3.

Firstly, a preliminary benchmark calculation has been performed with B3LYP in toluene which was employed to Rh catalyzed [5+1] and [4+1] cycloadditions of 3-acyloxy-1,4-enynes in Chapter 3.

The pivaloate group ($OCOC(CH_3)_3$) which was used in the experimental study of Tang et al. was replaced by the acetate group ($OCOCH_3$) for the benchmark to reduce the computational cost as it was successful in Chapter 3. Two trans conformers Ta and Td which give major and minor products, respectively, are modeled (Table 4-1).

Table 4.1 : The relative Gibbs free energies of trans-disubstituted cyclopropanes (with acyloxy group) optimized with B3LYP/LANL2DZ in toluene (kcal/mol).

	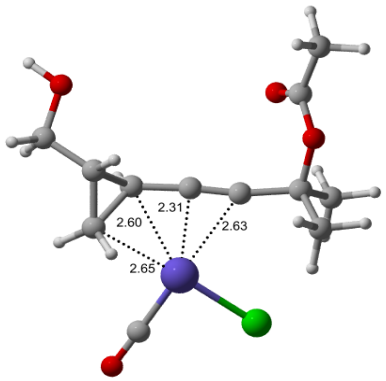	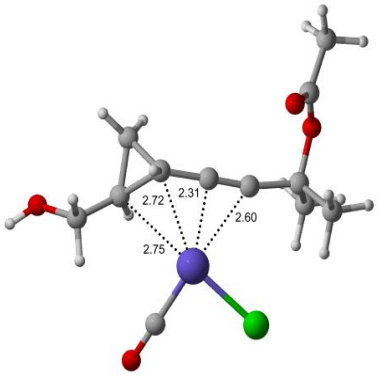
Conformers/ Structures	**Conformer Ta (OAc)**	**Conformer Td (OAc)**
1	0.0	1.6
TS-2	14.5	14.8
3	6.9	8.6
TS-4	7.1	8.4
5	-3.6	-2.4

However, Gibbs free energies of the transition states, 4 for the breaking of acetate group and the intermediates, 3, formed from the first step of the acyloxy group migration are nearly the same. Since no noticeable difference is seen between the energy values and the geometries of TS-4 and 3, another benchmark for all trans conformers has been done by using pivaloxy group to stick to the experimental conditions in Table 4-2. The structures of all conformers are presented in Figure 4.4.

Table 4.2 : The relative Gibbs free energies of trans-disubstituted cyclopropanes (with pivaloxy group) optimized with B3LYP/LANL2DZ in toluene (kcal/mol).

Conformers/ Structures	**Conformer Ta (OPiv)**	**Conformer Tb (OPiv)**	**Conformer Tc (OPiv)**	**Conformer Td (OPiv)**
1	0.3	0.0	2.2	1.7
TS-2	14.7	14.4	14.9	14.7
3	6.5	7.0	7.8	8.1
TS-4	6.1	6.6	7.3	7.6
5	-4.2	-4.2	-2.2	-2.3

The energy values and the optimized geometries for the breaking of OPiv group to form allene (transition states, 4 and intermediates, 3) are nearly same and indistinguishable for the conformers (Table 4-2) as in Table 4-1. According to Table 4-1 and Table 4-2, the conformers with acyloxy group or pivaloxy group have not made a significant difference in the energy comparison. A range separated functional is used since B3LYP has difficulty to capture the dispersion interactions.

Therefore, wB97XD, a range separated functional with dispersion correction, which has performed well on transition metal catalyzed cycloaddition reactions [119] has been employed with the same basis set. The optimized geometries and the energy values obtained from wB97XD have been consistent with the experimental observations. Thus, the energies discussed throughout the chapter are Gibbs free energies from the wB97XD calculations.

4.2 Results and Discussion

The aim of this study is to find out the cycloaddition mechanism of propargyl esters via a consecutive acyloxy migration and cyclopropyl ring opening to obtain the cyclic ketones. In addition, the regioselectivity of cyclopropane bond cleavage has been investigated for *trans*- and *cis*-disubstituted cyclopropanes. For this reason, we will consider the experimental results of Tang et. al. to highlight the tandem acyloxy migration carbocylization mechanisms [41].

In Rh catalyzed [5+1] cycloaddition of vinyl cyclopropanes, the cyclopropanes preferred to be cleaved on the least substituted C-C bond. *Cis*-disubstituted cyclopropane with hydroxyl methyl substituent gave only one kind of [5+1] cycloaddition product with the cleavage of less hindered monosubstituted C-C bond while its trans isomer led to two cyclohexenones with a high selectivity of the less hindered C-C bond [87].

In the highlight of these studies, we have modeled the cyclocarbonylation reaction of cis and trans conformers of 3-(2-Hydroxymethyl-cyclopropyl)-1,1-dimethyl-prop-2-ynyl ester and trans conformer of 3-(2-Phenyl-cyclopropyl)-1,1-dimethyl-prop-2-ynyl ester in toluene (Figure 4.3) [22]. Higher regioselectivity leading to alkylidene cyclohexenone P1 by the cleavage of less hindered bond “a” and P2 by the cleavage of most hindered bond “b” is observed in *cis*-disubstituted cyclopropane (P1:P2 ratio of 12:1) than the corresponding trans-counterpart (P1:P2 ratio of 3.5: 1). Also, trans conformers with hydroxymethyl and phenyl substitutents on the cyclopropane rings have opposite regioselectivities.

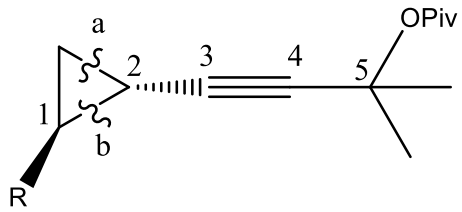

trans-disubstituted cyclopropane

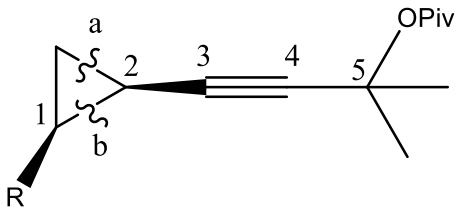

cis-disubstituted cyclopropane

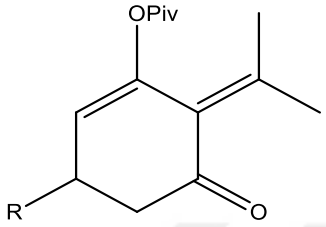

Alkylidene cyclohexenone **P1** (by the cleavage of bond "a")

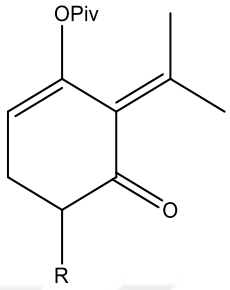

Alkylidene cyclohexenone **P2** (by the cleavage of bond "b")

Reactants		
R=MeOH ***trans***-disub-cyclopropane	3.5	1
R=MeOH ***cis***-disub-cyclopropane	12	1
R=Ph ***trans***-disub-cyclopropane	1	2.5

Figure 4.3 : Regioselectivity for the cleavage of C−C σ-bond in *trans*- and *cis*-disubstituted cyclopropanes [22].

In Part 4.2.1 and 4.2.2, Rh-catalyzed carbonylation mechanisms of *trans*-and *cis*-disubstituted cyclopropane with hydroxymethyl group have been discussed in detail. Part 4.2.3 presents the mechanistic study of trans-disubstituted cyclopropane with phenyl group. The lowest energy *trans*- and *cis*-disubstituted cyclopropane reactants are found by an extensive conformational search (Figure 4.4). Each isomer has 4 conformers according to the position of R group in cyclopropane (R is on the same carbon of cyclopropane in a and b vs c and d) and the position of H atom (H is in the front (b and d) or the back (a and c)).

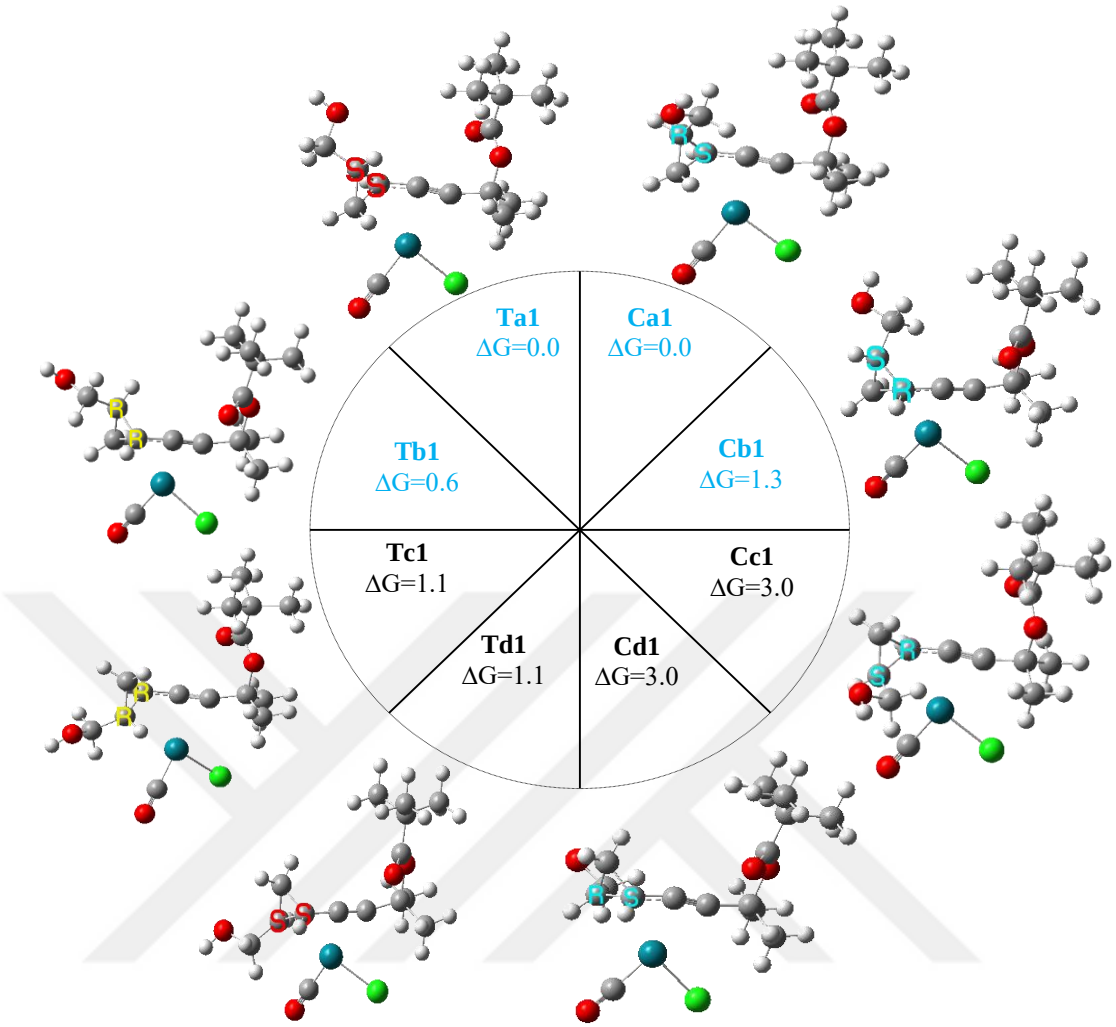

Figure 4.4 : The relative Gibbs free energies (in kcal/mol) of possible *trans*- and *cis*-disubstituted cyclopropane reactant conformers (T refers to *trans*, C refers to *cis*-disubstituted cyclopropane).

The trans and cis conformers of a and b (blue color) give major product, P1, with the cleavage of the least substituted bond of cyclopropane while c and d give minor product, P2 with the cleavage of the most substituted bond of cyclopropane. In both cis and trans conformers, c and d have higher reactant energies as compared to a and b. The free energies for cis conformers of Cc1 and Cd1 are higher than that of Ca1 and Cb1, which is consistent with the product distribution (12:1). On the other hand, the trans conformers are energetically close to each other (Figure 4.4). The difference in Gibss free energies for the reactants of trans isomers leading to major products (Ta1 and Tb1) and minor products (Tc1 and Td1) is also less that of cis isomers which is consistent with (12:1) vs (3.5:1) product ratio. The bond distances of the initial complexes, Ta1 and Ca1, have been shown in Figure 4.5.

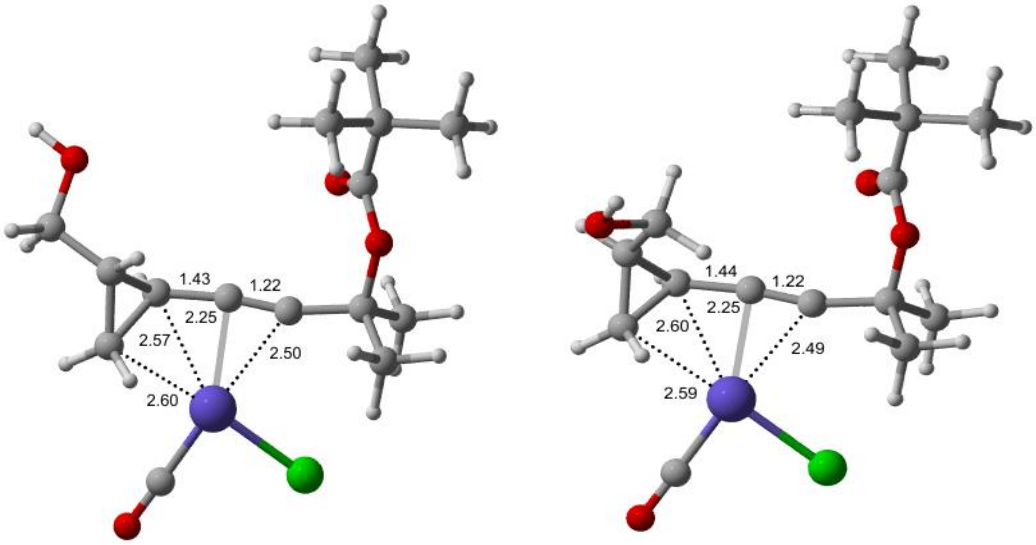

Ta1 **Ca1**

Figure 4.5 : 3D figures of *trans*- and *cis*-disubstituted cyclopropane reactants (T refers to *trans*, C refers to *cis*).

Trans- and *cis*-disubstituted conformers have been discussed in detail in the following parts.

4.2.1 The reaction mechanism of trans- hydroxymethyl cyclopropyl propargyl ester

The reaction mechanisms of all four trans conformers have been modelled because the reactants Ta1 (S,S) and Tb1 (R,R) giving major product P1 (0.0 kcal/mol and 0.6 kcal/mol, respectively) and Tc1 (R,R) and Td1 (S,S) giving minor product P2 (1.1 kcal/mol and 1.1 kcal/mol, respectively) have close free energies as seen in Figure 4.4. Tandem 1,3 acyloxy migration [5+1] cycloaddition of the reactant complexes, Ta1 and Tb1, have been evaluated in Figure 4.8. 1,3-acyloxy migration takes place via a step-wise mechanism (TS-2 and TS-4, Figure 4.6).

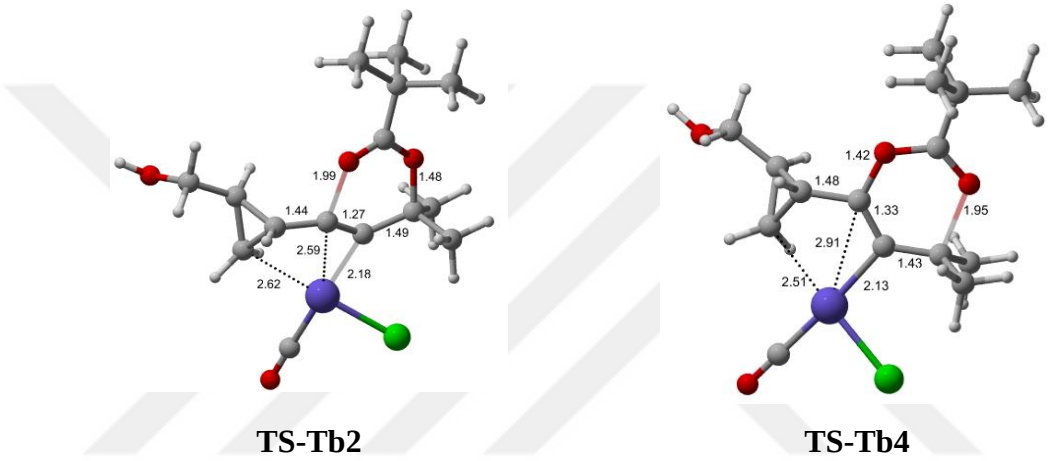

Figure 4.6 : 3D representation of a step-wise 1,3 acyloxy migration transition states of trans conformer b, TS-Tb2 and TS-Tb4.

In TS-2, acyloxy group is coordinated to C3 atom with energy barriers of 14.4 and 14.9 kcal/mol for Ta1 and Tb1, repectively and intermediate 3 forms where acyloxy group has an interaction with both C3 and C5. In TS-4, acyloxy group migrated to C3 at a relative free energy of 5.5 and 5.7 kcal/mol and Rh-allenyl complex 5 formation occurs exothermically at -3.5 and -3.7 kcal/mol for *trans*-conformers a and b, respectively. Rhodium catalyst attacked to allene and formed a bond with C3 and C4 of allenyl moiety of 6. The interaction of rhodium with C−C σ-bond of cyclopropane in 6 is also stronger than of 5. This is reflected in the shortening of Rh—C1 bond length (2.53A° vs 2.45A° for 5 vs 6, respectively) and Rh—C2 bond length (3.13A° vs 2.44A° for 5 vs 6, respectively) as shown in Figure 4.7. The intermediate 6 (-9.4 kcal/mol) is calculated to be more stable than 5 (-3.7 kcal/mol) by 5.7 kcal/mol.

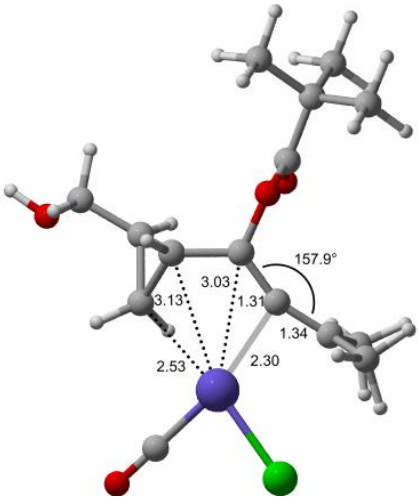

Tb5 (-3.7 kcal/mol)

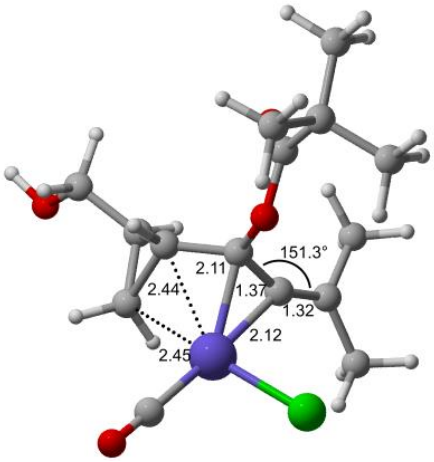

Tb6 (-9.4 kcal/mol)

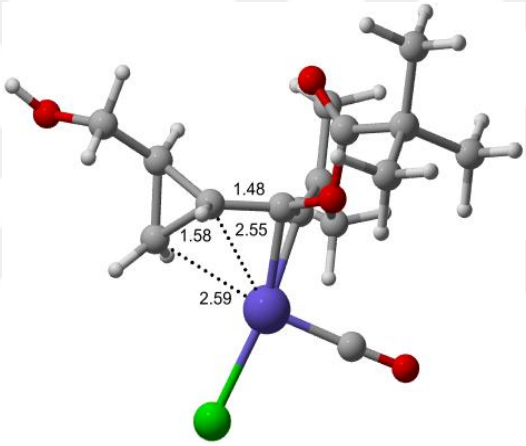

Tb7 (-26.3 kcal/mol)

Figure 4.7 : 3D representation of allenyl complexes Tb5, Tb6 and Tb7.

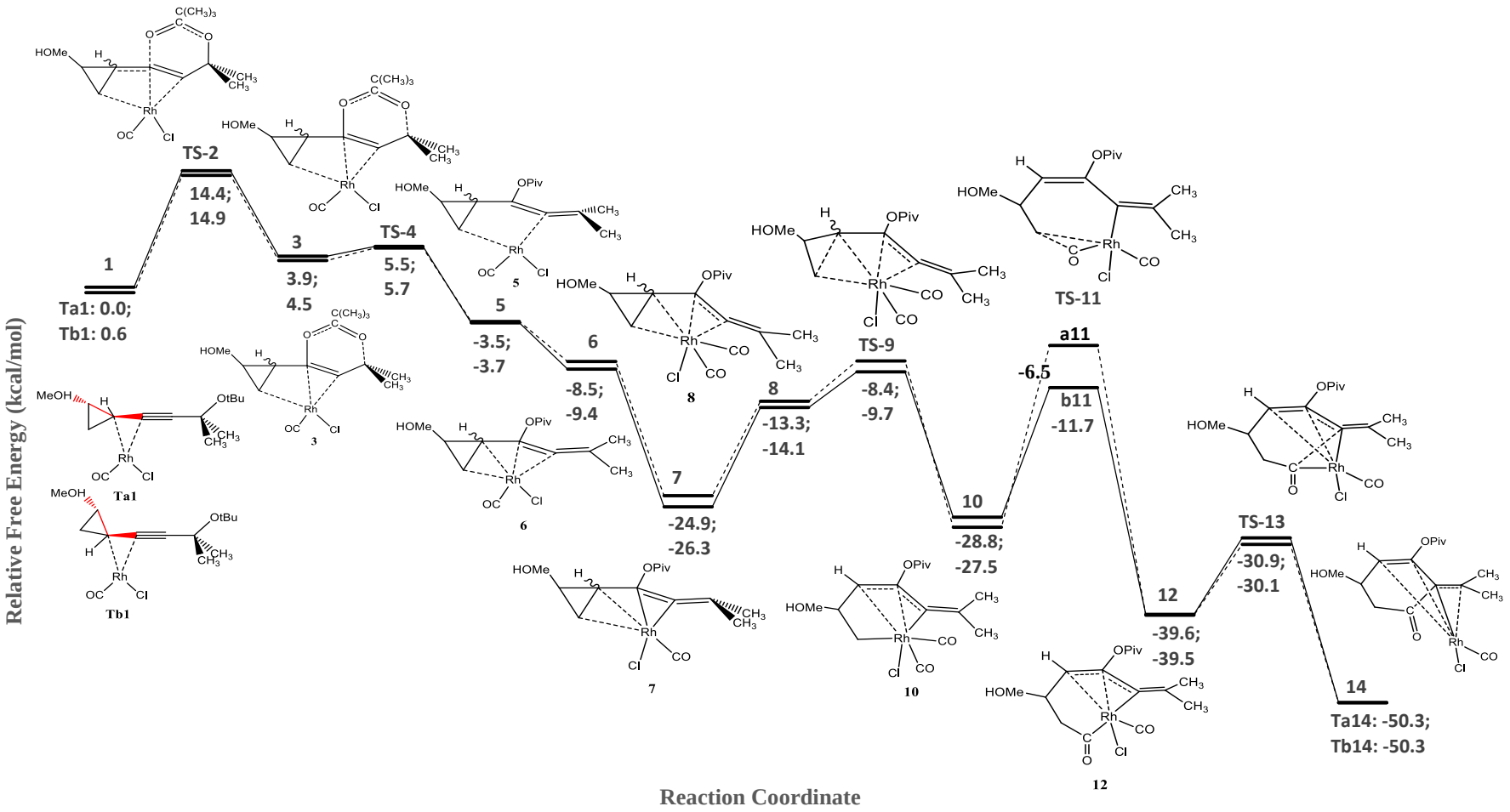

Figure 4.8 : Energy profile of the $[Rh(CO)_2Cl]_2$-catalyzed [5+1] cycloaddition reaction of trans- hydroxymethyl cyclopropyl propargyl esters (a and b) by CO in toluene. Energies are Gibbs free energies in kcal/mol.

The reaction path following 6 diverges into two possible paths where; (i) Cyclopropyl opening occurs first and then carbonyl addition takes place or (ii) CO addition is followed by ring expansion. In the first path (i), the cyclopropane ring opening of 6 or 7 (which is the isomerization intermediate) does not occur. Transition state is searched for both situations and only TS following 7 has a negative frequency which indicates the ring opening, however, IRC calculations do not proceed. Thus, the mechanism where cyclopropyl opening occurs first and then carbonyl addition takes place (i) is excluded. Then, the mechanism (ii) has been evaluated. Herein, the alternative mechanisms following through 6 are present and they will be discussed for one of the conformers in Figure 4.11 and then the whole mechanism in Figure 4.8 will be examined in detail. Conformer b is chosen to investigate the alternative mechanisms starting from 6b since the b conformer is energetically favored slightly more as compared to 6a (-9.4 kcal/mol *vs* -8.5 kcal/mol) to obtain the major product. Intermediate 6 can undergo either ring expansion following CO addition to Rh catalyst (8iii) or isomerization to 7 (Figure 4.7) followed by CO addition to Rh catalyst (8i and 8ii). In the first path, CO addition to Rh catalyst (from 6 to 8iii) in the resulting intermediate increase the free energy by 3.7 kcal/mol in 8iii and cyclopropyl opening takes place via TS-9iii (-3.7 kcal/mol). Rhodium metallacycle 10iii is obtained in an exergonic way at a relative free energy of -26.2 kcal/mol. In the other two alternative paths, isomerization to 7 takes place at first in a highly exergonic way (-26.3 kcal/mol) and then CO coordinated to Rh catalyst through two opposite directions (in 8i and 8ii) by an increase of ~12 kcal/mol of energy. Both complexes have still lower relative free energies (-14.1 and -14.3 kcal/mol for 8i and 8ii, respectively) than 8iii (-5.7 kcal/mol) as seen in Figure 4.9. This indicates that the pathway involving isomerization 7 and then CO addition 8i&8ii is an energetically favored path compared to direct CO addition to 6.

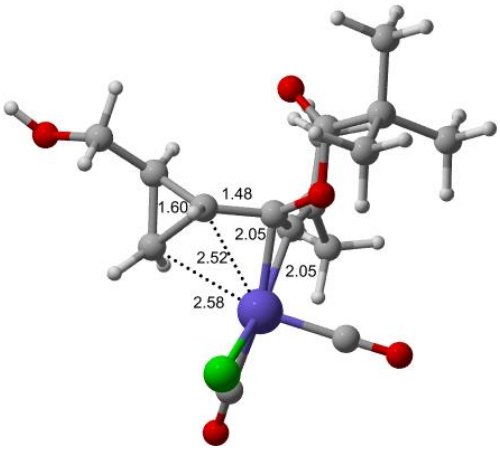

8i (-14.1 kcal/mol)

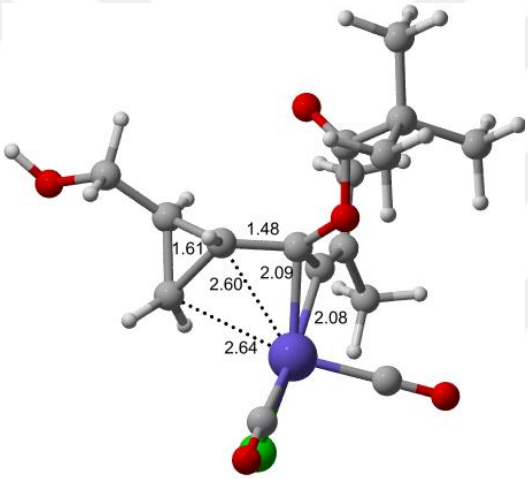

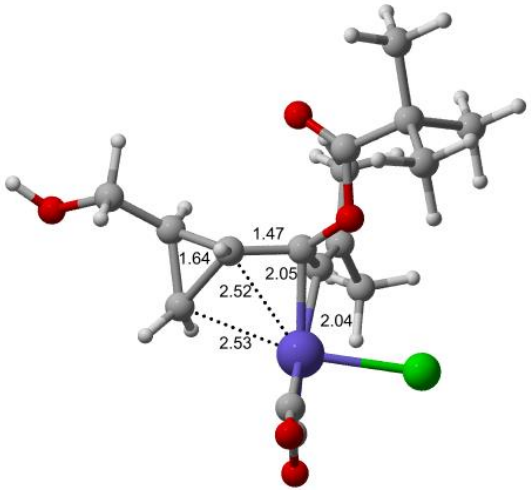

8ii (-14.3 kcal/mol)

8iii (-5.7 kcal/mol)

Figure 4.9 : 3D representation of CO addition intermediates 8i, 8ii and 8iii.

The formation of rhodium metallacycle 10i (-27.5 kal/mol) and 10ii (-23.3 kcal/mol) took place via energetically close transition states, TS-9i and TS-9ii (-9.7 and -9.4 kcal/mol) (Figure 4.11). The 4.2 kcal/mol of energy difference thermodynamically favors 10i but both paths are continued for CO insertion step. The six membered metallacycle (10i) is converted to a seven-membered rhodium metallacycle exothermically (12i at -39.5 kcal/mol via CO insertion (TS-11i) with a barrier of 15.8 kcal/mol. On the other hand, rhoda metallacycle 10ii should undergo 11ii-r before CO insertion (Figure 4.10). Rhodium loses its π-bonds with the double bond of cyclic structure in 11ii-r and it has only Rh-C σ-bonds. However, 11ii-r is an energetically

unfavored rhodacyclohexene. This is an endergonic process which needs an energy of 13.6 kcal/mol.

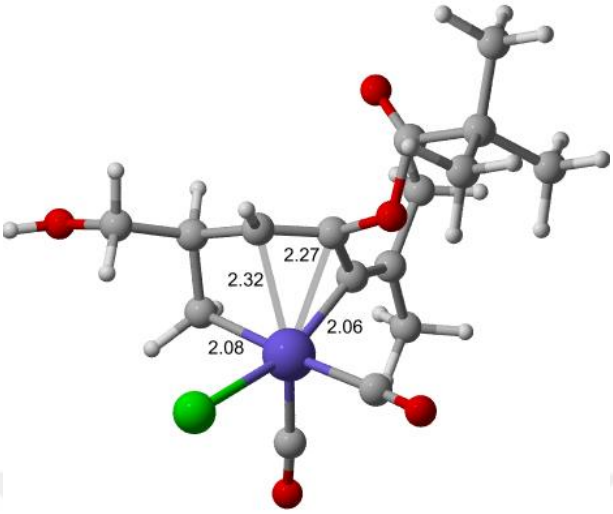

10i (-27.5 kcal/mol)

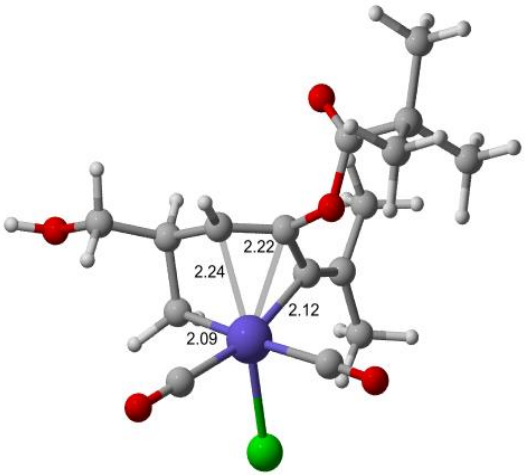

10ii (-23.3 kcal/mol)

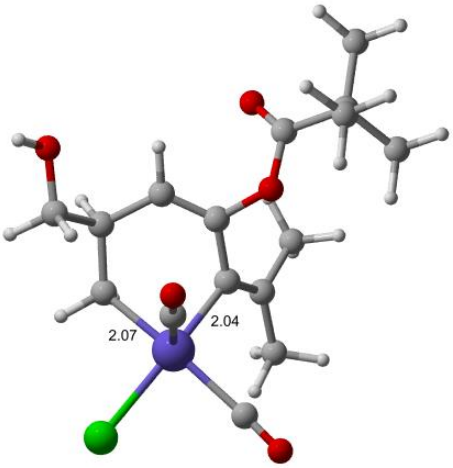

11ii-r (-9.7 kcal/mol)

Figure 4.10 : 3D representation of CO addition intermediates 10i, 10ii and 11ii-r.

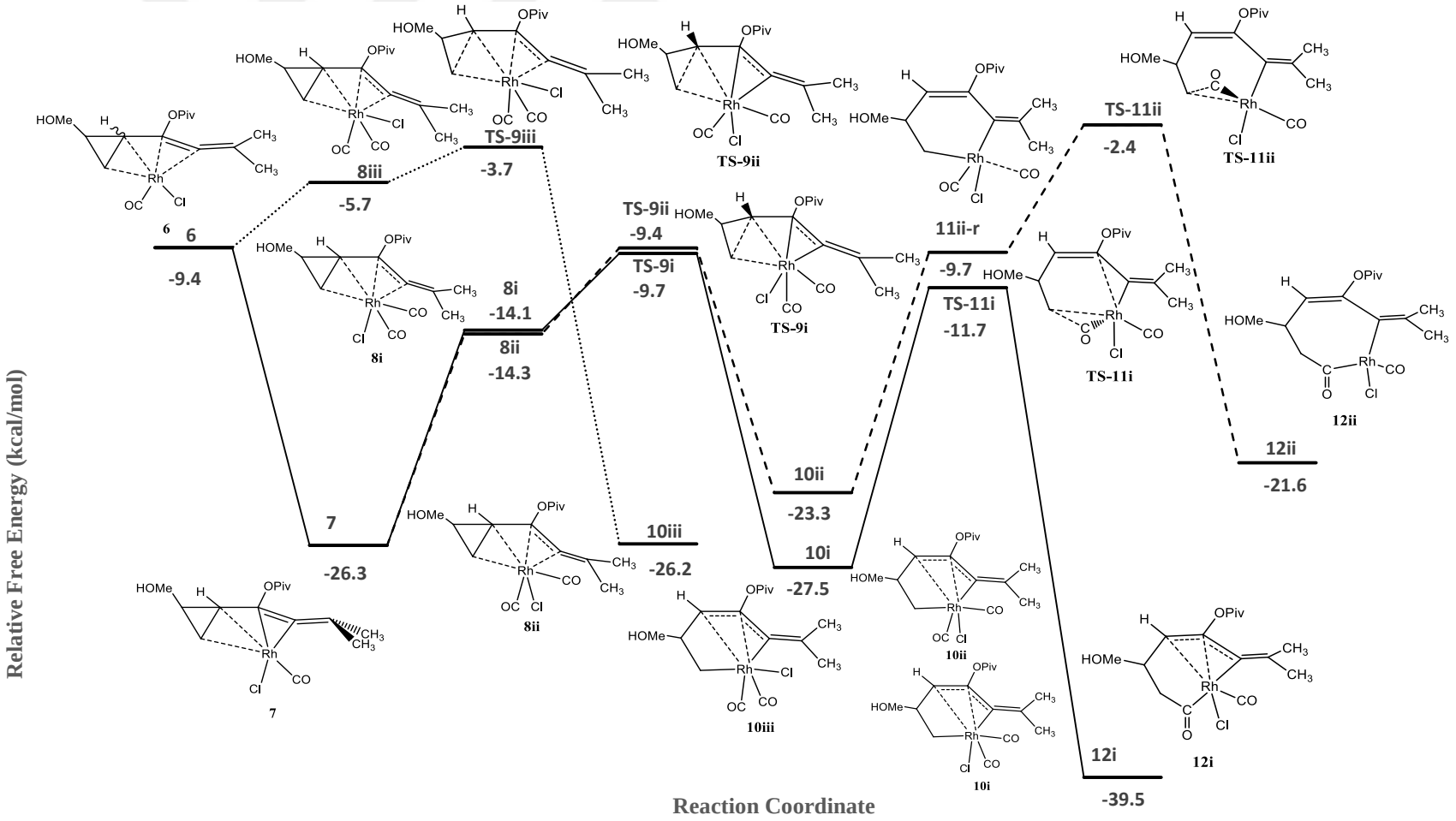

Figure 4.11 : The alternative mechanisms of [5+1] cycloaddition reaction of cyclopropyl substituted propargyl ester to allene intermediate 6 for trans-conformer b. Energies are Gibbs free energies in kcal/mol. The solid black line shows the more favorable pathway.

Unfavored rhodacyclohexene, 11ii-r is followed by CO insertion transition step TS-11ii (-2.4 kcal/mol). The relative free energy of TS-11ii is 9.3 kcal/mol higher than that of TS-11i (-11.7 kcal/mol) (Figure 4.12). Rhodium alkylidene cyclohexenone intermediate 12ii (-21.6 kcal/mol) has higher energy than the former intermediate 10ii (-23.3 kcal/mol). On the other hand, rhodium alkylidene cyclohexenone intermediate 12i is energetically favored (-39.5 kcal/mol) (Figure 4.12). From the calculations, we propose that the path through 8i to 12i more favorable over the others, thus, the mechanisms of all conformers will be investigated following this path.

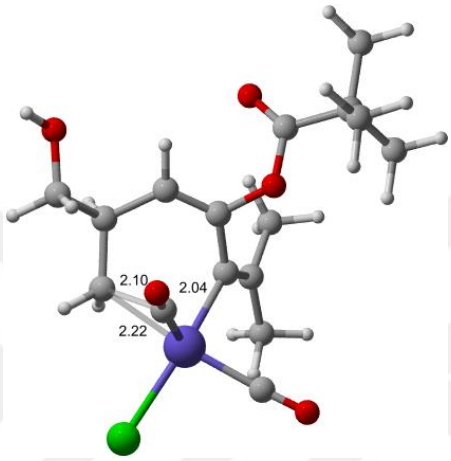

TS-11ii (unfavored TS, -2.4 kcal/mol**)**

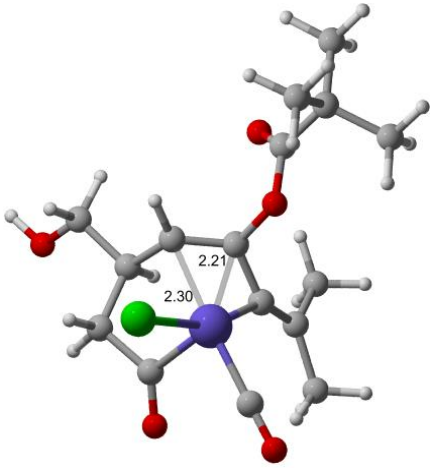

12i (favored, -39.5 kcal/mol)

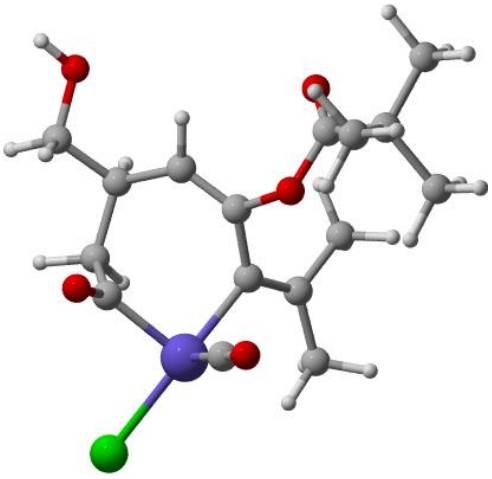

12ii (unfavored, -21.6 kcal/mol)

Figure 4.12 : 3D representation of CO insertion transition state TS-11i and the following intermediates 12i vs 12ii.

When continued with Figure 4.8, isomerization from 6 have revealed intermediates of a and b conformers at relative free energies of -24.9 kcal/mol (a7) and -26.3 kcal/mol (7b). CO addition to isomerized intermediates 7 increases the energies by ~12 kcal/mol for both conformers (Ta8 and Tb8). The ring opening transition state TS-9 to give a rhodium metallacycle 10 has a 1.5 kcal/mol of energy difference between a and b conformers which favors b. CO insertion transition state TS-a11 has a relative free energy of -6.5 kcal/mol. On the other hand, CO insertion transition state TS-b11 (-11.7 kcal/mol) is 5.2 kcal/mol more stable than TS-a11. The path following through conformer b is the favored path to obtain the major product P1. The seven-membered rhodium metallacycle, formed by by CO insertion has almost the same energies for Ta12 and Tb12 (-39.6 and -39.5 kcal/mol, respectively) and it is followed by C(carbonyl)-C(sp^2) reductive elimination via transition state TS-13 (-30.9 kcal/mol and -30.1 kcal/mol for Ta13 and Tb13 in Figure 4.13, respectively) leading to the same product π-complex, 14 (-50.3 kcal/mol).

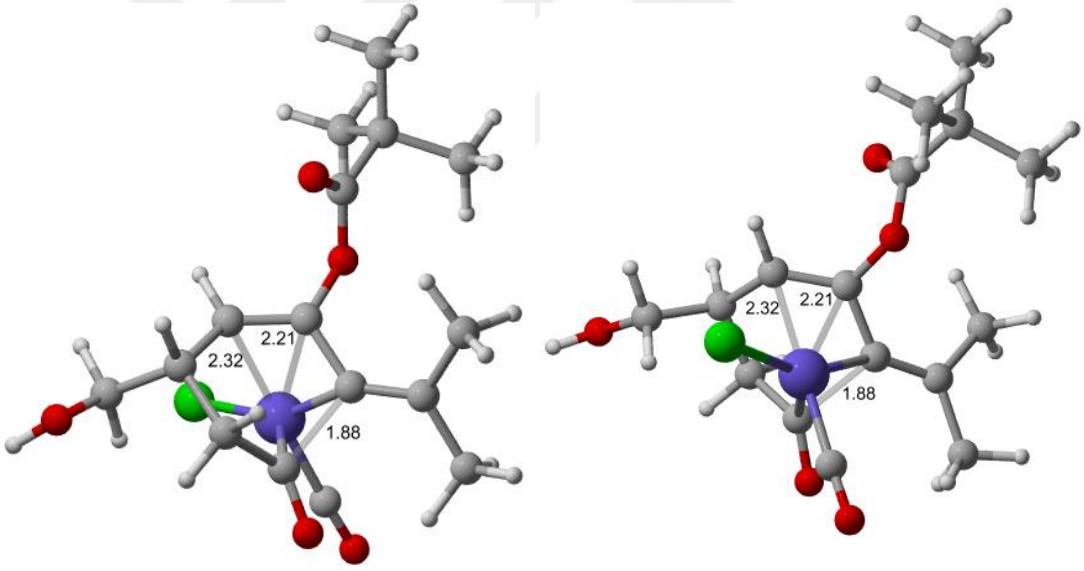

TS-Ta13 (-30.9 kcal/mol) **TS-Tb13** (-30.1 kcal/mol)

Figure 4.13 : 3D representation of reductive elimination transition states TS-Ta13 and TS-Tb13.

Kozuch S. et al. proposed a new concept which is called the energetic span model to conceptualize catalytic cycles [123]. In this model, the rate determining step or the slowest step of the reaction have been exchanged with the rate determining states which participated in the shaping of the kinetics, TDI (turnover frequency (TOF)-determining intermediate) and TDTS (TOF-determining transition state). The turnover

frequency (TOF) which determines the efficiency of the catalyst is given as the number of cycles per catalyst concentration per time. The energetic span terms (δE) which determine activation energies are consistent with DFT calculations in the preferred selectivity and the rate determining step is CO insertion step for conformer a while cyclopropyl ring opening for conformer b according to this model. The overall barrier calculated from Ta10 (TDI) to the next transition state TS-Ta11 (TDTS) has δE of 22.3 kcal/mol while the barrier calculated for cyclopropyl ring opening from Tb8 (TDI) to the next transition state TS-Tb9 (TDTS) have an energetic span δE of 16.6 kcal/mol.

Trans conformers c and d (switching the positions of H and cyclopropyl) in Figure 4.14 go through the same mechanisms as discussed in Figure 4.8. The free energies of the reactants Tc1 (1.1 kcal/mol) and Td1 (1.1 kcal/mol) are very close to the lowest free energy conformer of Ta1. The energy values for intermediates and transition states of trans conformers c and d in acyloxy migration steps are close to the values for trans conformers a and b through the mechanism. Allene intermediate 5 has -0.6 kcal/mol and -2.5 kcal/mol for c and d, respectively. The free energies of the conformers c and d have almost the same relative free energies for the following rearrangement (6), isomerization (7), CO addition to rhodium (8) and cyclization (TS-9 and 10) steps: However, CO insertion step TS-11 which is rate determining step requires a 3.7 kcal/mol of higher free energy for conformer d. The rate determining intermediate and the transition state obtained via the energetic span model are 10 and TS-11 for both c and d conformers. Conformer c has δE of 22.1 kcal/mol while conformer d has δE of 25.4 kcal/mol. The mechanism following conformer c is a plausible mechanism as compared to conformer d. It leads to a seven-membered rhodium metallacycle 12. The product π-complex 14 (-50.7 kcal/mol) is obtained through reductive elimination transition state, TS-13 (-29.0 kcal/mol).

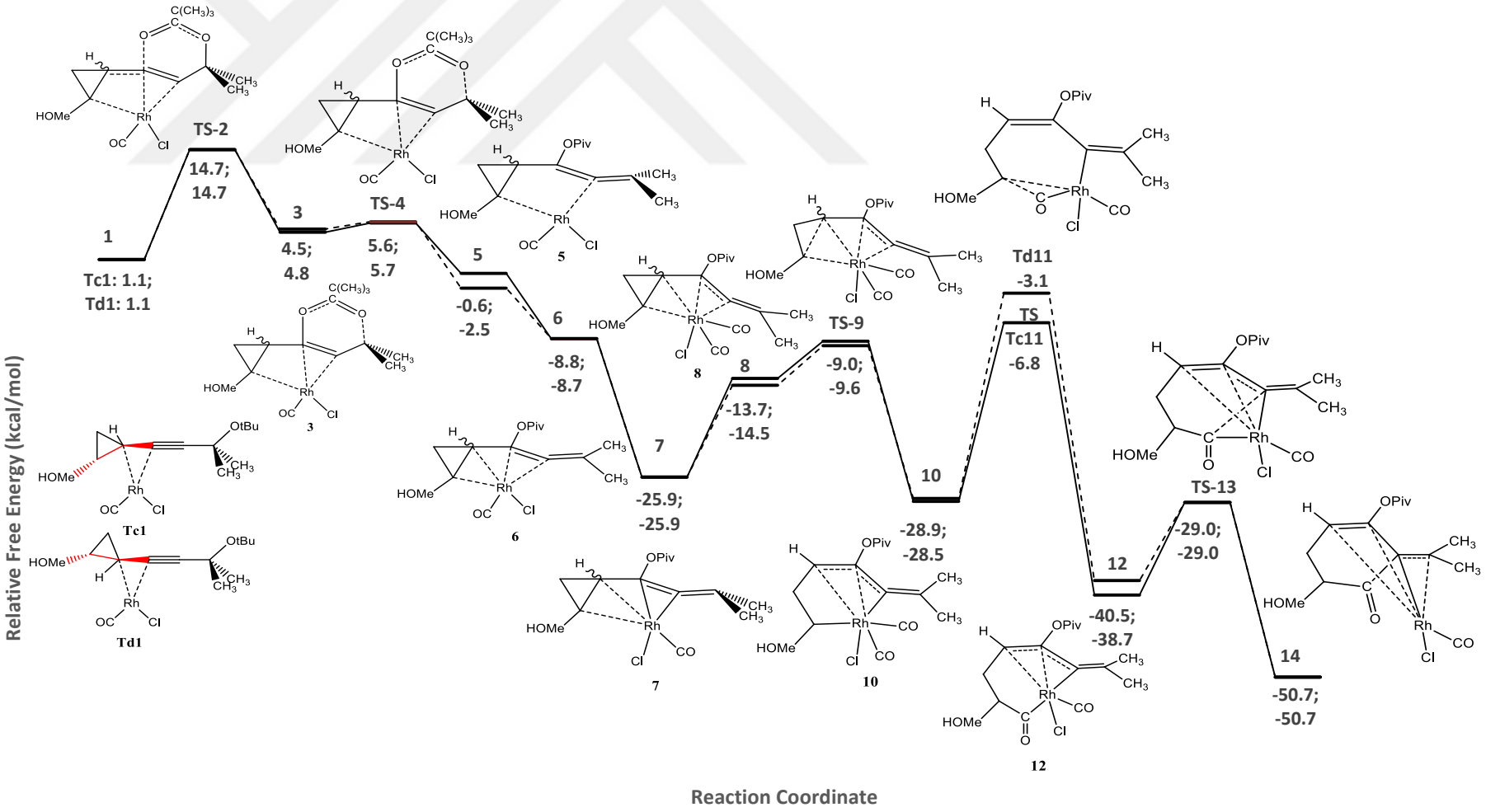

Figure 4.14 : The Gibbs free energy profile of the $[Rh(CO)_2Cl]_2$-catalyzed [5+1] cycloaddition reaction of trans- hydroxymethyl cyclopropyl propargyl esters (c and d) by CO in toluene. Energies are in kcal/mol.

In conclusion, the reactions following trans conformer b in Figure 4.8 and trans conformer c in Figure 4.14 are plausible mechanisms giving major product P1 and minor product P2, respectively, through the reaction pathways. A remarkable free energy difference is obtained in CO insertion transition state TS-11. Intermediate 10 has a free energy of -27.5 and -28.9 kcal/mol for trans conformers b and c, respectively. CO insertion TS-11 has a free energy barrier of 16.2 kcal/mol for conformer b while 22.1 kcal/mol for conformer c. The 4.9 kcal/mol of energy difference in TS-Tb11 and TS-Tc11 favors trans conformer b, leading to the major product alkylidene cyclohexanone, P1 (-37.8 kcal/mol) which has a ratio of 3.5:1 comparing to minor product, P2 (-36.4 kcal/mol) (Figure 4.15).

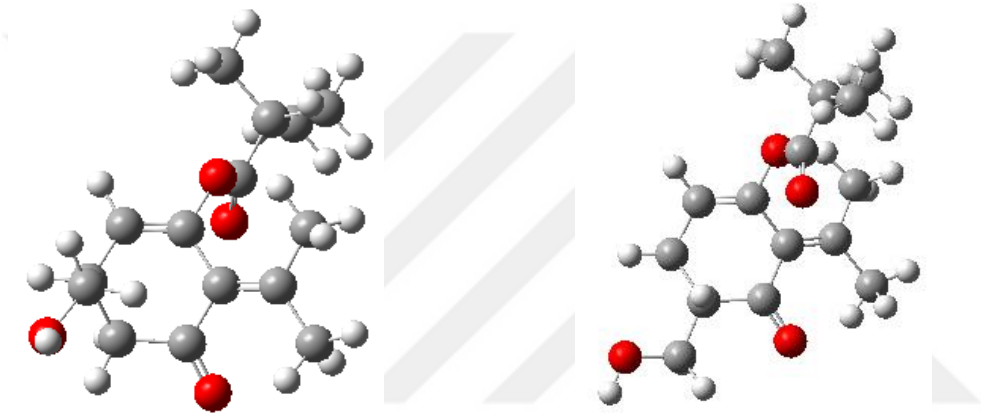

Tb15, major product, **P1**, -37.8 kcal/mol **Tc15**, minor product, **P2**, -36.4 kcal/mol

Figure 4.15 : The Gibbs free energies of major and minor products.

Tang et. al. accounted for this selectivity in their paper that the less hindered C−C σ-bond was selectively cleaved, presumably because of the steric interaction between the substituent R and the rhodium complex in the cyclization step. Our studies demonstrated that CO insertion to the cycle in TS-11 acoounted for this selectivity. The less hindered C-C σ-bond cleavage in trans-conformer b (-11.7 kcal/mol, TS-11) is energetically favored comparing to trans conformer c (-6.8 kcal/mol, TS-11) as seen in Figure 4.16.

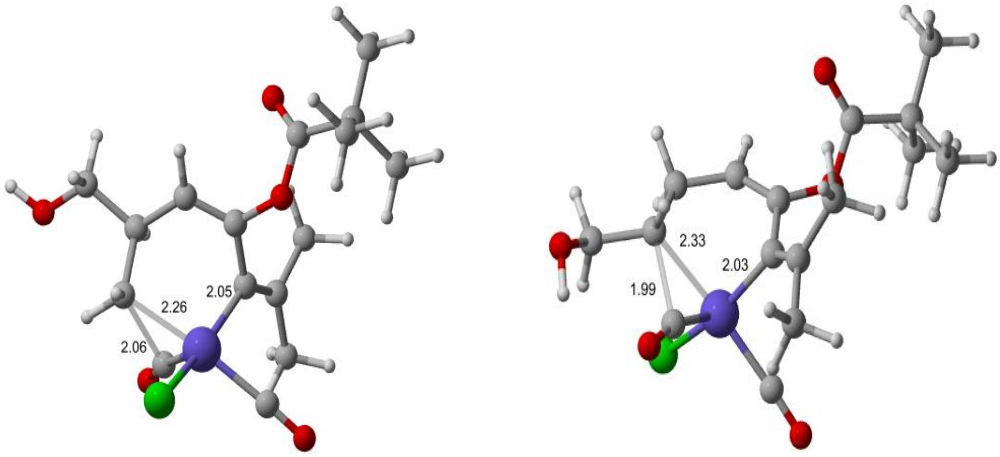

TS-Tb11 (-11.7 kcal/mol) **TS-Tc11** (-6.8 kcal/mol)

Figure 4.16 : 3D representation of CO insertion transition state TS-11 of trans conformers Tb and Tc.

4.2.2 The reaction mechanism of cis- hydroxymethyl cyclopropyl propargyl ester

For the *cis*-disubstituted case, conformers a and b which give major product P1 by the activation of the least substituted C-C bond of cyclopropane are compared with each other. The reactant of conformer a is 1.3 kcal/mol more stable than that of conformer b. Conversely, the reactants of conformers c and d which lead to minor product P2 by the activation of the most substituted bond of cyclopropane have the same free energy values. However, Rh atom interacts with hydrogen of hydroxymethyl group in the first acyloxy migration step which prevents conformer d to undergo acyloxy migration. In this respect, the cyclocarbonylation reaction mechanism of cis conformers a and c have been discussed in Figure 4.17.

The relative stability difference between Ca1 and Cc1 is 3 kcal/mol, favoring the complex Ca1 which gives the major product, P1 (P1:P2 ; 12:1). The first and second transition states in which acyloxy migration takes place (TS-2 and TS-4) have ~3 kcal/mol higher free energies in both TSs for conformer c. After the acyloxy migration, the allene intermediates (5) form with close Gibbs free energies (-2.7 kcal/mol and -2.3 kcal/mol for conformers a and c, respectively). Cc5 which has an interaction with both cyclopropane and allene directly undergoes isomerization Cc7 and CO addition Cc8. On the other hand, Ca5 rearranges to Ca6 (-8.7 kcal/mol) in which Rh interacts with both allene and cyclopropane. Same kind of bonding pattern or rearrangement is observed for trans conformers before CO addition takes place. Also, CO addition (from Ca7 to Ca8) is an endothermic process as it is in trans conformers. However,

CO addition in conformer c is an exothermic process (from Cc7 to Cc8) with a relative free energy of -29.9 kcal/mol. The following cyclopropyl ring opening requires a free energy of 24.5 kcal/mol for conformer c (from Cc8 to TS-9) while it needs a 14.8 kcal/mol of free energy for conformer a (from Ca7 to TS-9). CO insertion in rhodacyclohexane (10) has a barrier height of 19.5 kcal/mol (TS-11) and 22.4 kcal/mol and for conformers a and c, respectively. In other words, the corresponding C-C bond activation transition states TS-9 (-9.3 kcal/mol and -5.3 kcal/mol for Ca9 and Cc9, respectively) and CO insertion transition states TS-11 (-9.5 kcal/mol and -4.7 kcal/mol for Ca11 and Cc11, respectively) are in favor of activating the least substituted C-C bond by ~4-5 kcal/mol, suggesting that the cleavage of the least substituted C-C bond is kinetically preferred. The energy span model is consistent with the prediction and experimental result. The energetic span results show that CO insertion step (from Ca10 to TS-Ca11) is the rate determining step with δE=19.5 kcal/mol for conformer a. On the other hand, the rate determining step is determined by TDI where CO addition to Rh catalyst occurs (Cc8) and TDTS in which CO inserts to the cycle (TS-Cc11) for conformer c. The energetic span, δE, is 25.1 kcal/mol for conformer c. A highly exothermic rhodacycloheptanone 12 undergoes a reductive elimination TS-13 with a relative free energy of 30.8 kcal/mol and 29.9 kcal/mol leading to π-complex, 14 (-51.3 kcal/mol and 50.2 kcal/mol) for conformer a and c, respectively. 14 coordinates with another reactant molecule to generate the reactant 1 to complete the catalytic cycle. The major alkylidene cyclohexenone product, Ca15 has a free energy of -36.5 kcal/mol while the minor one, Cc15 has a free energy of -36.4 kcal/mol. Compared to its trans-counterpart, the cis isomer is found to have a more significant effect in product distribution due to the steric repulsion between the substituent on the cyclopropyl ring and the rhodium catalyst.

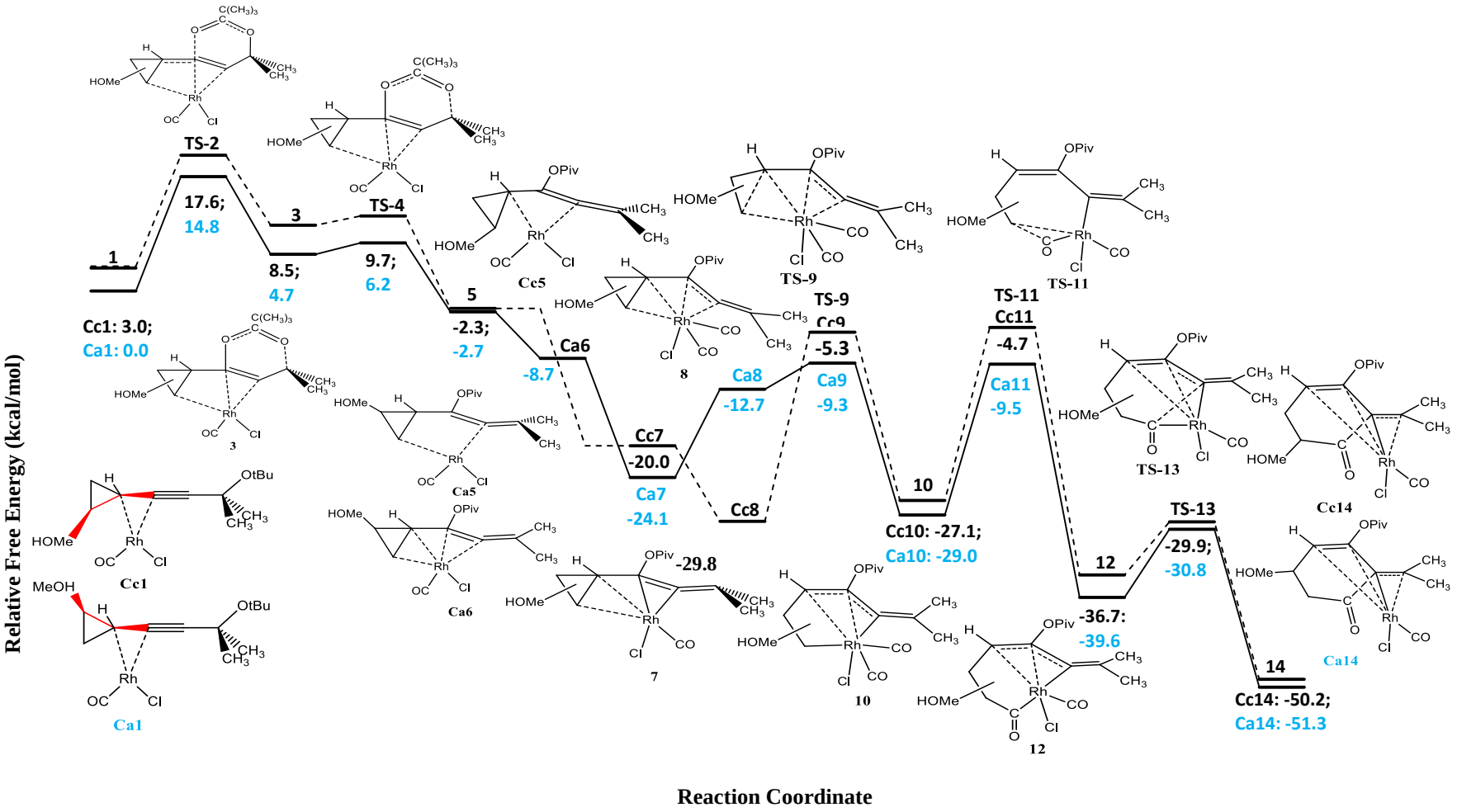

Figure 4.17 : The Gibbs free energy profile of the $[Rh(CO)_2Cl]_2$-catalyzed [5+1] cycloaddition reaction of cis- hydroxymethyl cyclopropyl propargyl esters (a and c) by CO in toluene. Energies are in kcal/mol.

4.2.3 The reaction mechanism of trans- phenyl cyclopropyl propargyl ester

In contrast to disubstituted cyclopropanes which prefer the cleavage of the least substituted C-C σ bond, *trans*-disubstituted cyclopropane with phenyl substitution is the only one which prefers the activation of the most substituted C-C bond of cyclopropane (P1:P2 ; 1:2.5).

In a former study, the selectivity of allenylcyclopropanes was explained by Saigo K. that the selectivity of the rearrangement of phenyl-substituted allenyl cyclopropanes depends on both the cationic character of the catalyst and the electron density of the allenyl group of the substrate. Allenylcyclopropane with a phenyl substituent has a high selectivity for the most substituted C-C bond of cyclopropane with the cationic complexes like $[Rh(cod)_2]^+BF_4^-$ and $[Rh(cod)(PPh_3)_2]^+BF_4^-$. On the other hand, the low selectivity is observed for the least substituted C-C bond (56:44) and a mixture of methylenecyclopentenones is obtained by a neutral catalyst, $[RhCl(PPh_3)_3]$. When phenyl is displaced by H or n-propyl, less hindered bond is preferred to be cleaved [124]. In this study, Tang et. al explained the opposite selectivity for trans- phenyl cyclopropyl propargyl ester that the C-C bond adjacent to the phenyl group was selectively cleaved due to the electronic effect of the adjacent π-system [41].

Herein, the selectivity of the cleavage of the most substituted C-C bond ("b") will be explained using quantum calculations. The reactants of conformers c and d which have lower free energies comparing to a and b give the major product P2 by the cleavage of bond "b". Fa1 and Fb1 have the same free energies which are higher than their counterparts Fc1 and Fd1 by 1.8 kcal/mol in Figure 4.18.

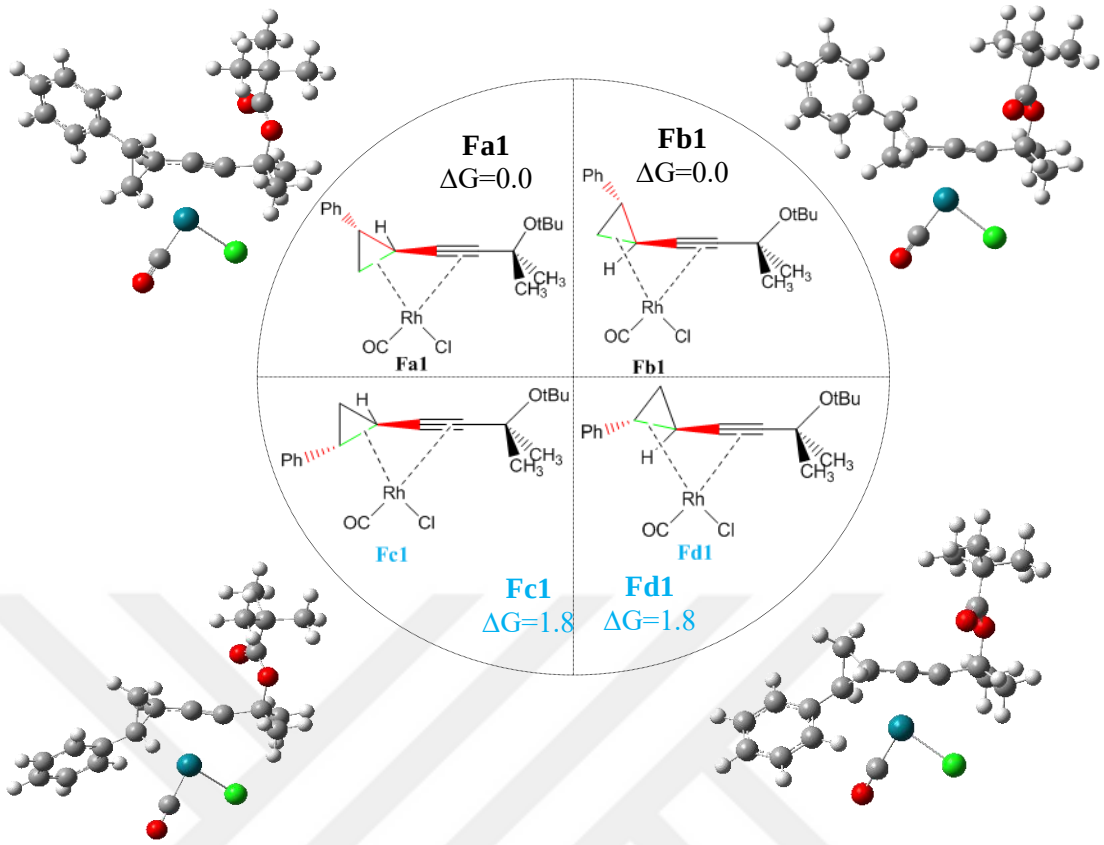

Figure 4.18 : The relative Gibbs free energies (in kcal/mol) of the reactants of possible *trans*-disubstituted cyclopropane conformers with phenyl substitution (conformers a&b give minor products, conformers c&d give major products, green bond refers to the bond which will be cleaved).

The CO insertion step is the rate determining step in the energy comparison of conformers which energetically favors conformer b to its counterpart a and conformer c to its counterpart d, respectively (Figure 4.19). Therefore, the computed reaction pathways for the conformers b and c are discussed in Figure 4.20.

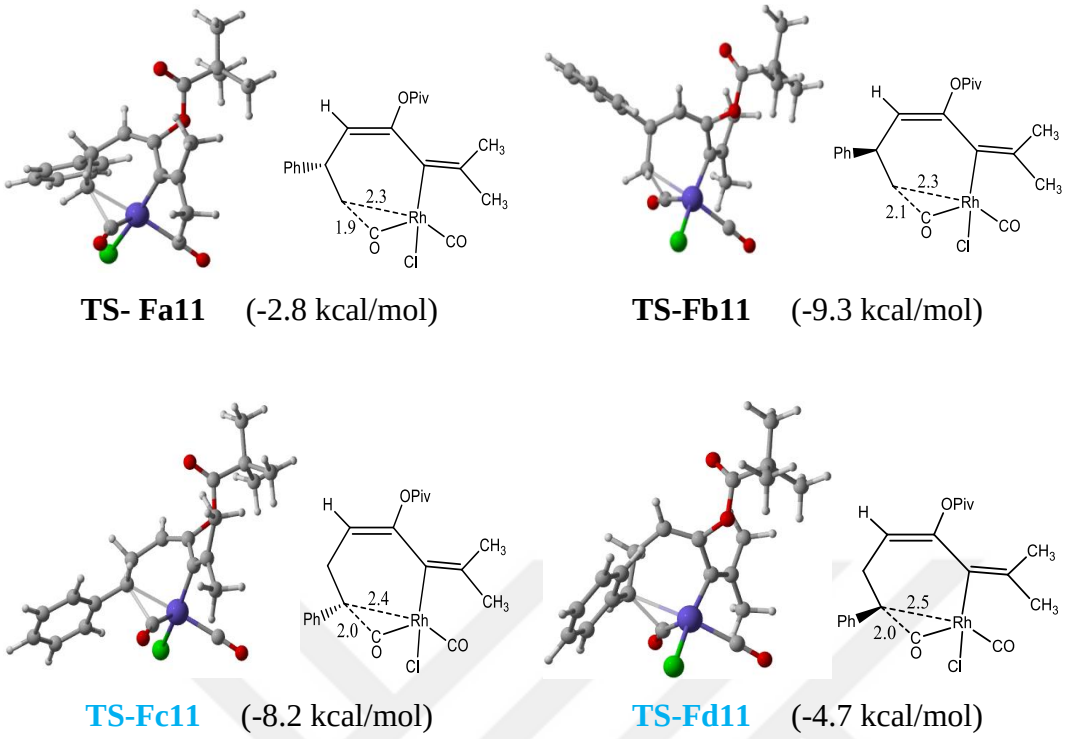

TS- Fa11 (-2.8 kcal/mol) **TS-Fb11** (-9.3 kcal/mol)

TS-Fc11 (-8.2 kcal/mol) **TS-Fd11** (-4.7 kcal/mol)

Figure 4.19 : The relative Gibbs free energies of CO insertion transition states for all four trans conformers.

Fc1 which gives the major product has a 1.8 kcal/mol of free energy lower than Fb1. Since the reaction path follows the reaction mechanism of trans- hydroxymethyl cyclopropyl propargyl ester investigated in Part 4.2.1, the details will not be discussed in this part. The acyloxy migration transition states of conformers b and c have close free energies. The first intermediate in which acyloxy group has an interaction with both C3 and C5 favors Fc3 by 1.3 kcal/mol of energy. Although the intermediates 5 formed after acyloxy migration have almost same energies, the rearranged intermediate Fc6 (-9.3 kcal/mol) is more stable than that of Fb6 (-7.7 kcal/mol). The intermediates formed through isomerization (7), CO addition to rhodium (8) and cyclopropyl ring opening (10) have close energies for both conformers. CO insertion in TS-11 has a barrier height of 17.2 and 18.5 kcal/mol for conformers b and c, respectively. The energetic span model is applied to find the rate determining step. CO insertion step (from 10 to TS-11) is the rate determining step for both conformers. The energetic span, δE, is 17.2 kcal/mol for conformer b and δE is 18.5 kcal/mol for conformer c. Although conformer c gives the major product, the energetic span model favors conformer b by 1.3 kcal/mol as with the computational results. The intermediate alkylidene rhodacycloheptanone, Fc12 has a 1.0 kcal/mol of lower free energy than

Fb12. While the reductive elimination transition states TS-13 have very close energies, the formed π-complexes between rhodium and alkylidene rhodacyclohexanone favors Fb14 by 2.5 kcal/mol of energy which is minor product. The final products have a free energy of -35.8 kcal/mol and -33.2 kcal/mol for Fb15 and Fc15, respectively. DFT results and the energetic spans prefer conformer b which gives the minor product. On the other hand, 1.8 kcal/mol and 1.6 kcal/mol of energy differences between two conformers in the reactant 1 and the allene intermediate 6, respectively, favor conformer c. To conclude, no conclusive conclusions from the calculations or the energetic span model can be drawn. Unlike the preferential cleavage of less hindered C-C bond in most cyclopropanes, the trans cyclopropane with phenyl substituent is the only one with the opposite selectivity but the preference is not that strong.

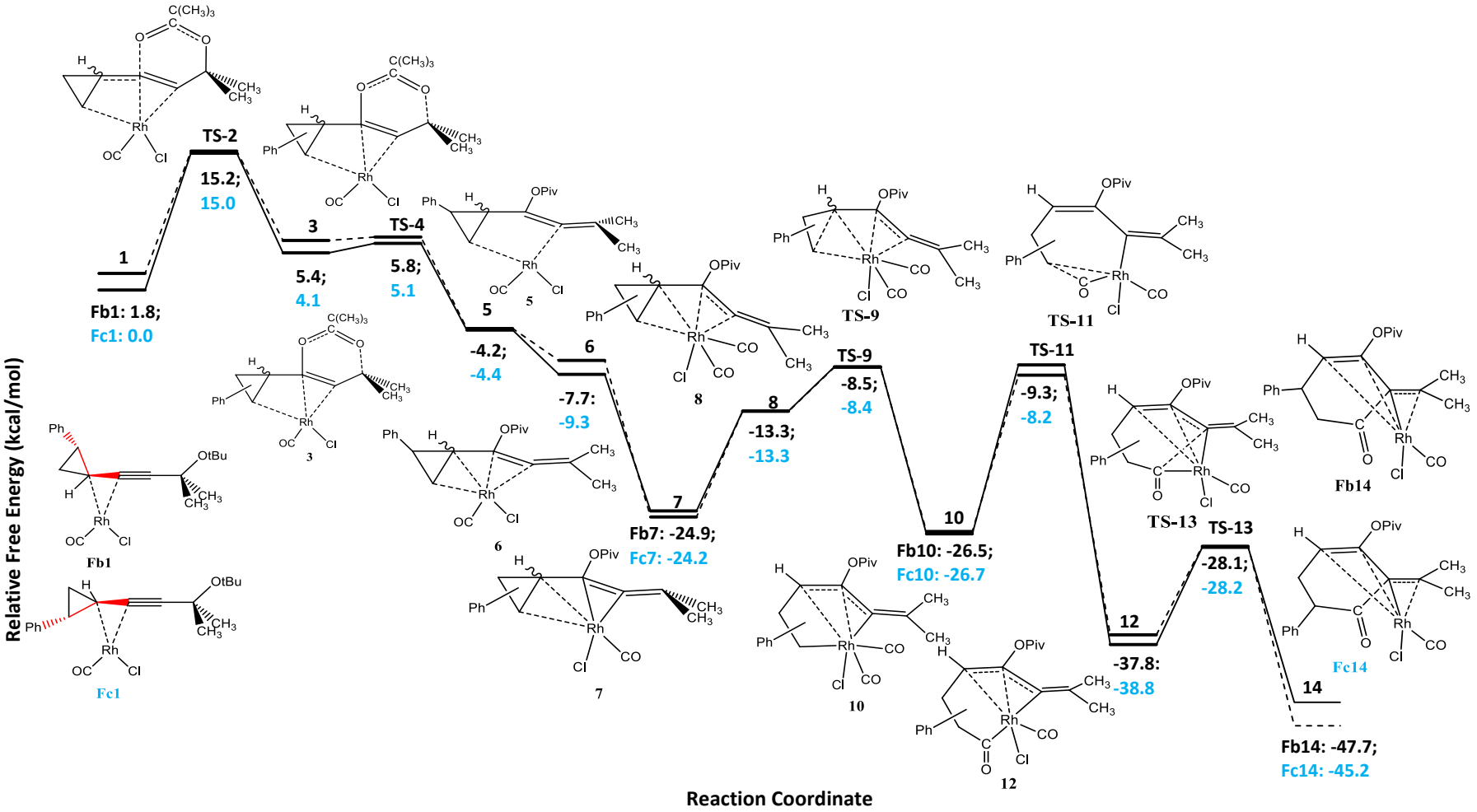

Figure 4.20 : The Gibbs free energy profile of the $[Rh(CO)_2Cl]_2$-catalyzed [5+1] cycloaddition reaction of trans- phenyl cyclopropyl propargyl esters (b and c) by CO in toluene. Energies are in kcal/mol.

5. CONCLUSIONS

In this thesis, tandem acyloxy migration cycloaddition reaction of two different propargyl esters have been investigated using quantum mechanical calculations.

In the first part, the mechanism of $[RhCl(CO)_2]_2$-catalyzed carbonylation of ACE with a cyclohexene moiety to form bicyclic cyclohexadienone and cyclopentenone derivatives have been explored using B3LYP functional. The effect of the nature of alkenes, terminal vs internal, has been rationalized by modelling possible intermediates and transition states for various possible transformations. The experimental preference of 1,2- vs 1,3-acyloxy migration of ACEs have been shown to depend on the type of alkynes in ACEs, such that terminal alkynes prefer to undergo a 1,2-acyloxy migration, whereas, ACEs with internal alkyne favors a 1,3-acyloxy migration.

Our calculations have reproduced this experimental trend and enabled us to predict the mechanism of tandem cycloaddition reactions. The migration step has been predicted to be the rate determining step in both terminal and internal alkyne cases. The calculations show that 1,3-acyloxy migration, whether with internal or terminal alkyne, takes place with the same barrier. 1,2- vs 1,3-selectivity is mainly determined by 1,2-migration becoming more facile with terminal alkyne. The favorable olefinic carbon being the more positive one shows that the electronic effects have significant impact in these investigated systems. The 1,3 selectivity in the internal alkynes is mainly dominated by the slightly lower energy barrier and more significantly by the 1,3-migration product being much more stable as compared to that of 1,2. For increasing 1,3-migration efficiency, experimentalists can focus on obtaining more stable allene intermediates with proper substitutions, ie. groups facilitating resonance stabilization through the olefinic carbon backbone. After the migration, CO addition to the Rh center can occur in the first step or after the isomerization. The calculations indicated that after the migration, isomerization step gave a ~6 kcal/mol lower energy complex in both types of alkynes and CO insertion took place from the side of the

cyclic structure to give a rhodacycle in terminal alkynes instead of a ketene formation [116].

In the second part of the thesis, $[RhCl(CO)_2]_2$ catalyzed [5+1] cycloadditions of propargyl esters via 1,3-acyloxy migration have been modeled for trans- and cis-hydroxymethyl and trans-phenyl cyclopropyl propargyl esters with their different conformers using WB97XD functional. Also, the regioselectivity associated with the different substituents on cyclopropyl group has been investigated.

First, the mechanism of trans- cyclopropyl propargyl ester with hydroxymethyl substitution has been highlighted. Then, cis counterpart has been modeled to compare the effect of trans and cis isomers on the selectivity of the preferred bond cleavage to obtain major product. The least substituted C-C σ-bond is kinetically preferred to be cleaved which leads to P1. Therefore, P1 is the major product for both trans and cis conformers and the regioselectivity increases in *cis*-disubstituted cyclopropanes (P1:P2 ; 12:1) compared to its trans-counterparts (P1:P2 ; 3.5:1).

Trans conformers a and b which give major product P1 have close energies through the reaction path but the energy difference which occurs in CO insertion transition state TS-11 favors conformer b by 5.2 kcal/mol. On the other hand, the trans conformers c and d give minor product P2. Conformer c is preferred energetically than conformer d by 3.7 kcal/mol in TS-11. Then, conformer b and c compared with each other to discuss about the regioselectivity leading to major and minor products P1 and P2, respectively. During the path, both structures have close energies but CO insertion steps of conformers b and c need a free energy of -11.6 kcal/mol and -6.7 kcal/mol, respectively. Therefore, CO insertion is suggested as the rate determining step and 4.9 kcal/mol of energy difference favor conformer b which leads to major product P1.

In the comparison of cis conformers of a and c, the reaction mechanism favors conformer a energetically through the reaction path. Conformer a is more stable than c by about ~3 kcal/mol when each transition states and intermediates are compared. This might be the reason of the high regioselectivity in *cis*-disubstituted conformer (P1:P2 ; 12:1). Here, the less hindered C−C σ-bond was selectively cleaved, presumably because of the steric interaction between hydroxymethyl moiety and the rhodium catalyst.

Trans-phenyl cyclopropyl propargyl ester has been discussed due to the opposite selectivity. Although the less hindered C-C σ bond was selectively cleaved for all *cis*- and *trans*-disubstituted cyclopropanes in the experiment study of Tang et. al. [41], the most substituted C-C σ bond is preferred to be cleaved only in the case of *trans*-disubstituted cyclopropane having phenyl group. Our theoretical work indicated that 1.8 kcal/mol and 1.6 kcal/mol of energy differences in the comparison of the reactants 1 and the allene intermediates 6, respectively, favor conformer c which give P2 as major product (P1:P2 ; 1:2.5). The selectivity of the cleavage of the most substituted C-C bond in the case of phenyl substituted cyclopropane can be the result of the electronic effect of the adjacent π-system.

Although trans phenyl and hydroxymethyl disubstituted cyclopropanes show an opposite selectivity, the same conformers b and c with (R,R) stereochemistry having lower energies coumparing to their counterparts undergo the cleavage to obtain two isomers.

In conclusion, the effect of terminal and internal alkynes on acyloxy migration and the corresponding cycloaddition have been evaluated with CO for 3-acyloxy 1,4-enynes. Also, the regioselectivity of the conformers which leads to two isomers and the cyclopropyl ring opening to obtain carbocyclic structures with CO have been investigated. We believe that the calculations presented herein will contribute to understanding and controlling this effective Rh (I) catalyzed transformation reactions of 1,2- and 1,3-acyloxy migration followed by cycloaddition for further carbocyclic derivatives in obtaining custom made products. In further studies, the calculated reaction mechanism in this thesis can be extended to model similar reactions in the literature to test the mechanism and to predict the outcome.

REFERENCES

[1] **Lautens, M., Klute, W., & Tam, W**. (1996). Transition metal-mediated cycloaddition reactions. *Chemical reviews*, *96*(1), 49-92.

[2] **Frühauf, H. W.** (1997). Metal-assisted cycloaddition reactions in organotransition metal chemistry. *Chemical reviews*, 97(3), 523-596.

[3] **Trost, B. M., & Krische, M. J**. (1998). Transition metal catalyzed cycloisomerizations. *Synlett*, *1998*(01), 1-16.

[4] **Evans, P. A. (Ed.).** (2005). *Modern rhodium-catalyzed organic reactions* (pp. 215-299*)*. Weinheim: John Wiley & Sons.

[5] **Michelet, V., Toullec, P. Y., & Genêt, J. P**. (2008). Cycloisomerization of 1, n-Enynes: Challenging Metal-Catalyzed Rearrangements and Mechanistic Insights. *Angewandte Chemie International Edition*, *47*(23), 4268-4315.

[6] **Aubert, C., Buisine, O., & Malacria, M.** (2002). The behavior of 1, n-enynes in the presence of transition metals. *Chemical reviews*, *102*(3), 813-834.

[7] **Michelet, V., Toullec, P. Y., & Genêt, J. P.** (2008). Cycloisomerization of 1, n-Enynes: Challenging Metal-Catalyzed Rearrangements and Mechanistic Insights. *Angewandte Chemie International Edition*, *47*(23), 4268-4315.

[8] **Marco-Contelles, J., & Soriano, E.** (2007). Recent Developments in the Metal-Catalyzed Reactions of Metallocarbenoids from Propargylic Esters. *Chemistry-A European Journal*, *13*(5), 1350-1357.

[9] **Ota, K., Lee, S. I., Tang, J. M., Takachi, M., Nakai, H., Morimoto, T., ... & Chatani, N.** (2009). Rh (II)-Catalyzed Skeletal Reorganization of 1, 6- and 1, 7-Enynes through Electrophilic Activation of Alkynes. *Journal of the American Chemical Society*, *131*(42), 15203-15211.

[10] **Sato, K., Tomonaga, H., Yamamoto, T., Matsumura, S., Zulkifli, N. D. B., Ishimoto, T., ... & Nagaoka, K.** (2016). A Synthetic Pseudo-Rh: NOx Reduction Activity and Electronic Structure of Pd–Ru Solid-solution Alloy Nanoparticles. *Scientific reports*, 6, 28265.

[11] **Colby, D. A., Bergman, R. G., & Ellman, J. A**. (2009). Rhodium-catalyzed C− C bond formation via heteroatom-directed C− H bond activation. *Chemical reviews*, 110(2), 624-655.

[12] **Lin, M., & Sen, A.** (1994). Direct catalytic conversion of methane to acetic acid in an aqueous medium. *Nature*, 368(6472), 613-615.

[13] **Ota, K., Lee, S. I., Tang, J. M., Takachi, M., Nakai, H., Morimoto, T., ... & Chatani, N.** (2009). Rh (II)-Catalyzed Skeletal Reorganization of 1, 6- and 1, 7-Enynes through Electrophilic Activation of Alkynes. *Journal of the American Chemical Society*, *131*(42), 15203-15211.

[14] Chatani, N., Furukawa, N., Sakurai, H., & Murai, S. (1996). PtCl2-catalyzed conversion of 1,6-and 1,7-enynes to 1-vinylcycloalkenes. Anomalous bond connection in skeletal reorganization of enynes. *Organometallics*, *15*(3), 901-903.

[15] Chatani, N., Inoue, H., Morimoto, T., Muto, T., & Murai, S. (2001). Iridium (I)-Catalyzed Cycloisomerization of Enynes. *The Journal of organic chemistry*, *66*(12), 4433-4436.

[16] Chatani, N., Inoue, H., Kotsuma, T., & Murai, S. (2002). Skeletal reorganization of enynes to 1-vinylcycloalkenes catalyzed by GaCl3. *Journal of the American Chemical Society*, *124*(35), 10294-10295.

[17] Marion, N., & Nolan, S. P. (2007). Propargylic esters in gold catalysis: Access to diversity. *Angewandte Chemie International Edition*, 46(16), 2750-2752.

[18] Mauleón, P., Krinsky, J. L., & Toste, F. D. (2009). Mechanistic studies on Au (I)-catalyzed [3,3]-sigmatropic rearrangements using cyclopropane probes. *Journal of the American Chemical Society*, *131*(12), 4513-4520.

[19] Garayalde, D., Gómez-Bengoa, E., Huang, X., Goeke, A., & Nevado, C. (2010). Mechanistic insights in gold-stabilized nonclassical carbocations: gold-catalyzed rearrangement of 3-cyclopropyl propargylic acetates. *Journal of the American Chemical Society*, *132*(13), 4720-4730.

[20] Brancour, C., Fukuyama, T., Ohta, Y., Ryu, I., Dhimane, A. L., Fensterbank, L., & Malacria, M. (2010). Synthesis of functionalized resorcinols by rhodium-catalyzed [5+1] cycloaddition reaction of 3-acyloxy-1,4-enynes with CO. *Chemical Communications*, *46*(30), 5470-5472.

[21] Shu, X. Z., Shu, D., Schienebeck, C. M., & Tang, W. (2012). Rhodium-catalyzed acyloxy migration of propargylic esters in cycloadditions, inspiration from the recent "gold rush". *Chemical Society Reviews*, *41*(23), 7698-7711.

[22] Saucy, V. G., Marbet, R., Lindlar, H., & Isler, O. (1959). Über eine neue Synthese von Citral und verwandten Verbindungen. *Helvetica Chimica Acta*, *42*(6), 1945-1955.

[23] Rautenstrauch, V. (1984). 2-Cyclopentenones from 1-ethynyl-2-propenyl acetates. *The Journal Of Organic Chemistry*, *49*(5), 950-952.

[24] Shi, X., Gorin, D. J., & Toste, F. D. (2005). Synthesis of 2-cyclopentenones by gold (I)-catalyzed Rautenstrauch rearrangement. *Journal of the American Chemical Society*, *127*(16), 5802-5803.

[25] Gorin, D. J., Dubé, P., & Toste, F. D. (2006). Synthesis of benzonorcaradienes by gold (I)-catalyzed [4+3] annulation. *Journal of the American Chemical Society*, *128*(45), 14480-14481.

[26] **Zi, W., Wu, H., & Toste, F. D.** (2015). Gold (I)-Catalyzed Dearomative Rautenstrauch Rearrangement: Enantioselective Access to Cyclopenta [b] indoles. *Journal of the American Chemical Society*, *137*(9), 3225-3228.

[27] **de Haro, T., Gómez-Bengoa, E., Cribiú, R., Huang, X., & Nevado, C.** (2012). Gold-Catalyzed 1,2-/1,2-Bis-acetoxy Migration of 1,4-Bis-propargyl Acetates: A Mechanistic Study. *Chemistry-A European Journal*, *18*(22), 6811-6824.

[28] **Wang, S., & Zhang, L.** (2006). A highly efficient preparative method of α-ylidene-β-diketones via Auiii-catalyzed acyl migration of propargylic esters. *Journal of the American Chemical Society*, *128*(26), 8414-8415.

[29] **Cho, E. J.** (2012). Factors Controlling the Equilibrium of Pt-Catalyzed [1,2]-versus [1,3]-Acyloxy Migration. *Chemistry-A European Journal*, *18*(15), 4495-4498.

[30] **Cariou, K., Mainetti, E., Fensterbank, L., & Malacria, M**. (2004). Tandem $PtCl_2$ catalyzed–thermal [3,3] rearrangements of enyne acetates. *Tetrahedron*, *60*(43), 9745-9755.

[31] **Fürstner, A., & Hannen, P.** (2006). Platinum-and Gold-Catalyzed Rearrangement Reactions of Propargyl Acetates: Total Syntheses of (−)-α-Cubebene,(−)-Cubebol, Sesquicarene and Related Terpenes. *Chemistry-A European Journal*, *12*(11), 3006-3019.

[32] **Yi, T. F., Yang, S. Y., & Xie, Y.** (2015). Recent advances of $Li_4Ti_5O_{12}$ as a promising next generation anode material for high power lithium-ion batteries. *Journal of Materials Chemistry A*, *3*(11), 5750-5777.

[33] **Miki, K., Ohe, K., & Uemura, S.** (2003). Ruthenium-catalyzed cyclopropanation of alkenes using propargylic carboxylates as precursors of vinylcarbenoids. *The Journal of organic chemistry*, *68*(22), 8505-8513.

[34] **Miki, K., Ohe, K., & Uemura, S.** (2003). A new ruthenium-catalyzed cyclopropanation of alkenes using propargylic acetates as a precursor of vinylcarbenoids. *Tetrahedron letters*, *44*(10), 2019-2022.

[35] **Tenaglia, A., & Marc, S.** (2006). $CpRuCl(PPh_3)_2$-Catalyzed Cyclopropanation of Bicyclic Alkenes with Tertiary Propargylic Acetates. *The Journal of organic chemistry*, *71*(9), 3569-3575.

[36] **Fehr, C., Farris, I., & Sommer, H.** (2006). Copper-Catalyzed Cycloisomerizations of 5-En-1-yn-3-ols. *Organic letters*, *8*(9), 1839-1841.

[37] **Fehr, C., & Galindo, J.** (2006). Synthesis of (-)-Cubebol by Face-Selective Platinum-, Gold-, or Copper-Catalyzed Cycloisomerization: Evidence for Chirality Transfer. *Angewandte Chemie*, *118*(18), 2967-2970.

[38] **Fehr, C., Winter, B., & Magpantay, I.** (2009). Synthesis of (-)-Cubebol by Face-Selective Platinum-, Gold-, or Copper-Catalyzed Cycloisomerization: Evidence of Chirality Transfer and Mechanistic Insights. *Chemistry-A European Journal*, *15*(38), 9773-9784.

[39] **Fukuyama, T., Ohta, Y., Brancour, C., Miyagawa, K., Ryu, I., Dhimane, A. L., ... & Malacria, M.** (2012). Rh-Catalyzed [5+ 1] and [4+ 1] Cycloaddition Reactions of 1, 4-Enyne Esters with CO: A Shortcut to Functionalized Resorcinols and Cyclopentenones. *Chemistry-A European Journal*, *18*(23), 7243-7247.

[40] **Li, X., Huang, S., Schienebeck, C. M., Shu, D., & Tang, W.** (2012). Rhodium-catalyzed Carbonylation of 3-Acyloxy-1,4-enynes for the Synthesis of Cyclopentenones. *Organic letters*, *14*(6), 1584.

[41] **Shu, D., Li, X., Zhang, M., Robichaux, P. J., Guzei, I. A., & Tang, W.** (2012). Rhodium-catalyzed carbonylation of cyclopropyl substituted propargyl esters: a tandem 1,3-acyloxy migration [5+1] cycloaddition. *The Journal of organic chemistry*, *77*(15), 6463.

[42] **Soriano, E., Ballesteros, P., & Marco-Contelles, J.** (2005). Theoretical investigation on the mechanisms of the $PtCl_2$-mediated cycloisomerization of polyfunctionalized 1,6-enynes.2.Propargylic carboxylates. *Organometallics*, *24*(13), 3182-3191.

[43] **Bhanu Prasad, B. A., Yoshimoto, F. K., & Sarpong, R.** (2005). Pt-Catalyzed Pentannulations from In Situ Generated Metallo-Carbenoids Utilizing Propargylic Esters. *Journal of the American Chemical Society*, *127*(36), 12468-12469.

[44] **Murakami, M., Itami, K., & Ito, Y.** (1996). A Study on Rhodium–Vinylallene Complexes Leading to a New Reaction, Rhodium-Catalyzed Carbonylative [4+1] Cycloaddition. *Angewandte Chemie International Edition*, *34*(23-24), 2691-2694.

[45] **Murakami, M., Ubukata, M., Itami, K., & Ito, Y**. (1998). Rhodium-Catalyzed Intermolecular [4+2] Cycloaddition of Unactivated Substrates. *Angewandte Chemie International Edition*, *37*(16), 2248-2250.

[46] **Huang, S., Li, X., Lin, C. L., Guzei, I. A., & Tang, W.** (2012). Rhodium-catalyzed 1, 3-acyloxy migration and subsequent intramolecular [4+2] cycloaddition of vinylallene and unactivated alkyne. *Chemical Communications*, *48*(16), 2204-2206.

[47] **Jiang, G. J., Fu, X. F., Li, Q., & Yu, Z. X**. (2012). Rh (I)-Catalyzed [5+1] Cycloaddition of Vinylcyclopropanes and CO for the Synthesis of α, β- and β, γ-Cyclohexenones. *Organic letters*, *14*(3), 692-695.

[48] **Yao, Z. K., Li, J., & Yu, Z. X.** (2010). Rh-Catalyzed [7+1] Cycloaddition of Buta-1,3-dienylcyclopropanes and CO for the Synthesis of Cyclooctadienones. *Organic letters*, *13*(1), 134-137.

[49] **Li, X., Zhang, M., Shu, D., Robichaux, P. J., Huang, S., & Tang, W.** (2011). Rhodium-Catalyzed Ring Expansion of Cyclopropanes to Seven-membered Rings by 1,5 C-C Bond Migration. *Angewandte Chemie*, *123*(44), 10605-10608.

[50] **Shibata, Y., Noguchi, K., & Tanaka, K.** (2010). Cationic rhodium (I) complex-catalyzed [3+2] and [2+1] cycloadditions of propargyl esters with electron-deficient alkynes and alkenes. *Journal of the American Chemical Society*, *132*(23), 7896-7898.

[51] **Shu, X. Z., Li, X., Shu, D., Huang, S., Schienebeck, C. M., Zhou, X., ... & Tang, W.** (2012). Rhodium-catalyzed intra-and intermolecular [5+ 2] cycloaddition of 3-acyloxy-1, 4-enyne and alkyne with concomitant 1, 2-acyloxy migration. *Journal of the American Chemical Society*, *134*(11), 5211-5221.

[52] **Schienebeck, C. M., Li, X., Shu, X. Z., & Tang, W.** (2014). 3-Acyloxy-1,4-enyne: A new five-carbon synthon for rhodium-catalyzed [5+2] cycloadditions. *Pure and Applied Chemistry*, *86*(3), 409-417.

[53] **Lytollis, W., Scannell, R. T., An, H., Murty, V. S., Reddy, K. S., Barr, J. R., & Hecht, S. M.** (1995). 5-Alkylresorcinols from Hakea trifurcata that cleave DNA. *Journal of the American Chemical Society*, *117*(51), 12683-12690.

[54] **Barr, J. R., Murty, V. S., Yamaguchi, K., Singh, S., Smith, D. H., & Hecht, S. M.** (1988). 5-Alkylresorcinols from Hakea amplexicaulis that cleave DNA. *Chemical research in toxicology*, *1*(4), 204-207.

[55] **Kubo, I., Himejima, M., & Muroi, H.** (1991). Antimicrobial activity of flavor components of cardamom Elettaria cardamomum (Zingiberaceae) seed. *Journal of agricultural and food chemistry*, *39*(11), 1984-1986.

[56] **Correa, A., Marion, N., Fensterbank, L., Malacria, M., Nolan, S. P., & Cavallo, L.** (2008). Golden carousel in catalysis: the cationic gold/propargylic ester cycle. *Angewandte Chemie*, *120*(4), 730-733.

[57] **Mauleón, P., Krinsky, J. L., & Toste, F. D.** (2009). Mechanistic studies on Au (I)-catalyzed [3, 3]-sigmatropic rearrangements using cyclopropane probes. *Journal of the American Chemical Society*, *131*(12), 4513.

[58] **Chen, W., Tay, J. H., Yu, X. Q., & Pu, L.** (2012). Diastereoselective [4+1] Cycloaddition of Alkenyl Propargyl Acetates with CO Catalyzed by $[RhCl(CO)_2]_2$. *The Journal of organic chemistry*, *77*(14), 6215-6222.

[59] **Cho, E. J.** (2012). Factors Controlling the Equilibrium of Pt-Catalyzed [1,2]-versus [1,3]-Acyloxy Migration. *Chemistry-A European Journal*, *18*(15), 4495-4498.

[60] **Xu, X., Liu, P., Shu, X. Z., Tang, W., & Houk, K. N.** (2013). Rh-catalyzed (5+2) cycloadditions of 3-acyloxy-1,4-enynes and alkynes: Computational study of mechanism, reactivity, and regioselectivity. *Journal of the American Chemical Society*, *135*(25), 9271.

[61] **Katritzky, A. R., & Dennis, N.** (1989). Cycloaddition reactions of heteroaromatic six-membered rings. *Chemical Reviews*, *89*(4), 827-861.

[62] **Gothelf, K. V., & Jørgensen, K. A.** (1998). Asymmetric 1,3-dipolar cycloaddition reactions. *Chemical Reviews*, *98*(2), 863-910.

[63] **Goodall, G. W., & Hayes, W.** (2006). Advances in cycloaddition polymerizations. *Chemical Society Reviews*, *35*(3), 280-312.

[64] **Ylijoki, K.E. and Stryker, J.M.,** (2012). [5+2] Cycloaddition reactions in organic and natural product synthesis. *Chemical reviews*, *113*(3), pp.2244-2266.

[65] **Hong, X., Trost, B. M., & Houk, K. N.** (2013). Mechanism and origins of selectivity in Ru (II)-catalyzed intramolecular (5+2) cycloadditions and ene reactions of vinylcyclopropanes and alkynes from density functional theory. *Journal of the American Chemical Society*, *135*(17), 6588-6600.

[66] **Shu, D., Li, X., Zhang, M., Robichaux, P. J., & Tang, W**. (2011). Synthesis of Highly Functionalized Cyclohexenone Rings: Rhodium-Catalyzed 1,3-Acyloxy Migration and Subsequent [5+1] Cycloaddition. *Angewandte Chemie*, *123*(6), 1382-1385.

[67] **Nishiwaki, N. (Ed.).** (2013). *Methods and applications of cycloaddition reactions in organic syntheses* (pp. 551-564). New Jersey: John Wiley & Sons Inc.

[68] **Lautens, M., Klute, W., & Tam, W.** (1996). Transition metal-mediated cycloaddition reactions. *Chemical reviews*, *96*(1), 49-92.

[69] **Ojima, I., Tzamarioudaki, M., Li, Z., & Donovan, R. J.** (1996). Transition metal-catalyzed carbocyclizations in organic synthesis. *Chemical reviews*, *96*(2), 635-662.

[70] **Inglesby, P. A., & Evans, P. A.** (2010). Stereoselective transition metal-catalysed higher-order carbocyclisation reactions. *Chemical Society Reviews*, *39*(8), 2791-2805.

[71] **Broere, D. L., & Ruijter, E.** (2012). Recent advances in transition-metal-catalyzed [2+2+2]-cyclo (co) trimerization reactions. *Synthesis*, *44*(17), 2639-2672.

[72] **Burnie, A. J., & Evans, P. A.** (2017). Recent Developments in Rhodium-Catalyzed Cyclocarbonylation Reactions. In *Rhodium Catalysis* (pp. 167-230). Springer, Cham.

[73] **Boeckman, R. K., del Rosario Rico Ferreira, M., Mitchell, L. H., & Shao, P.** (2002). An enantioselective total synthesis of (+)-and (−)-saudin. Determination of the absolute configuration. *Journal of the American Chemical Society*, *124*(2), 190-191.

[74] **Modugu, N. R., & Mehta, G.** (2015). An approach toward novel bioactive natural products antroquinonols: de novo construction of the carbocyclic core. *Tetrahedron Letters*, *56*(44), 6030-6033.

[75] **Mac, D. H., Samineni, R., Sattar, A., Chandrasekhar, S., Yadav, J. S., & Grée, R.** (2011). Total synthesis of gabosines via an iron-catalyzed intramolecular tandem aldol process. *Tetrahedron*, *67*(48), 9305-9310.

[76] **Nakayachi, T., Yasumoto, E., Nakano, K., Morshed, S. R. M., Hashimoto, K., Kikuchi, H., ... & Sakagami, H.** (2004). Structure-activity relationships of α, β-unsaturated ketones as assessed by their cytotoxicity against oral tumor cells. *Anticancer research*, *24*(2B), 737-742.

[77] **Mori, K.** (1989). Synthesis of optically active pheromones. *Tetrahedron*, *45*(11), 3233-3298.

[78] **Plummer, E. L., Stewart, T. E., Byrne, K., Pearce, G. T., & Silverstein, R. M.** (1976). Determination of the enantiomeric composition of several insect pheromone alcohols. *Journal of Chemical Ecology*, *2*(3), 307-331.

[79] **Mori, K., Tamada, S., Uchida, M., Mizumachi, N., Tachibana, Y., & Matsui, M.** (1978). Synthesis of optically active forms of seudenol, the pheromone of douglas fir beetle. *Tetrahedron*, *34*(13), 1901-1905.

[80] **Ben-Shoshan, R., & Sarel, S.** (1969). Reaction of 1, 1-dicyclopropylethylene with pentacarbonyliron: a novel carbon monoxide insertion coupled with a double cyclopropane ring-opening. *Journal of the Chemical Society D: Chemical Communications*, (15), 883-884.

[81] **Victor, R., Ben-Shoshan, R., & Sarel, S.** (1970). Photochemically induced 1, 5-insertion of carbon monoxide into vinylcyclopropane systems. A novel synthesis of cyclohexenones mediated by iron carbonyl. *Tetrahedron Letters*, *11*(49), 4253-4256.

[82] **Sarel, S.** (1978). Metal-induced rearrangements and insertions into cyclopropyl olefins. *Accounts of Chemical Research*, *11*(5), 204-211.

[83] **Aumann, R.** (1974). Reactions of strained carbon-carbon bonds with transition metals. 7. Iron carbonyl complexes from vinylcyclopropane. *Journal of the American Chemical Society*, *96*(8), 2631-2632.

[84] **Cho, S. H., & Liebeskind, L. S.** (1987). Practical organic synthesis with strained ring molecules. Rhodium catalyzed carbonylation of cyclopropenecarboxylate esters and cyclopropenyl ketones to. alpha.-pyrones and of vinylcyclopropenes to phenols. *The Journal of Organic Chemistry*, *52*(12), 2631-2634.

[85] **Kurahashi, T., & de Meijere, A**. (2005). [5+1] Cocyclization of (Cyclopropylmethylene) cyclopropanes and other Vinylcyclopropanes with Carbon Monoxide Catalyzed by Octacarbonyldicobalt. *Synlett*, *2005*(17), 2619-2622.

[86] **Liu, C. H., Zhuang, Z., Bose, S., & Yu, Z. X.** (2016). $Fe_2(CO)_9$-mediated [5+1] cycloaddition of vinylcyclopropanes and CO for the synthesis of α, β-cyclohexenones. *Tetrahedron*, *72*(22), 2752-2755.

[87] **Jiang, G. J., Fu, X. F., Li, Q., & Yu, Z. X.** (2012). Rh(I)-Catalyzed [5+1] Cycloaddition of Vinylcyclopropanes and CO for the Synthesis of α, β- and β, γ-Cyclohexenones. *Organic letters*, *14*(3), 692-695.

[88] **Liu, C. H., & Yu, Z. X.** (2016). Rh-catalysed [5+1] cycloaddition of allenylcyclopropanes and CO: reaction development and application to the formal synthesis of (−)-galanthamine. *Organic & biomolecular chemistry*, *14*(25), 5945-5950.

[89] **Murakami, M., Itami, K., Ubukata, M., Tsuji, I., & Ito, Y.** (1998). Iridium-catalyzed [5+1] cycloaddition: allenylcyclopropane as a five-carbon assembling unit. *The Journal of organic chemistry*, *63*(1), 4-5.

[90] **Zhang, M., & Tang, W.** (2012). Synthesis of functionalized cyclohexenone core of welwitindolinones via rhodium-catalyzed [5+1] cycloaddition. *Organic letters*, *14*(14), 3756.

[91] **Cramer, C. J. (2004).** *Essentials of computational chemistry: theories and models*. (pp. 106-110, 187-190, 419-420). England: John Wiley & Sons Ltd.

[92] **Hohenberg, P., & Kohn, W.** (1964). Inhomogeneous electron gas. *Physical review*, *136*(3B), B864.

[93] **Kohn, W., & Sham, L. J.** (1965). Self-consistent equations including exchange and correlation effects. *Physical review*, *140*(4A), A1133.

[94] **Lewars, E. G.** (2011). *Computational chemistry: introduction to the theory and applications of molecular and quantum mechanics* (pp. 445-456, 521-527). Springer. 2nd Edition

[95] **Becke, Axel D.** (1993) Density-functional thermochemistry. III. The role of exact exchange, *The Journal of Chemical Physics 98, 5648-5652*.

[96] **Stephen, P. J., Devlin, F. J., Chabalowski, C. F., & Frisch, M. J**. (1994). Ab Initio Calculation of Vibrational Absorption and Circular Dichroism Spectra Using Density Functional Force Fields. *The Journal of Physical Chemistry, 98(45),* 11623-11627.

[97] **Slater, J. C.** (1951). A simplification of the Hartree-Fock method. *Physical Review*, *81*(3), 385.

[98] **Vosko, S. H., Wilk, L., & Nusair, M.** (1980). Accurate spin-dependent electron liquid correlation energies for local spin density calculations: a critical analysis. *Canadian Journal of physics*, *58*(8), 1200-1211.

[99] **Becke, A. D**. (1988). Density-functional exchange-energy approximation with correct asymptotic behavior. *Physical review A*, *38*(6), 3098.

[100] **Becke, A. D.** (1992). Density-functional thermochemistry. I. The effect of the exchange-only gradient correction. *The Journal of chemical physics*, *96*(3), 2155-2160.

[101] **Lee, C., Yang, W., & Parr, R. G. (**1988). Development of the Colle-Salvetti correlation-energy formula into a functional of the electron density. *Physical review B*, *37*(2), 785.

[102] **Chai, J. D., & Head-Gordon, M.** (2008). Long-range corrected hybrid density functionals with damped atom–atom dispersion corrections. *Physical Chemistry Chemical Physics*, 10(44), 6615-6620.

[103] Zhao, Y., & Truhlar, D. G. (2006). A new local density functional for main-group thermochemistry, transition metal bonding, thermochemical kinetics, and noncovalent interactions. *The Journal of chemical physics*, 125(19), 194101.

[104] Jensen, F. (2007). *Introduction to computational chemistry* (2nd Ed.) (pp. 416-418, 497-499). England: John Wiley & Sons.

[105] Gonzalez, C., & Schlegel, H. B. (1989). An improved algorithm for reaction path following. *The Journal of Chemical Physics*, 90(4), 2154-2161.

[106] Gonzalez, C., & Schelgel, H. B. (1990). Reaction path following in mass-weighted internal coordinates. *Journal of Physical Chemistry*, *94*(14), 5523-5527.

[107] Young, D. C. (2001). *Computational Chemistry: A Practical Guide for Applying Techniques to Real-World Problems* (pp. 159-162). New York: John Wiley & Sons, Inc.

[108] Tomasi, J., Mennucci, B., & Cammi, R. (2005). Quantum mechanical continuum solvation models. *Chem. Rev*, *105*(8), 2999-3094.

[109] Wang, H., Sawyer, J. R., Evans, P. A., & Baik, M. H. (2008). Mechanistic Insight into the Diastereoselective Rhodium-Catalyzed Pauson-Khand Reaction: Role of Coordination Number in Stereocontrol. *Angewandte Chemie*, *120*(2), 348-351.

[110] Hay, P. J., & Wadt, W. R. (1985). Ab initio effective core potentials for molecular calculations. Potentials for the transition metal atoms Sc to Hg. *The Journal of chemical physics*, *82*(1), 270-283.

[111] Hay, P. J., & Wadt, W. R. (1985). Ab initio effective core potentials for molecular calculations. Potentials for K to Au including the outermost core orbitals. *The Journal of Chemical Physics*, *82*(1), 299-310.

[112] Wadt, W. R., & Hay, P. J. (1985). Ab initio effective core potentials for molecular calculations. Potentials for main group elements Na to Bi. *The Journal of Chemical Physics*, *82*(1), 284-298.

[113] Frisch, M. J., Trucks, G. W., Schlegel, H. B., Scuseria, G. E., Robb, M. A., Cheeseman, J. R., ... & Millam, J. M. (2004). Gaussian 03, revision C. 02; Gaussian, Inc. *Wallingford, CT*, *26*.

[114] Fukui, K. (1970). Formulation of the reaction coordinate. *The Journal of Physical Chemistry*, *74*(23), 4161-4163.

[115] Fukui, K. (1981). The path of chemical reactions-the IRC approach. *Accounts of chemical research*, *14*(12), 363-368.

[116] Ke, X. N., Schienebeck, C. M., Zhou, C. C., Xu, X. F., & Tang, W. P. (2015). Mechanism and reactivity of rhodium-catalyzed intermolecular [5+1] cycloaddition of 3-acyloxy-1,4-enyne (ACE) and CO: A computational study. *Chinese Chemical Letters*, *26*(6), 730-734.

[117] Jiang, J., Liu, Y., Hou, C., Li, Y., Luan, Z., Zhao, C., & Ke, Z. (2016). Rationalization of the selectivity between 1,3-and 1,2-migration: a DFT study on gold(I)-catalyzed propargylic ester rearrangement. *Organic & biomolecular chemistry*, *14*(14), 3558-3563.

[118] **Coskun, D., & Tüzün, N. Ş.** (2017). A DFT study on the mechanism of Rh-catalyzed competitive 1,2- versus 1,3-acyloxy migration followed by [5+1] and [4+1] cycloadditions of 1,4-enynes with CO. *Journal of Organometallic Chemistry*, *851*, 97-103.

[119] **Boz, E., & Tüzün, N. Ş.** (2016). Ag-catalyzed azide alkyne cycloaddition: a DFT approach. *Dalton Transactions*, *45*(13), 5752-5764.

[120] **Legault, C. Y.** (2009). CYLview, 1.0 b, Université de Sherbrooke.

[121] **Mbaezue, I. I., & Ylijoki, K. E.** (2017). [5+ 1+ 2+ 1] vs [5+1+ 1+ 2] Rhodium-Catalyzed Cycloaddition Reactions of Vinylcyclopropanes with Terminal Alkynes and Carbon Monoxide: Density Functional Theory Investigations of Convergent Mechanistic Pathways and Reaction Regioselectivity. *Organometallics*, *36*(15), 2832-2842.

[122] **Taber, D. F., Kanai, K., Jiang, Q., & Bui, G.** (2000). Enantiomerically pure cyclohexenones by Fe-mediated carbonylation of alkenyl cyclopropanes. *Journal of* the *American Chemical Society*, *122*(28), 6807-6808.

[123] **Kozuch, S., & Shaik, S.** (2010). How to conceptualize catalytic cycles? The energetic span model. *Accounts of chemical research*, *44*(2), 101-110.

[124] **Hayashi, M., Ohmatsu, T., Meng, Y. P., & Saigo, K.** (1998). Rhodium (I)-Catalyzed Regioselective Ring-Expanding Rearrangement of Allenylcyclopropanes into Methylenecyclopentenes. *Angewandte Chemie International Edition*, *37*(6), 837-839.

CURRICULUM VITAE

Name Surname **:** Dilek COŞKUN

Place and Date of Birth **:** Geyve, 1985

E-Mail **:** okusdilek@itu.edu.tr

EDUCATION **:**

- **B.Sc.** **:** 2008, Middle East Technical University (METU), Faculty of Education, Department of Chemistry Education, Ankara, Turkey
- **M.Sc.** **:** 2010, Middle East Technical University (METU), Graduate School of Natural and Applied Science, Master of Science in Chemistry, Ankara, Turkey

PROFESSIONAL EXPERIENCE AND REWARDS:

- 2008 Project Assistant, METU (with Prof. Mürvet Volkan, METU), Synthesis of silver nanowires through polyol process
- 2008- 2010 Research Assistant, METU Chemistry Department, Working as an instructor for chemistry in the laboratories and assisting students during the experiment process, preparing and evaluating exams during the semester, doing research on polymer composites.
- 2008- 2010 Project Assistant, ARCELIK A.S. (with Prof. Teoman Tinçer, METU) Development of "Bituminous Composites", Preparing

and testing mechanical, thermal and flow properties of bituminous composites to decrease the amount of sound and heat in dishwashers for Arcelik company in Turkey

- 2009- 2010 Project Assistant, GISAM (Audio-Visual Systems Research and Application Center) Integrating General Chemistry experiments in the laboratory to the electronic environment
- 2011 The OCW Consortium Award for METU OpenCourseWare in the Video and Multimedia, Category at the 2011 global conference of OpenCourseWare Consortium in Massachusetts Institute of Technology-MIT
- 2008-2010 TUBITAK Graduate Achievement Scholarship for Master Students, 2 years in a row
- 2010-2015 TUBITAK Graduate Achievement Scholarship for Doctorate Students, 5 years in a row

PUBLICATIONS, PRESENTATIONS AND PATENTS ON THE THESIS:

Coskun, D., & Tüzün, N. Ş., (2017) A DFT study on the mechanism of Rh-catalyzed competitive 1, 2-versus 1, 3-acyloxy migration followed by [5+1] and [4+1] cycloadditions of 1, 4-enynes with CO. *Journal of Organometallic Chemistry*, *851*, 97-103.

Coskun, D., & Tüzün, N. Ş., (2017) Rh-catalyzed [5+1] and [4+1] cycloadditions of 1,4-enynes by CO with concominant 1,2- versus 1,3-acyloxy migrations: A DFT study, Chemistry Via Computation, Boğaziçi University, Istanbul/Turkey